SYNTHESIS AND CHARACTERISATION OF AMINOPOLYCARBOXYLIC ACID BASED METAL COMPLEXES AS PHOTOLUMINESCENT MATERIALS

MERLINVINOLIYA J E

21PCH013

Dissertation work submitted to
Avinashilingam Institute for Home Science and Higher Education for Women
Coimbatore- 641 043

In Partial Fulfilment of the Requirements for the Degree Of

MASTER OF SCIENCE IN CHEMISTRY

MAY – 2023

SYNTHESIS AND CHARACTERISATION OF AMINOPOLYCARBOXYLIC ACID BASED METAL COMPLEXES AS PHOTOLUMINESCENT MATERIALS

MERLINVINOLIYA J E

21PCH013

Dissertation work submitted to
Avinashilingam Institute for Home Science and Higher Education for Women
Coimbatore- 641 043

In Partial Fulfilment of the Requirements for the Degree Of

MASTER OF SCIENCE IN CHEMISTRY

MAY - 2023

M. Amuthaselvi 19/5/23
Signature of the
Supervisor

R. Rani 19/5/23
Signature of the
for Head of the Department

ACKNOWLEDGEMENT

Every work succeeds by the blessings of Lord Almighty. Hence, I bow my head at the feet of the Lord Almighty for his blessings rendered with good health and clear mind throughout my work.

I am grateful to **Dr. S.P. Thyagarajan, Chancellor**, Avinashilingam Institute for Home Science and Higher Education for Women, Coimbatore, for providing a learning opportunity being in this university.

I owe my sincere thanks to **Dr. Bharathi Harishankar, Vice Chancellor**, Avinashilingam Institute for Home Science and Higher Education for Women, Coimbatore, for providing a learning opportunity at this university.

I am thankful to **Dr. S. Kowsalya, Registrar**, Avinashilingam Institute for Home Science and Higher Education for Women, Coimbatore, for extending adequate facilities for the progress of the work.

I am highly thankful to **Dr.G.Padmavathi, Dean** of School of Physical Sciences and Computational Sciences, Avinashilingam Institute for Home Science and Higher Education for Women, Coimbatore, for making all necessary arrangements during the course of the work.

With great pleasure and respect, I would like to express my affable and cordial thanks to **Dr.R.Saratha**, Professor and **Head**, Department of Chemistry, Avinashilingam Institute for Home Science and Higher Education for Women, Coimbatore, for being a great support and for extending all the facilities during the entire course of work.

With deep sense of gratitude and respect, I humbly extend my heartfelt thanks to my guide, **Dr. M. Amutha Selvi,** Assistant professor, Department of Chemistry, Avinashilingam Institute for Home Science and Higher Education for Women, Coimbatore, for her care, innovative ideas, highly motivating guidance, encouragement and constant support during the entire course of the work.

I also thank all my staff members of Chemistry Department, Avinashilingam Institute for Home Science and Higher Education for Women, Coimbatore, for extending their support and encouragement.

I wish to thank all my senior research scholars and my friends of the Chemistry Department for their help, moral support and encouragement.

I also wish to extend a word of appreciation for the non-teaching staff, Department Of Chemistry, Avinashilingam Institute for Home Science and Higher Education for Women, Coimbatore, for their cooperation and timely help.

I owe my gratitude to all those who rendered their help for the completion of my work in the form of physical help and mental strength.

At length, with deep respect and honour my gratitude highlights on my parents, my siblings and all my family members for without them there is no glossary to my glory.

MERLINVINOLIYA J E

CONTENT

LIST OF TABLES

LIST OF FIGURES

LIST OF ABBREVIATIONS

MRI	Magnetic Resonance Imaging
Gd	Gadolinium
Mn	Manganese
Fe	Iron
GBCA	Gadolinium Based Contrast Agent
BM	Bohr Magneton
NSF	Nephrogenic Systemic Fibrosis
DPDP	Dipyridoxyldiphosphate
EDTA	Ethylenediamine tetra acetic acid
Ln	Lanthanum
Ca	Calcium
DTPA	Diethylenetriamine penta acetic acid
DMF	Dimethyl formamide
NaHCO3	Sodium bicarbonate
HCl	Hydrochloric acid
DMSO	Dimethyl sulphoxide
FTIR	Fourier Transform Infrared

INTRODUCTION

1.INTRODUCTION

Magnetic Resonance Imaging (MRI) is a potent non-invasive diagnostic imaging technique [1]. It can reach a depth of 1 mm to 1 m inside soft tissues and can take three-dimensional images with exceptional resolution [2]. MRI does not use any dangerous high-energy radiation, unlike other diagnostic procedures like X-ray computer tomography (CT), single-photon emission computed tomography (SPECT), or positron emission tomography (PET) [3].

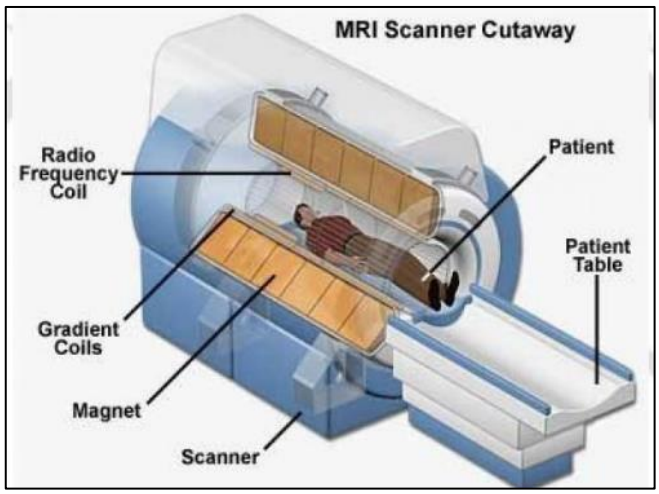

Fig 1.1: Basic components present in an MRI scanner [4]

The essential parts that make up an MRI machine are (a) sizable magnet, (b) gradient coils, (c) a radio frequency coil, (d) a patient table, (e) an antenna with a computer system. The gradient coils spatially encode the treated nuclei with various resonance frequencies when a static magnet is present. Free induction decay signal is Fourier transformed to generate images based on the strength of the NMR signal following the application of a radio frequency pulse.

Primarily, MRI detects endogenous water molecules, which make about 70% of the human body [5]. Different tissues found in various places of our body contain varying amounts of water, and these water molecules have unique physical and magnetic properties. Protons from water molecules found in human bodily tissue (a sample) are used by the MRI machine to produce NMR signals [6]. Images are acquired from the fluctuation of these water molecules' longitudinal ($R_1 = 1/T_1$) and transverse ($R_2 = 1/T_2$) relaxation rates [7]. The signals assess the

local surroundings of the tissues being investigated. Eventually, using image contrast, the variation in tissue relaxation rates reveals the anatomy and pathology of the studied tissue.

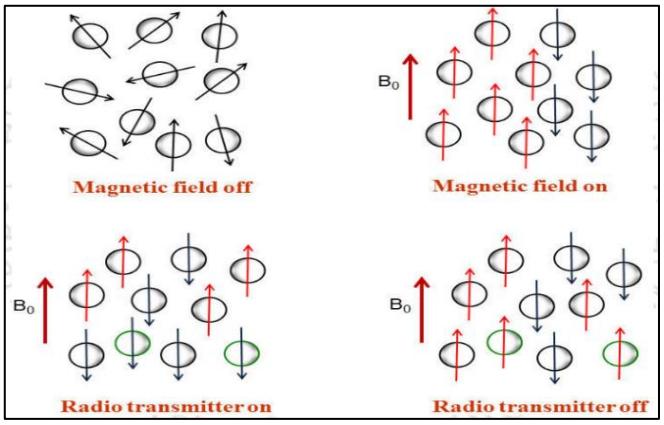

Fig 1.2: Arrangement of protons during MRI experiment.

The magnetic moment connected to a positively charged, spinning proton is the basis of the MRI's physical operation. When there is no external field present, these charged spheres in motion behave like tiny magnets that are randomly orientated. These spinning charged spheres align themselves in either the parallel (low energy) or antiparallel (high energy) directions of the applied magnetic field after the MRI machine applies a magnetic field. The population of the lower energy state is higher than that of the higher energy state, and the population differential varies depending on the measurement's magnetic field and temperature. When a radio frequency pulse with a frequency equal to the Larmor frequency is applied, some charged spheres absorb the energy and jump to a higher energy level by flipping their orientation, at which point they all begin to precess in phase. It establishes transverse magnetization and causes a decrease in net longitudinal magnetization. The entire system returns to its equilibrium state once the radio frequency pulse ends through a process known as relaxing (Fig 1). The relaxation process is divided into two categories depending on how one returns to the equilibrium state.

1.1 Longitudinal relaxation (T1 relaxation):

By transferring energy to its surrounding lattice, magnetization grows exponentially along the z-direction to its initial maximum value (M_0) throughout the relaxation phase. Spin-lattice relaxation or thermal relaxation are other names for this. T_1 is the amount of time necessary to regain 63% of its initial magnetization in the z-direction.

$$M_z = M_0 (1 - e^{-t/T_1})$$

1.2Transverse relaxation (T_2 relaxation):

Net magnetization in the xy plane diminishes during this relaxation process as a result of the loss of spin coherence. Spin-spin relaxation is the term used to describe this. Transverse magnetization, which is determined by the equation, falls to 37% of its initial value in T_2.

$$M_{xy} = M_0 e^{-t/T_2}$$

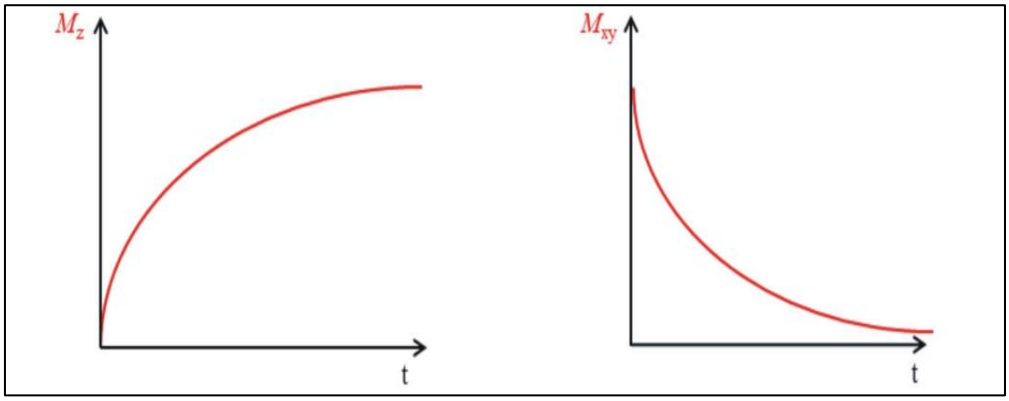

Fig 1.3: Variation of magnetization in returning back to equilibrium position, (A) on z-axis in longitudinal relaxation, and (B) on xy-plane in transverse relaxation.

The biochemical parameters of the tissues being studied (such as water concentration, pH, temperature, salt concentration, etc.) have a significant impact on T_1 and T_2 relaxation times. Malignant tissues have much longer T_1 and T_2 relaxation durations than healthy ones. Hence, any abnormalities found in the tissues under examination can be identified by an MRI experiment. Table 1 compares the T_1 relaxation durations of normal and cancerous tissues from various human body areas.

Table 1: T_1 relaxation times in normal and malignant human tissues [8]

Tissue	**T_1 Tumour**	**T_2 Tumour**
Liver	0.832	0.570
Lung	1.110	0.788
Breast	1.080	0.367
Bone	1.027	0.554
Skin	1.047	0.616

Images can be classified as T_1-weighted or T_2-weighted images based on two different relaxation durations. In an MRI scan, the region with high signal intensity is brighter than the region with low signal intensity. Tissues with short T_1 seem brighter in T_1-weighted imaging because most of their longitudinal magnetizations have regained, producing a strong MR signal. As a result of their inability to recover the majority of their longitudinal magnetization, tissues with long T_1 appear dark and produce weak signals. White matter, which contains a large proportion of fat, appears brighter as a result, while compartments containing a higher proportion of water, such as Cerebrospinal fluid seem darker. (Fig 1.3A).

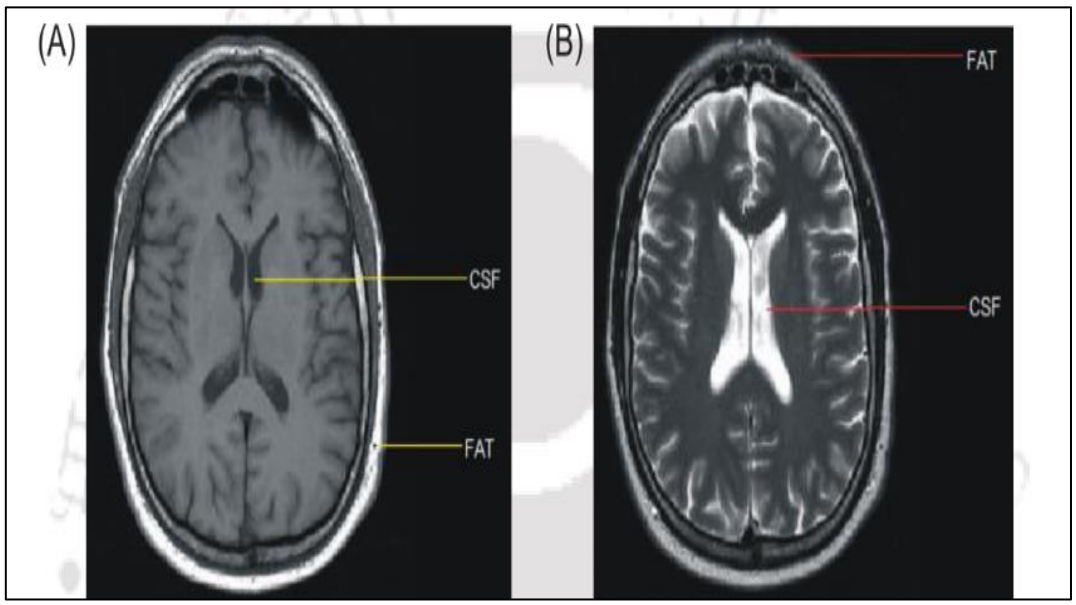

Fig 1.4: Image contrast between fat and CSF in; (A) T_1-weighted, and (B) T_2-weighted MR imaging [9]

T_2-weighted imaging causes tissues with short T_2 to appear black since the whole signal has been lost. Tissues with a long T_2 emit a stronger signal, which makes them appear brilliant. In contrast to fat with a short T_2 value, CSF with a long T_2 value appears brighter on T_2 -weighted pictures. (Fig 1.3B)

1.3 MRI Contrast Agents

Even while MRI scans naturally have a high level of contrast, some diagnostic questions cannot be fully resolved by this method. It becomes important to adjust the visual contrast by using certain external agents called as contrast agents when it is unable to achieve intrinsic contrast throughout any experiment [10]. The relaxation durations of bulk water molecules can be catalytically shortened by these external agents, which are often paramagnetic, superparamagnetic, or ferromagnetic substances (Figure 1.4) [11]. Despite the fact that all contrast agents can reduce T_1 and T_2 relaxation durations, they are primarily divided into two groups based on their dominating effect.

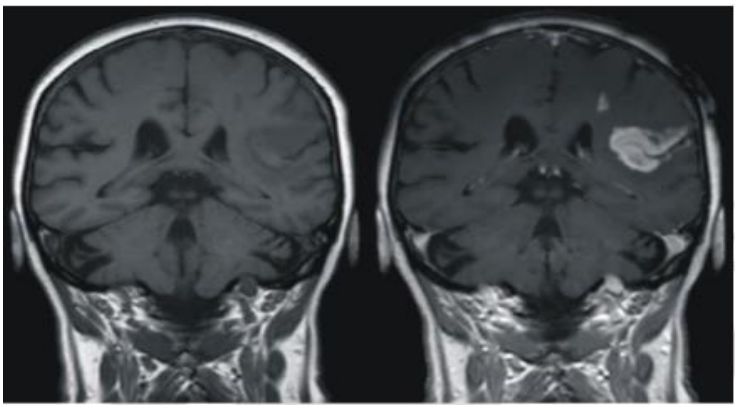

Pre Post

Fig 1.5: Effect of contrast agent on the images detecting blood-brain barrier after stroke.

1.3.1 T_1-Contrast Agents:

Image contrast can be increased by using a variety of paramagnetic metal ions, such as Gd (III), Mn (II), Mn (III), Fe (III), etc., that have a lot of unpaired electrons [12]. Unpaired electrons have the ability to effectively relax adjacent nuclei and generate a high fluctuating magnetic field. They are primarily responsible for decreasing T_1 relaxation durations, which increases signal intensity. They are referred to as positive contrast agents.

1.3.2 T_2-Contrast Agents:

These are super paramagnetic and ferromagnetic substances which effect predominantly in lowering T_2 relaxation times. Reduction in T_2 relaxation times decreases MRI signal intensity. These contrast agents are known as negative contrast agents. Iron oxide nanoparticles are mostly used as T_2 contrast agent. These particles are behaving as small

movable magnets, which finally create a strong magnetic field. They are again classified according to their sizes [13].

(a)Super paramagnetic iron oxides (SPIO), average diameter > 50 nm, and
(b) Ultra-small super paramagnetic iron oxides (USPIO), average diameter < 50 nm.

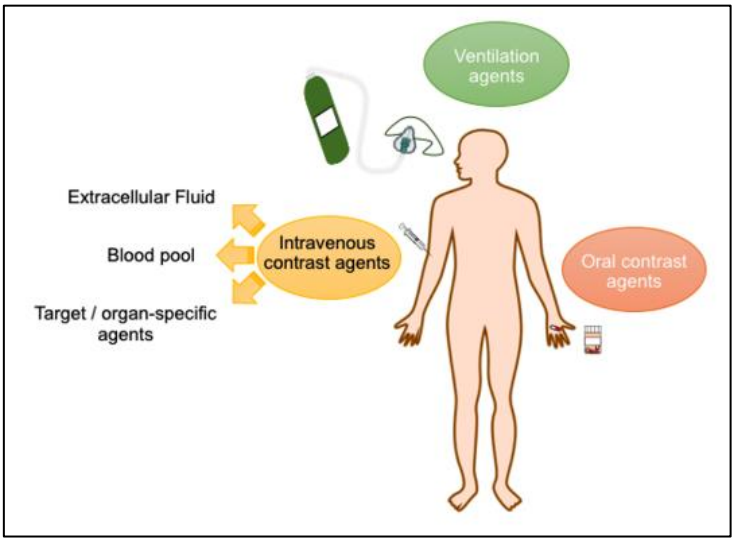

Fig 1.6: Route of administration of MRI contrast agents

A contrast agent for MR must have good tolerance and be able to effectively reduce T_1 and/or T_2 in tissues at low doses (μM to mM). The most significant characteristics of paramagnetic MRI contrast agents are listed below, with an emphasis on the GBCAs [14].

***High Relaxivity*:**

The "relaxivity" of each agent, denoted by r_1 and r_2, is its fundamental capacity to decrease T_1 and/or T_2. At similar doses, a substance with a higher relaxivity will lower the T_1 and/or T_2 more than a substance with a lower relaxivity. The benefit that results from this difference can be exploited to lower the dose or provide greater signal at appropriate doses, potentially reducing toxicity [15].

High Stability:

Stability is the capacity of the chelating agent to keep the metal ion from being lost. The shelf-life of an MRI contrast agent, which is normally 2-3 years from manufacture to usage, must be kept as low as possible in terms of metal dissociation from the chelating agent,

but more importantly, dissociation in vivo must be kept to a minimum. The chelating agents must be exceptionally potent in order to do this [16].

Specific Biodistribution:

In order to reduce the required contrast agent dose and/or boost the sensitivity of lesion identification, tissue specificity refers to the distribution of contrast agents to select organs or tissues with a higher concentration than to others. Agents that use the hepatobiliary, renal, or both renal and hepatobiliary modes of excretion are now available. Biologic target-specific contrast compounds are being investigated for application in imaging biochemical processes at the cellular and molecular levels [17].

Rapid Clearance:

After injection and subsequent imaging, MRI contrast agents should be quickly and effectively eliminated from the body. This is required to stop the slow deposition of dissociated free metal ions in certain tissues or organs, which causes chronic toxicity. Except where natural barriers (like the blood-brain barrier) prohibit it, these agents spread quickly to extracellular spaces [18].

Low Toxicity:

The acute toxicity of contrast agents should be modest, and they shouldn't cause any immediate side effects, including allergic or anaphylactoid reactions, or alterations to the normal range of blood values. Usually, ratios greater than 30 are desired between rodent LD50 and human dosages. There should be no issues with long-term toleration of the agents. Certain patient populations, such as those with renal impairment, require specific attention [19].

1.4 MRI Contrast Mechanisms:

The difference in signal intensities between the tissues in an image is what primarily determines MRI contrast. Spin density (primarily the spins of water protons), intrinsic tissue T_1 and T_2, the presence of naturally occurring paramagnetic ions, magnetic susceptibility, and diffusion or perfusion of the imaged water molecules in and out of voxels during scanning are some of the factors that affect MRI signal intensity. The T_1 and T_2 relaxation times are the parameters that MRI contrast agents focus on changing the most [20]. Although using contrast agents somewhat compromises the non-invasive nature of MRI, there are still several benefits that come with it. The ability to visualise inflammatory tissues, such

as those found in arthritis, tumour angiogenesis, atherosclerotic plaques, and the breakdown of the blood-brain barrier associated with diseases like multiple sclerosis is considerably improved by the use of contrast agents in conjunction with MRI [21].

1.5 Relaxivity Theory:

The capacity of a paramagnetic metal ion to affect the protons on most or all of the water molecules in the bulk solution via its magnetic moment is necessary for successful water proton relaxation enhancement (or tissues). The paramagnetic or superparamagnetic ion(s), specifically $Gd^{3+,}$ Mn^{2+}, or $Fe^{3+,}$ have all been present in the intravenous MRI contrast agents approved clinically to date as the active component. These ions provide a strong net magnetic moment and effective T_1 and/or T_2 relaxivities because they have either five (Fe^{3+} and Mn^{2+}) or seven (Gd^{3+}) unpaired electrons. The ions must be very labile, fast exchanging water molecules, and have an equal number of unpaired electrons to d or f orbitals in order to have a powerful effect. Both the relaxivity of the agent and the tissue's innate relaxation rate should be taken into account when developing experiments and new contrast agents because both have a role in the signal change that is detected. T_2 values for tissues during transverse relaxation are typically quite low and tend to fall as field strength rises. As a result, to substantially impact T_2, much greater concentrations of contrast agent and/or much higher relaxivities are needed. Many additional paramagnetic ions are inappropriate for a variety of chemical or biological reasons, but mostly because they do not fit electron orbitals and have an inertia to exchange water [21].

1.6 Contrast Agents with Gd (III) ions:

Gd (III) is a perfect target for use as a relaxation agent due to its high paramagnetic properties, seven unpaired electrons, and prolonged electronic relaxation time [22]. Gd (III) ion is a significant T1-weighted contrast agent that is used because of its high magnetic moment (7.9 BM) and completely symmetric electronic configuration, which results in a long electronic relaxation time (10^{-8}-10^{-9} s). The water protons return to their equilibrium locations as a result of the high magnetic moment of electrons. An electron's magnetic moment is 658 times stronger than a proton's magnetic moment. Unpaired electrons are therefore more efficient in the relaxing process and can produce great image contrast**.** However, due to the severe toxicity of Gd (III) ion in aqua form [23], strong organic ligand framework coordination of Gd (III) ion is required prior to in vivo application**.** The clinically used Gd (III) complexes is shown below [24].

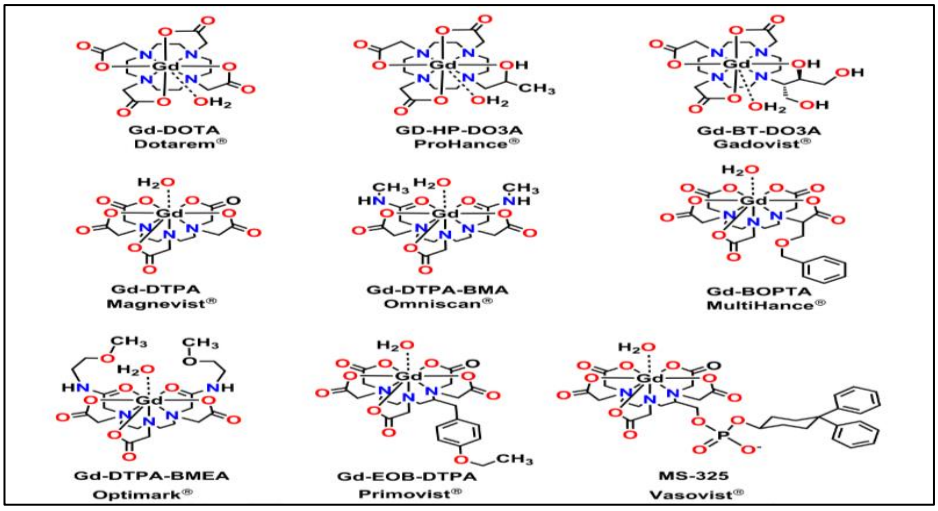

Fig1.7: Commercially available Gd (III)-based MRI contrast agents

Nephrogenic Systemic Fibrosis (NSF) is a systemic illness that is characterised by skin and connective tissue fibrosis (development of scar tissue). The disease is fatal and typically results in disability and death. Usually, red, itchy rashes occur as the initial NSF sign, progressing to hardness and hyperpigmentation**.** Other symptoms like pain, inflammation, nausea, vomiting, muscle weakness, and joint stiffness are frequently present together with the skin changes. Visceral fibrosis of the heart, lungs, and other organs is another effect that this disorder causes. In 2000, there was a first-case report of NSF. Initially, this was thought to be an unexplained outbreak of an unidentified disease, but subsequent research showed that all patients had chronic kidney disease and gadodiamide contrast enhanced MRIs prior to the onset of the symptoms [25]. After multiple retrospective investigations of NSF cases revealed that nearly all NSF patients had received a Gd^{3+}-based contrast agent prior to disease start in 2006, it was hypothesised that there was a link between NSF and Gd^{3+}-based MRI contrast agents. Subsequent analysis of NSF cases around the world showed that a small percentage of individuals with substantially impaired renal function are affected by NSF. After administering numerous doses of contrast agent, the condition progresses more quickly, hence the effect of Gd^{3+} is cumulative. Although the precise pathophysiology of NSF has not yet been completely outlined, various potential causes of skin lesion formation have been suggested. They include accumulation of the whole Gd(L) complex, the ligand released from the complex depleting endogenous metal ions, and the toxicity of the released free Gd^{3+} was found in the skin lesions of NSF patients, and a connection between NSF and MRI contrast agents with low kinetic inertness strongly suggests that free Gd^{3+} is what causes NSF [25]. This leads to a new road in the development of contrast agents where scientists concentrated on finding an alternative to gadolinium.

1.7 Mn^{2+}-based contrast agents:

The discovery of NSF has stimulated fresh research to create safer MRI contrast agents. The utilisation of some paramagnetic transition metal ions that may effectively relax the water protons is a potential strategy for developing substitute contrast agents for Gd^{3+} chelates. Mn^{2+} and Fe^{3+}, two metal ions that have significant biological roles and are less harmful than Gd^{3+}.However, due to their lower magnetic moments, fewer unpaired electrons (Mn^{2+} and Fe^{3+} both have d^5 electron configurations), and slightly faster electronic relaxation durations than $Gd^{3+,}$ these metals are less desirable for MRI applications. Presently, Mn^{2+} - dipyridoxyl diphosphate, Mn $(DPDP)^{3-}$ is the only Mn^{2+} based contrast agent available for use in liver imaging [26]. The complex [Mn $(DPDP)]^{3-}$ was in fact given the go-ahead to be used as a liver imaging agent. It has been demonstrated that [Mn $(DPDP)]^{3-}$ partially dechelates in plasma, with the Mn^{2+} ion being swiftly absorbed by hepatocytes, pancreatic tissue, and cardiomyocytes. The potential and difficulty of employing Mn^{2+} are both shown by [Mn $(DPDP)]^{3-.}$ In addition to highlighting the great lability of the Mn^{2+} ion and the difficulty of creating a stable Mn-chelate, [Mn $(DPDP)]^{3-}$ produced excellent picture contrast that showed the effectiveness of a Mn-based method. The negatively charged oxygen and nitrogen donor atoms are preferred by the "hard" Mn^{2+} ion. As a result of their symmetrical d^5 electron configuration and lack of ligand field stabilisation energy, most Mn^{2+} complexes follow the Irving-Williams order of relative stability. Hence, among the divalent first-row transition metal high spin complexes, Mn^{2+} complexes have the lowest stability. It makes sense to design chelators that enable stable Mn^{2+} complexes suitable for the same MR imaging applications as Gd-based probes, including bifunctional Mn^{2+} chelators that can be used in molecular MR applications and small, hydrophilic complexes useful for angiography, lesion identification, and characterization of tissue perfusion [27]. This also demonstrates the difficulty in creating Mn^{2+}-based MRI contrast agents. The Mn^{2+} ion typically has a coordination number of 6 or 7, and the most stable complexes are those generated with ligands that have a corresponding number of donor atoms [28]. Fast water exchange, acceptable T1 relaxivities, the possibility of undergoing redox chemistry in vivo, and other characteristics of high-spin Mn^{2+} complexes make them appealing as MRI agents.

1.8 LIGAND STRATEGY TO DESIGN MRI CONTRAST AGENTS:

A sort of bonding between ions and molecules and metal ions is called chelation. A polydentate (many bound) ligand and a single central metal atom form or already have one or

more distinct coordinate bonds. These ligands are also known as chelators, sequestering agents, chelants, or chelating agent. Chelates can best be visualized as a lobster's claw (appropriate since the word chelate comes from a Greek word meaning claw) made of carbon and hydrogen atoms holding the metal ion. The more bonds, called ligands, that form between the ion and the carbon atoms, the stronger the ion is held within the chelate. Chelation can be used to provide nutritional supplements, chelation therapy, contrast agents for MRI scanning, homogeneous catalysts for manufacturing, chemical water treatment to help remove metals from water, fertilisers, and other purposes. One of the earliest complexes to be investigated as a potential MRI contrast agent was Gd (EDTA). Gd (EDTA) was not given consideration for future commercial development as a contrast agent due to a number of drawbacks, including relatively low thermodynamic stability, adverse kinetic inertness, and formation of ternary complexes with other biomolecules (extracellular). The Ln (III) complexes of this hexadentate ligand are made more stable and slightly more kinetically inert by replacing the ethylenediamine (ED) backbone of EDTA with the more rigid 1,2-cyclohexyldiamine bridge to yield DCTA, but this structural modification did not completely prevent the formation of ternary complexes. This led to the conclusion that hexadentate ligands cannot be used as a platform for contrast agents because, despite being advantageous for relaxivity, having many inner-sphere water coordination sites proved detrimental when such complexes are exposed to a biological matrix. Nonetheless, interesting EDTA and DCTA derivatives have been described in which one or more carboxylates are substituted with picolinate or phosphonate groups. In aqueous solution, it was discovered that these ligands formed comparatively stable complexes with Ln^{3+} ions. This implies that derivatives with a structure similar to Gd (EDTA) could be employed as contrast agents in a biological setting.

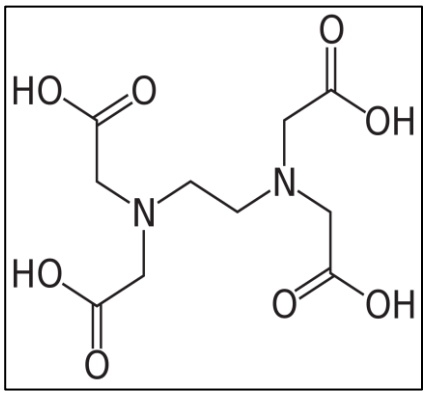

Fig 1.8: Structure of EDTA

The amino poly carboxylic acid ethylenediaminetetraacetic acid (EDTA) has the formula $[CH_2N(CH_2CO_2H)_2]_2$. Even at neutral pH levels, this white, water-insoluble solid is

frequently employed to bind to calcium (Ca^{2+}) and iron (Fe^{2+}/Fe^{3+}) ions, generating water-soluble complexes. Hence, it is employed to transport iron ions in environments where its oxides are intractable as well as to dissolve scale that contains Fe and Ca. Disodium EDTA, sodium calcium EDTA, and tetrasodium EDTA are some of the salt forms of EDTA that are available, but they all perform comparable functions [29]. Chelation therapy, such as the treatment of lead and mercury poisoning, uses sodium calcium edetate, an EDTA derivative, to bind metal ions. Similar techniques are applied to get rid of extra iron from the body. Similar to how it would be used to treat thalassaemia, this therapy is used to alleviate the side effect of frequent blood transfusions [30]. Moreover, chelation of the metal ion necessary for catalytic activity allows EDTA to block a variety of metallopeptidases. Heavy metal bioavailability in sediments can also be tested using EDTA. Yet, given its numerous uses and applications, it may affect the bioavailability of metals in solution, raising questions about its effects on the environment [31]. Ferdinand Münz, who synthesized the chemical from ethylenediamine and chloroacetic acid, published the first description of it in 1935 [32]. Nowadays, formaldehyde, sodium cyanide, and ethylenediamine (1,2-diaminoethane) are used mostly in the manufacture of EDTA. In coordination chemistry, $EDTA^{4-}$ is a member of the amino polycarboxylic acid family of ligands. $EDTA^{4-}$ usually binds to a metal cation through its two amines and four carboxylates, i.e., it is a hexadentated ('six-toothed') chelating agent. Many of the resulting coordination compounds adopt octahedral geometry. Although of little consequence for its applications, these octahedral complexes are chiral. Due to the development of an extra bond to water, resulting in seven-coordinate complexes, or the displacement of one carboxylate arm by water, many $EDTA^{4-}$ complexes take on more complicated structures. EDTA has an iron (III) complex with seven coordinates. When combined with Mn (II), Cu (II), Fe (III), Pb(II), and Co (III), EDTA forms very potent compounds [33].

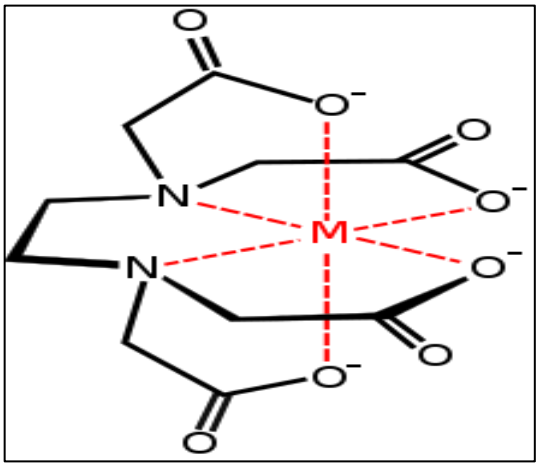

Fig 1.9: Metal EDTA chelate as in Co (III) complex

Diethylenetriaminepentaacetic acid (DTPA), also known as pentetic acid, is an aminopolycarboxylic acid made composed of a diethylenetriamine backbone and five carboxymethyl groups. The molecule functions similarly to EDTA and can be thought of as an enlarged form of it. It is a white substance that only partially dissolves in water.

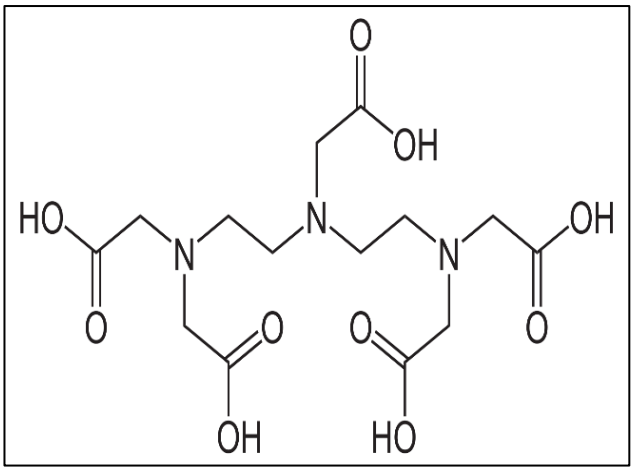

Fig 1.10: Structure of DTPA

Metal cations have a strong affinity for the conjugate base of DTPA. Assuming that each nitrogen centre and each -COO group count as coordination centres, the penta-anion

$DTPA^{5-}$ might be an octadentate ligand. Its complexes' formation constants are about 100 times larger than those of EDTA. DTPA forms up to eight bonds to encircle a metal ion while acting as a chelating agent [34]. An additional water molecule that coordinates the metal ion may be present in its complexes. However, less than eight coordination bonds typically form in the case of transition metals. As demonstrated by its derivative pendetide, DTPA can still attach to other chemicals even after creating a complex with a metal. For instance, DTPA binds in a hexadentate fashion to copper (II) by using three of the five carboxylates and the three amine centres [35]. Similar to the more popular EDTA, the main application of DTPA is as a chelating agent for complexing and retaining metal ions. DTPA is also employed as an MRI contrast material. By creating a soluble complex with a gadolinium (Gd^{3+}) ion and altering the magnetic resonance behaviour of the protons of adjacent water molecules, DTPA enhances the resolution of magnetic resonance imaging (MRI) and raises the contrast of the images. To stop the oxidative cell damage caused by superoxide and hydrogen peroxide, DTPA is more effective than EDTA at deactivating redox-active metal ions such Fe (II)/(III), Mn (II)/(IV), and Cu(I)/(II). Moreover, DTPA is utilised in bioassays that use redox-active metal ions [36].

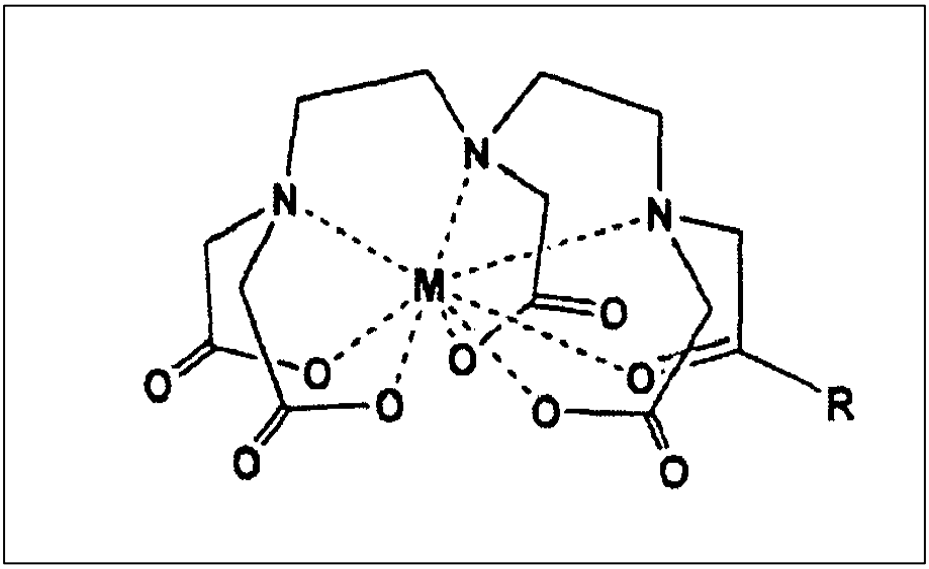

Fig 1.11: Metal – DTPA chelate as found in complex

SCOPE OF THE WORK:

Gd^{3+} complexes are commercially accessible MRI contrast agent that are utilised in roughly 40% of all MRI exams in clinics. When metal complexes bind to the target protein, they produce a good contrast and also boost the metal complex's relaxivity. Nephrogenic systemic fibrosis (NSF), particularly in patients with renal insufficiency, has been linked to Gd-based CA. Manganese (II) is getting greater attention for the next generation of effective MRI contrast agents in order to overcome the drawbacks of Gd-based CA, particularly liver and kidney damage. (Ferenc K. Kalman, Viktoria Nagy et al.,2020) When we compare the relaxivities of Mn based CA's, MNP-PEG-Mn is much higher than that of Gadodiamide (Xiaodong Li et al., 2020) (Mauro Botta et al., 2019). According to Y. Huang et al.., (2011), it is advantageous to bind Mn (II) ions to optimal ligands such Benzothiazole aniline (BTA), Phenylpentadecanoic Acid (PPDA), Diethyelenetriamine Penta Acetic Acid (DTPA), Dipyridoxy diphosphate (DPDP), and Ethylene Diamine Tetra Acetic Acid (EDTA). High chelation effectiveness and minimal leakage of free Mn (II) ions into the circulation are both characteristics of Mn (II)-DTPA contrast agent. Therefore, the search for potentially useful Mn (II)-based MRI contrast agents has never ended. The MRI technology uses the Mn-DTPA contrast agent extensively. This work concentrates on preparing DTPA and EDTA based manganese complexes which can be further studied to be used as contrast agent.

REVIEW OF LITERATURE

2. REVIEW OF LITERATURE

37. **Christoph J. Z Ech et al., (2017**) reviewed the use of liver-specific contrast agents which has been limited as a result of the inability to complete both the necessary vascular and liver-specific phase within a reasonable amount of time and in a single examination following a single injection of contrast agent. Liver-specific contrast agents have been particularly helpful in detecting and precisely characterising focal liver lesions. Gadolinium-ethoxybenzyl (Gd-EOB)-DTPA, a hepatobiliary contrast agent, now permits integrated dynamic imaging and hepatocyte-specific imaging in a single examination. As a bolus injection, Gd-EOB-DTPA exhibits the enhanced traits and vascularity of liver lesions. Gd-EOB-DTPA is selectively taken up by active hepatocytes during the delayed phase, which is best acquired 20 minutes after injection. Active hepatocytes selectively take up Gd-EOB-DTPA. Consequently, the surrounding liver parenchyma does not absorb contrast into malignant liver lesions, such as metastases. The liver around them is bright, but these lesions are hypointense. Using imaging examples of patients with liver metastases, the most recent research and provide a useful method for Gd-EOB-enhanced MR imaging are reviewed.

38. H. P. Niendorf et al., (2001) reviewed information on the paramagnetic contrast agent Gd-general DTPA's and renal tolerance following intravenous injection. In cranial, spinal, and body MR applications, Gd-DTPA was typically supplied at a dose level of 0.1 to 0.2 mmol/kg body weight (range: 0.005-0.25 mmol/kg body weight). Data on tolerance were gathered using a standardised technique, and a metanalysis of the results was done. 1.15 percent of the patients experienced adverse events (AEs), regardless of the drugs involved. The adverse events (AEs) that were seen were similar to those that occurred after receiving iodinated non-ionic X-ray contrast material intravenously. Hemo dialysis has been found to entirely remove Gd-DTPA. Injections given quickly tolerated without additional risk. Regardless of the injection speed and underlying renal impairment, Gd-DTPA demonstrated a favourable safety profile after intravenous administration of diagnostic doses to patients of all age groups. 1-2% was determined to be the overall incidence of adverse events following intravenous administration of 0.1 or 0.2 mmol Gd-DTPA/kg body weight.

39.The poly (lactic-co-glycolic acid) (PLGA) microbubbles loaded with Gd-DTPA were created by **Meng Ao et al., (2009)** for MRI and ultrasound imaging. Gadolinium diethylenetriamine penta acetic acid (Gd-DTPA) and fluorocarbon-filled microbubbles were

employed to create a contrast agent, and a biodegradable high-molecular-weight poly (lactic-co-glycolic acid) (PLGA) was used as the encapsulating medium. They evaluated the shape, dimension, and Gd loading capability of PLGA microparticles. After the contrast agent was injected into rabbits, the liver parenchyma and hepatic vessels were imaged in vivo to determine the contrast agent's effectiveness for ultrasound and magnetic resonance (MR) imaging. Moreover, there is a favourable correlation between the concentrations of Gd-DTPA encapsulated and the increase in signal intensity and relaxation properties. Further tests using in vivo imaging showed that the Gd-PLGA contrast agent also improved in vivo MR and ultrasonic imaging.

40. A hepatobiliary contrast agent for MR imaging that **Gabriele Schuhmann-Giampie et al., (1992)** have studied is called Gd-EOB-DTPA. As a paramagnetic contrast agent, they introduced Gd-DTPA covalently coupled to the lipophiic ethoxybenzyl (EOB) moiety (Gd-EOB-DTPA), which has high T1 relaxivity and high in vivo complex stability as well as good tolerance and strong hepatobiliary specificity. It has been shown to have high hepatic uptake, high T1 relaxivity, good tolerance, and high in vivo stability. According to MR imaging, Gd-EOB-DTPA is enabled for the precise delineation of the bile ducts and of tiny liver tumours.

41. In order to develop biodegradable blood-pool MRI contrast agent **Xiaoxia Wen, et al., (2004)** manufactured and analysed poly (L-glutamic acid) (PG) gadolinium chelates. With the aid of difunctional and monofunctional DTPA precursors, two PG chelates of gadolinium diethylenetriaminepentaacetic acid (Gd-DTPA) were created. The molecular weight and molecular weight distribution, gadolinium concentration, relaxivity, and degradability of the conjugates were all characterised. By injecting ^{111}In-labeled polymers intravenously into mice carrying murine breast cancers, it was possible to map the distributions of the polymeric MRI contrast agents in various organs. PG-Bz-DTPA-Gd is an advantageous macromolecular MRI contrast agent due to its capacity to be eliminated from the body.

42. The creation of a novel gadolinium compound with a lipophilic moiety was reported by **Luciano Lattuada et al., (2003)**. It's the first time a Gd-DTPA complex has been

joined to cholesterol. The process of creating the pentaester is simple and basic, and it makes use of the extremely valuable bifunctional pro-chelating agent that was combined with cholesteryl chloroformate. The DTPA-cholesterol ligand was produced by deprotecting this with formic acid at 100°C, and it was then reacted with gadolinium chloride to produce the desired complex in an overall yield of 50%.

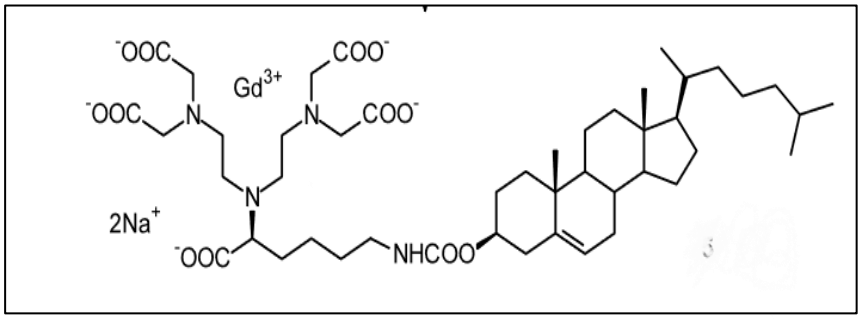

Fig 2.1: Gd-DTPA-cholesterol

43.For better MRI of melanomas in local lymph nodes, tissue-specific drugs are needed. Given that a significant enhancement effect was shown in nude mice with melanoma xenografts**, D. Shahbazi-Gahrouei et al., (2001**) have demonstrated that MRI with Gd-DTPA-9.2.27 gives the benefit of tissue contrast enhancement and precise anatomic localization of the tumours. Gd-TCP (Gd-tetra-carboranylmethoxyphenyl-porphyrin) can also be utilised as a radiation sensitizer for NCT and as a dual probe for an MRI contrast agent. This might make it easier to find tumours and arrange treatments, and it might help radiation oncologists and radiologists diagnose and define the radiation treatment field.

44. Regarding longitudinal and transverse relaxivities in mouse blood plasma, concentration detection limits in vitro, and in vivo contrast-enhanced MR imaging (CE-MRI) in mice, **Sander Langereis et al., (2005**) studied various generations of Gd (III)DTPA-terminated poly (propylene imine) dendrimers and reference Gd (III)DTPA complex. With increasing molecular weight, Gd (III)DTPA-terminated poly (propylene imine) dendrimers exhibit higher T_1 and T_2 relaxivities. The blood plasma relaxivity findings are in good agreement with earlier studies made in citrate buffer, demonstrating that these dendritic contrast agents little interact with the proteins in blood plasma. These dendritic contrast compounds are particularly suited for imaging of blood vessels smaller than one millimetre and analysing

tumour microcirculatory features in mice. The kidneys were found to remove even the largest MRI contrast agent, ^{64}Gd (III) ions.

45. Magnetic resonance imaging (MRI) contrast agents were created using biocompatible polysuccinimide (PSI) derivatives coupled with gadolinium diethylenetriaminepentaacetic acid (DTPA-Gd). In this study, **Ha Young Lee et al., (2006**) created PSI derivatives with DTPA-Gd as the contrast agent, methoxy-poly (ethylene glycol) (mPEG) as the hydrophilic ligand, and hexadecylamine as the hydrophobic ligand. The compounds have been put to the test to see if they might work as carriers and contrast agents. In comparison to commercially available products, the produced micelles demonstrated an increase in MRI contrast over five times in vitro. According to these findings, PSI conjugates with mPEG, a hydrophobic ligand, and DTPA-Gd may be used as carriers and contrast agents because of their biocompatibility, high stability, and effective contrast imaging.

46. Gadolinium-diethylenetriamine pentaacetic acid-deoxyglucosamine (Gd-DTPA-DG), which is a d-glucosamine metabolic MR imaging contrast agent, was synthesised by **Wei Zhang et al. in 2010.** The drug produced good T_1 and visual enhancement of the tumour by MR imaging in vitro and utilising a human lung cancer xenograft animal model in vivo. After administering Gd-DTPA-DG, the imaging of cancer structures remained improved for 2 hours. Gd-DTPA-DG has a longer retention time in tumour tissue compared to the standard contrast agent and more accurately depicts the elevated level of tumour cell metabolism compared to normal tissues. The application of Gd-DTPA-DG holds considerable potential for the early monitoring of original tumours, the detection of tumour metastasis, and the detection of tumour recurrence.

47.**Guoying Sun et al., (2003)** used Gadolinium-diethylenetriaminepenta-acetic acid (Gd-DTPA) to synthesise and analyse macromolecular conjugates of two different types of natural polysaccharides, those from Panax quinquefolium linn (PQPS) and Ganoderma applanatum pat (GAPS), which had better T_1 -relaxivity. The in vitro stability of these two macromolecular contrast agents is good. In contrast to the albumin-based product, the

hydrolysable linkages between Gd-DTPA and the polysaccharide backbone speed up the compound's metabolism and elimination in vivo.

48. In order to create nanodiamond (ND) particles with an organogadolinium moiety added chemically for use as an MRI contrast agent, **Takako Nakamura et al. (2012)** have established a straightforward and practical procedure. The condensation of ND with diethylenetriaminepentaacetic acid (DTPA), followed by treatment with $GdCl_3$, was used to add the organogadolinium moiety to the surface of the ND particles. The high signal strength of the Gd-DTPA-ND particles was seen in MRI experiments on T_1-weighted images. These particles had a strong signal intensity on the T_1-weighted MRI images that were produced. This alteration has the benefit of being simple to handle and makes it possible to create Gd-DTPA-ND particles from the initial ND samples in two straightforward steps for future practical manufacturing. A promising new MRI agent are the modified ND particles.

49. The objective of **Amber L. Doiron et al., (2007)** study was to produce polymeric particles of a small size with a high loading of gadolinium (III) diethylenetriaminepentaacetic acid (Gd-DTPA) and show their utility for MRI. To concentrate the MRI agent at an imaging site, a poly(lactide-co-glycolide) (PLGA) or polylactide-poly (ethylene glycol) (PLA-PEG) particle was created using a water-in-oil-in-oil double emulsion solvent evaporation technique. It was possible to produce PLGA particles with two different average sizes of 1.83 m and 920 nm as well as PLA-PEG particles with a mean diameter of 952 nm. Upto 30% wt of Gd-DTPA could be loaded, and a 5-hour in vitro release time was achieved. The polymeric contrast agent formulation's capacity to produce contrast was comparable to that of Gd-DTPA by itself. These findings show the potential value of the polymeric particles loaded with contrast agents for MRI plaque detection.

50.**Abishek Gupta et al., (2013**) described the incorporation of Gd (III) chelated DTPA amphiphiles with an oleyl chain (Gd-DTPA-MO) in the self-assembly matrix of glycerol monooleate (GMO), an inverse cubic phase forming system, at various compositions. The potential for the dispersed colloidal nanoassemblies to serve as an MRI contrast agent was investigated. At both low and high magnetic field strengths, all of the colloidal dispersions

showed improved longitudinal relaxivities per Gd compared to Magnevist, a contrast agent that is commercially available. It is reasonable to anticipate orders of magnitude higher relaxivity per supramolecular nanoassembly given the substantial payload of Gd-chelates per cubosome. Moreover, cubosomes with broad water channels, 3D-periodic internal nanostructures, and high interfacial surface area demonstrated potential as high field contrast agents. These stable colloidal particles may potentially be employed as dual-purpose delivery matrices for medicines and diagnostics.

51. The self-assembly of Gd (III) chelated DTPA-monophytanyl (Gd-DTPA-MP) amphiphiles contained within phytantriol (PT), an inverse bicontinuous cubic phase generating matrix, was described by **Abhishek Gupta et al., (2015).** At various magnetic field intensities, the dispersed colloidal nanoassemblies were assessed as prospective MRI contrast agents. All of the dispersions were subjected to in vitro relaxivity tests, and the results were contrasted against Magnevist, a readily accessible contrast agent. In comparison to Magnevist, all of the dispersions displayed much higher relaxivities at both low and high magnetic field strengths. With the same Gd concentration and 11.74 T, it was discovered that the image contrast of the nano assemblies was significantly better than Magnevist. Also, under high magnetic fields, the Gd-DTPA-MP/PT dispersions outperformed the pure Gd-DTPA-MP dispersion in terms of relaxivities.

52.**Enik Molná et al. (2014)** reported the synthesis of the ligand Hnompa (6-((1,4,7-triazacyclononan-1-yl) methyl) picolinic acid) and a thorough description of the Mn^{2+} complexes generated by this ligand, as well as the related ligands Hdompa (6-((1,4,7,10-tetraazacyclododecan-1-yl)methyl)picolinic acid. In aqueous solutions, these ligands create thermodynamically stable complexes. The results of this research also demonstrate the challenges in predicting the solution structure of Mn^{2+} complexes with polyaminocarboxylates because of the metal ion's symmetrical high-spin d^5 configuration. Yet, in solution, the metal ion is six-coordinated by the pentadentate ligand and an inner-sphere water molecule, contrary to the solid state where the Mn^{2+} complex of Nompa was discovered to be seven-coordinated.

53. **Bohuslav Draho˘s et al., (2011)** described although Mn^{2+} complexes are not all kinetically labile, the dissociation kinetic analysis of $[Mn(dota)]^{2-}$ and $[Mn(nota)]^{-}$ revealed unexpectedly high kinetic inertness. The saturation of the coordination sphere of Mn^{2+} solely by the ligand donor atoms (no inner-sphere water) can also contribute to this kinetic inertness,

in addition to the complex's great thermodynamic stability. In both experimental and physiologically relevant conditions, the dissociation is significantly pH-dependent and occurs 15 times more quickly for $[Mn(nota)]^-$ than for $[Mn(dota)]^{2-}$ This difference is due to the higher predicted rate constants for both spontaneous and proton-assisted dissociation. For $[Mn(dota)]^{2-}$, the influence of the dinuclear complex formation is more important; this is also demonstrated by the stability constant of its Mn^{2+} -L-Zn^{2+} combination, which has a value that is 20 times greater. DOTA-type ligands are excellent agents for the creation of Mn^{2+} based MRI probes due to the strong kinetic inertness of $[Mn(dota)]^{2-}$

54. Using the method **Rocío Uzal-Varela et al., (2022)** used for Gd, they made use of the vast amount of published stability constant data to construct quantitative structure-stability correlations to forecast stability constants. Notwithstanding recognised variations in experimental stability constants caused by the use of various ionic fluids and ionic strengths, the empirical relations reported are very precise. This study's prediction of the coordinated ligand's denticity when multidentate ligands are employed, for example, $[Mn(DOTA)]^{2-}$'s eight-coordinate Mn(II) (confirmed by X-ray crystallography), whereas the projected stability constant for $[Mn(DTPA)]^{3-}$'s seven-coordinate Mn(II), is fascinating. Their method also helps to spot potentially inaccurate published stability constant data. This method permits the prediction of stability constants and the ability to disqualify the synthesis of potentially inferior complexes for the development of innovative Mn (II) complexes. Last but not least, the quantification of many structural characteristics like the type of chelate ring or the donor atom enables the building of novel complexes that may have the best stability. This work's technique requires stability constant data for certain donors or ligand archetypes, which is a restriction. It therefore does not account for novel chelators like bispidines. However, once stability constant information is gathered for a few samples, these kinds of ligands can be added to the model.

55. **Maxim L. Belyanin et al., (2016)** discussed the initial synthesis and assessment of a brand-new Mn (II) complex (DTPA-PPDA Mn (II)) that has a C-15 fatty acid moiety that has a strong affinity for the heart muscle. According to quantum chemistry technique, the complexation energy of DTPA-PPDA Mn (II) is essentially greater than that of the known DTPA Mn (II) complex. DTPA-PPDA Mn (II) complex has a lower rate of decomposition because it is more stable than the DTPA-Mn (II) complex that was previously examined. To give good relaxometric qualities, the interior sphere comprises two water molecules. The b-oxidation of DTPA-PPDA Mn (II) can occur when it is successfully transported to the mitochondrial membrane, according to molecular docking simulations. The proposed

combination has a far higher affinity to the heart-type transport protein H-FABP than lauric acid, according to molecular docking. The developed contrast agent offers MR imaging equivalent to gadopentetic acid in phantom studies in low-field MRI.

56. CMCS-$(Mn\text{-}DTPA)_n$, a biocompatible macromolecular MRI contrast agent based on O-carboxymethyl chitosan (CMCS), was developed and synthesised by **Xianghui Wang et al., (2018)** . In aqueous solution, the relaxivity of CMCS-$(Mn\text{-}DTPA)_n$ is about 3.5 and 5.5 times higher than that of Gd-DTPA and Mn-DPDP, respectively. At the dose required for MRI imaging, CMCS-$(Mn\text{-}DTPA)_n$ exhibits good cellular and blood biocompatibility. With a dose of 0.03 mM Mn/kg b.w. CMCS-$(Mn\text{-}DTPA)_n$ accompanied by a lengthy effective imaging window, Sprague Dawley (SD) rats' MRI signal intensity in the kidney and liver is dramatically increased.

57. $[Tb_2L_6\ (H_2O)_2]_2$ (1), $[Tb_2L_6\ (H_2O)]\ H_2O$ (2), and $Tb[(phen)_2L_2(H_2O)_2]\ 4H_2O$ phenL (3) are three novel rare earth p-aminobenzoic acid complexes. (HL: p-aminobenzoic acid; phen: 1, 10-phenanthroline) are described in a variety of structural configurations by **Chao-Hong Ye (2004).** A polymolecule called Complex 1 has a two-dimensional plane structure. Whereas compound 3 looks to be a mononuclear complex, compound 2 is a binuclear molecule. In contrast to 1, which has just one coordination water molecule, 2, which has two, exhibits greater fluorescence intensity, fluorescence lifetime, and emission quantum yield. In the context of common fluorescent rare earth complexes, this is a unique phenomenon. The fluorescence performance of complex 3 is the least desirable of the three. These crystal structures show that the coordination mode of the ligand plays a significant role in influencing the luminescence properties of a fluorescent rare earth complex.

58. By enhancing the lesion-to-liver contrast, liver-specific contrast agents (CAs) can enhance the Magnetic resonance imaging (MRI) identification of focal and diffuse liver lesions in terms of a liver-specific MRI contrast agent, a novel Mn (II) complex, Mn-BnO-TyrEDTA by **Keyu Chen et al., (2021)** which outperforms Gd-EOB-DTPA. This complex has a lipophilic group-modified ethylenediaminetetraacetic acid (EDTA) structure as a ligand to control its behaviour in vivo. Mn-BnO-TyrEDTA can be rapidly taken up by hepatocytes with a combination of hepatobiliary and renal clearance pathways, according to a mouse MRI research. The mechanism of hepatic targeting of Mn- BnO-TyrEDTA was confirmed by studies on bromosulfophthalein (BSP) inhibition imaging, biodistribution, and cellular uptake to be

the hepatic uptake of the amphiphilic anion contrast agent mediated by organic anion transporting polypeptides (OATPs) expressed by functional hepatocytes.

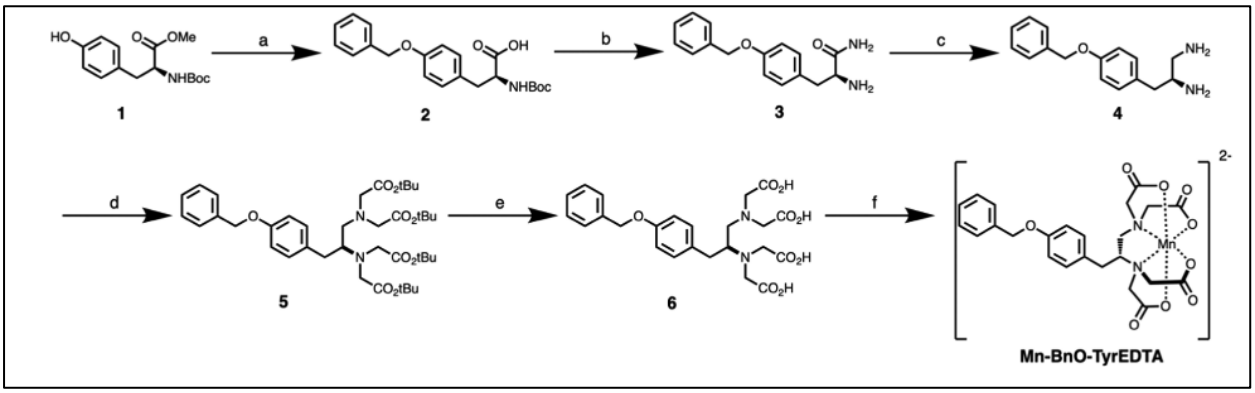

Fig 2.2: Synthesis Procedure of the Mn-BnO-TyrEDTA Complex

59. By conjugating ethylene diamine tetraacetic acid (EDTA) to one or more C20 isoprenoid-type chains (phytanyl) via an ester link, chelating amphiphiles of EDTA have been created by **Minoo J. Moghaddam et al., (2010)**. Many metal ions, including transition metal ions and paramagnetic metal ions like manganese (Mn) and gadolinium, can be sequestered by EDTA-mono and bis phytanyl (EDTA-MP and EDTA-BP) (Gd). In the solid state and as hydrated lyotropic liquid crystalline phases, ordered self-assembled structures of both amphiphiles and their metal complexes were investigated. Whereas its Mn complexed conjugate showed an ordered lamellar phase with molten chains, the bis-phytanyl conjugate showed a less ordered structure. Low field NMR measurements were used to analyse the contrast agents (CAs) for magnetic resonance imaging that were dispersed Mn and Gd complexed particles. Compared to Mn-EDTA and Gd-EDTA, respectively, Mn and Gd complexed nanostructured particles showed improved relaxivity. These chelating amphiphiles have the potential to be used as MRI contrast agents due to the creation of highly ordered nanostructured self-assembled materials and their capacity to bind a range of metal ions, including paramagnetic metal ions.

60. For usage as a liver-specific MRI contrast agent with excellent chelation stability, a new manganese (II) complex (Mn-EDTA-BTA) based on an ethylene- diaminetetraacetic acid (EDTA) coordination cage containing a benzothiazole aniline (BTA) moiety was developed and produced by **Md. Kamrul Islam et al., (2017).** This novel Mn chelate was quickly absorbed by liver hepatocytes, formed a hydrophilic, stable complex with $Mn^{2+,}$ and was then eliminated by the kidneys and biliary system. The compound has much higher kinetic inertness and R_1 relaxivity than mangafodipir trisodium (MnDPDP), a therapeutically approved liver-specific MRI contrast agent. The high-sensitivity tumour detection in an animal model of liver cancer served as a demonstration of the novel Mn complex's diagnostic value in MRI.

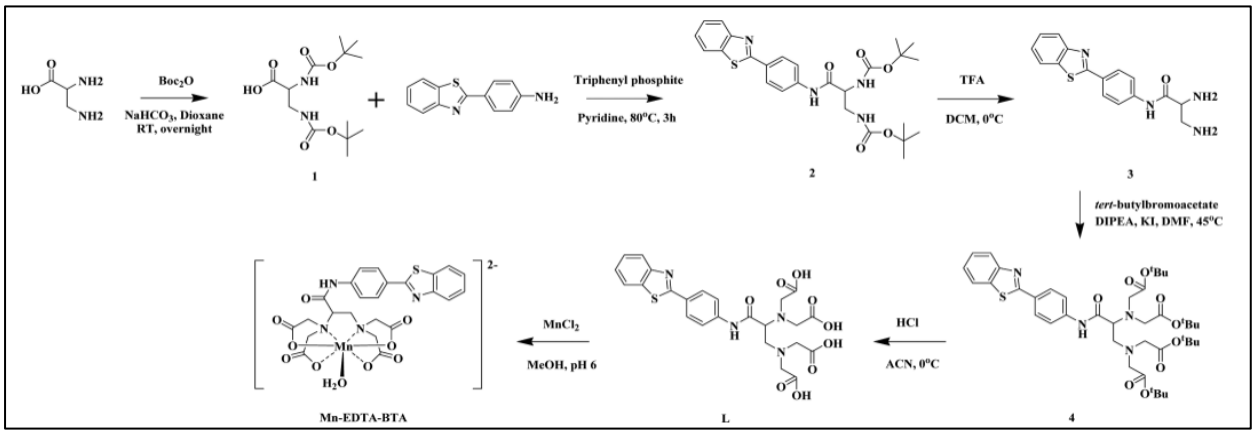

Fig 2.3: Synthesis of Mn-EDTA-BTA

61. **Joan F. Carvalho et al., (1992**) produced a number of macrocyclic DTPA and EDTA bis(amide) derivatives. Potentiometric titrations were used to determine the protonation constants, Gd^{3+} complex stability constants, and Zn^{2+} complex stability constants of these ligands. The DTPA bis(amide) macrocycle series' stability constants for the Gd^{3+} complexes rise as the ring size increases, showing the increased involvement of the amide carbonyl oxygens in metal ion coordination. On the other hand, there is no clear pattern in the stability constants of the Zn^{2+} complexes over the course of the series. The difference between the logarithmic stability constants of Gd(EDTA-DAM) and Zn(EDTA-DAM) is 6.12, which is the logarithmic selectivity constant of the 15-membered EDTA-DAM ligand for Gd^{3+} over $Zn^{2+.}$

62. The following ligands were employed by **Steven T. Frey et al., (1993)** to create solution complexes, which were then characterised using Eu^{3+} luminescence spectroscopy: 4,10,13-tris(carboxymethyl1)-8,15-dioxo-1,4,7,10,13 penta azacyclo pentadecane(edta-dam); 1,4,7-tris(carboxymethyl)-9,14-dioxo-1,4,7,10,13-pentaazacyclopentadecane(dtpa-eam);

1,4,7-tris(carboxymethyl)-9 (piperazine do3a-dimer). The Eu^{3+} complex is seen in a single isomeric state with each ligand. Whereas bis(dtpa-eam) and the do3a-dimer create 2:1 stoichiometric metal-ligand complexes, edta-dam, dtpa-eam, and dtpa-oam form stoichiometric metal-ligand complexes at a 1:1 ratio. The dtpa-eam, dtpa-oam, and edta-dam Eu^{3+} complexes have their formation constants measured. Competition experiments for dtpa-eam, dtpa-oam, and edta-dam were used to measure the relative formation constants for the other lanthanide series members. For each ligand's Eu^{3+} complex, it was calculated how many water molecules were coordinated. In dinuclear complexes of bis(dtpa-eam) and the piperazine do3a-dimer, inter-metal ion energy transfer between the Eu^{3+} ion and many other coordinated lanthanide ions has been seen. Molecular mechanics calculations and the number of coordinated water molecules discovered from excited-state lifetime measurements in H_2O and D_2O were used to make deductions about the makeup of the initial coordination sphere of the Eu^{3+} ion.

63. The large spin number, extended electronic relaxation period, and labile water exchange are only a few of the beneficial characteristics of the manganese (II) ion that suggest prospective applications as an MRI contrast agent. A novel Mn (II) complex (MnL1) based on EDTA is designed, synthesised, and evaluated by **Jeffrey S. Troughton et al., (2004)**. The complex also includes a moiety that noncovalently binds serum albumin, the same moiety found in the gadolinium-based contrast agent MS-325. Measurements of ultrafiltration albumin binding at 0.1 mM, pH 7.4, and 37°C showed that the complex binds to plasma proteins well. Imaging at 1.5T was used to validate the Mn (II)-based contrast agent. MnL_1 distinguished between healthy tissue and areas of vascular damage, clearly defining both arteries and veins in a rabbit model of carotid artery injury. High-resolution imaging of blood arteries was made possible by binding to serum albumin, which also retained the complex in the bloodstream. Images with a strong contrast-to-noise ratio were captured in a rabbit model, making it possible to discern between healthy and wounded arteries caused by stenosis and inflammation. Although there was no acute cardiotoxicity seen, more research on in vivo stability and toxicity is required.

64. As possible "smart" magnetic resonance imaging contrast agents, three novel Gd DO3A-type bis macrocyclic complexes were created and conjugated to Ca^{2+} chelating molecules such ethylenediamine-tetraacetic acid and diethylenetriamine pentaacetic acid bisamides by **Anurag Mishra et al., (2007).** Using relaxometric titrations, their sensitivity to Ca^{2+} was investigated. For Gd_2L_1, Gd_2L_2, and Gd_2L_3, respectively, a maximum relaxivity

increase of 15, 6, and 32% was seen upon Ca2+ binding (L 1) N,N-bis {1-[{[({1-[1,4,7-tris(carboxymethyl)-1,4,7,10-tetraazacyclododecane-10-yl]eth-2-yl}amino)carbonyl] -methyl}-(carboxymethyl)amino]eth-2-yl}aminoacetic acid; L2) N,N-bis[1-({[({R-[1,4,7-tris(carboxymethyl)-1,4,7,10- stetraazacyclododecane-10-yl]-p-tolylamino}carbonyl)methyl]-(carboxymethyl)}amino)eth-2-yl]aminoacetic acid; L3) \s1,2-bis[{[({1-[1,4,7-tris(carboxymethyl)-1,4,7,10-tetraazacyclododecane-10-yl]eth-2-yl}amino)carbonyl]methyl}-s(carboxymethyl)amino]ethane). A combined nuclear magnetic relaxation dispersion (NMRD) and ^{17}O NMR investigation was used to evaluate the factors affecting the proton relaxivity of the Gd^{3+} complexes. Compared to GdL_3, water exchange is slower on Gd_2L_1 and Gd_2L_2. It is concluded that the increase in relaxivity that was observed after the addition of Ca^{2+} can be mostly attributed to the rise in hydration number and, to a lesser extent, to the rigidification of the complex that Ca^{2+} causes.

65. **Dong-Sheng Liu et al., (2011)** designed a reaction of $MnCl_2 .4H_2O$ and H_4edta under hydrothermal conditions produced a new Mn(II) complex, $[Mn_2 (edta)(H_2O)]_n .nH2O$ (1) (H_4edta = ethylenediaminetetraacetic acid), which was characterised by single-crystal X-ray diffraction study, variable temperature (1.8-300 K) magnetic measurement, and thermal gravity analysis. Complex 1 is the first two-dimensional (2D) Mn-edta coordination polymer with a grid-like (4,4) structure, according to the results of X-ray crystallographic research. It is composed of Mn-carboxylate chains and fully deprotonated edta4 ligands with a maximum denticity. Complex 1 exhibit substantial antiferromagnetic coupling, according to the changing temperature magnetic data. With a maximum denticity of twelve and using all 10 donor atoms for coordination, the edta4 coordination fashion—rarely observed—is discovered in 1. Complex 1 has high antiferromagnetic couplings, according to magnetic studies.

66. A novel tetranuclear lead-edta compound $[Pb_4(edta)(H_2O)_2 (N_3)_4]_n$ (1) (H_4edta = ethylenediaminetetraacetic acid) has been synthesised by the reaction of PbF_2 with H_4edta and NaN_3 mixed-ligands under hydrothermal conditions, and was characterised by elemental analysis, thermal analysis, luminescence, powder X-ray diffraction\sand single-crystal X-ray diffraction. According to the findings of X-ray crystallography, compound 1 is the first 3D Pb(II)-edta coordination polymer with a significant lead content. Surprisingly, the edta4 ligand utilises all 10 of its donor atoms (8 O & 2 N) to couple to Pb (II) ions and create a 2D layer. The inorganic chain $[Pb_5(N_3)_{10}]_n$ connects the complicated 3D coordination polymer to the 2D layers further. According to calculations using time-dependent density functional theory (TDDFT), the mechanism of fluorescence emission for compound 1 is mostly caused by

ligand-to-metal charge transfer (LMCT), which is in good accord with its fluorescence spectra and crystal structure. According to optical absorption spectra, material 1 can be employed as a broad optical band-gap semiconductor material since it has wide optical band-gaps.

67. Gd(III)-complexes have been used as MRI contrast agents for more than 25 years. Considerations regarding the potential toxicity of remaining gadolinium in patients with severe kidney disorders have prompted researchers to consider alternative approaches, like Mn(II)-complexes, to shorten T1 and obtain good image contrast over the past ten years. In this study, **S. Baroni et al., (2016)** described the synthesis of a novel Mn (II)-chelate with a deoxycholic acid residue that has been specifically engineered to interact reversibly with serum albumin and increase the typically low relaxivity associated with Mn (II)-complexes. Its thorough relaxometric research and investigation of albumin binding behaviour revealed exceptional features, suggesting its potential application as an MRI blood pool agent. The strong reversible binding of this unique conjugate to HSA increases the Mn (II)-complex's relaxivity value in human serum to a re-markable value of 32.72 mM^{-1} s^{-1} (298 K, 20 MHz). These outcomes highlight the importance of this HSA-targeting strategy in the development of effective and safe MRI blood pool agents.

68. The compounds in the title, $(NH_4)_2$ [Mn II (edta)(H_2O)] $(NH_4)_2$ [Mn II (cydta)(H_2O)], 3H2O (H_4 edta = ethylenediamine-N,N",N'"- tetraacetic acid), K_2 [Mn II (Hdtpa)] and $4H_2O$ (H_4 cydta = trans-1,2-cyclohexanediamine-N,N',N",N""-tetraacetic acid). $5H_2O$ (H 5 dtpa = diethylenetriamine-N,N,Nc,Ns,Ns-pentaacetic acid) were synthesised by **X.F. Wang et al., (2008)** their compositions and structures were determined using the single-crystal X-ray diffraction technique and elemental analysis. The Mn^{2+} ions are all seven-coordinated and arranged in a pseudo-monocapped trigonal prismatic shape in these three complexes. In the P-1 space group, the triclinic system crystallises all three complexes. The three complexes use a pseudo-monocapped trigonal prismatic structure with seven coordinates. There is a free, uncoordinated carboxyl group present in the K_2 [MnII (Hdtpa)] complex. In contrast, the Mn^{2+} ion is coordinated with an edta or cydta ligand and an extra water molecule in the complexes with edta and cydta. The three complexes all have layered crystal structures, and the isolated chemicals are all water-soluble.

69. A new dimeric manganese (III) porphyrin (MnP_2) was examined in vitro and in vivo as a potential gadolinium-free blood-pool agent by **Weiran Cheng et al.** in the year **2021**. The

researchers showed through numerous spectroscopic studies that MnP_2 strongly binds to Human Serum Albumin (HSA). On HSA binding, MnP_2 shows a moderate relaxivity reduction. Yet, MnP_2 -HSA has a molar relaxivity at 3T that is twice that of the gadofosveset-HSA complex due to the distinct field-dependent relaxation behaviours and the dimeric design (two Mn (III) ions per complex). All of these findings showed that MnP_2 is a novel class of gadolinium-free blood-pool agents that can be used in both low-field and high-field applications. In both in vitro and in vivo tests, it functioned as a potential dual MR contrast enhancer with T1- and T2-weighted contrast capabilities.

70. **Kenneth N. Raymond et al., (2004)** reviewed that due to their increased number of coordinated water molecules and nearly ideal water exchange rates—which are several orders of magnitude faster than those of commercial agents—hydroxypyridinone-based Gd (III) complexes demonstrated noticeably better relaxivities. The NMRD profiles, which often exhibit a peak in relaxivity at high magnetic fields while the relaxivities of commercial agents drop, reflect this ideal m. The nine-coordinate intermediate is near in energy to the eight-coordinate ground state, and as a result, this mechanism leads to the quick water exchange. By attaching lengthy poly (ethylene glycol) chains to the pendant acid of a mixed hydroxypyridinone terephthalamide complex, this exchange rate can be further adjusted. In comparison to current commercial products, these complexes exhibit higher thermodynamic stability and the ligands are more selective for Gd (III) than physiologically accessible cations like Ca (II) and Zn (II).

71. Iodinated and gadolinium- (Gd) based CT and MRI contrast media are not routinely used in individuals with renal impairment due to safety concerns. Contrast media that can be used in situations where renal impairment exists are desperately needed, as an estimated 14% of the US population suffers from chronic kidney disease (CKD). As a Gd substitute, **Eric M. Gal et al.,** provide the novel manganese (II) complex $[Mn(PyC_3A)(H_2O)]$. At pH 7.4, $[Mn(PyC_3A)(H_2O)]^-$ is one of the Mn(II) complexes with the highest stability (log KML = 11.40). $[Mn(PyC_3A)(H_2O)]^-$ is 20 times more resistant to dissociation than $[Gd(DTPA)(H_2O)]$ in the presence of 25 mol equiv. Zn at pH 6.0, 37 °C. Blood plasma's $[Mn(PyC_3A)(H_2O)]^-$ has a similar relaxivity to commercial Gd contrast agent .$[Mn(PyC_3A)(H_2O)]^-$ clears via a mixed renal/ hepatobiliary pathway with >99% clearance by 24h, according to biodistribution study. In order to create a bifunctional chelator, $[Mn(PyC_3A)(H_2O)]^-$ was modified, and Mn-FBP was created by conjugating 4 chelates to a peptide that targets fibrin. With a K_d of 110 nM, Mn-FBP binds the soluble fibrin fragment DD(E). When fibrin is present, Mn-per-Mn FBP's

relaxivity increases by 60% and is 4-times larger than $[Mn(PyC_3A)(H_2O)]^-$, which is consistent with binding. No indication of dechelation is seen in the examination of Mn metabolites, and the probe was >99% removed after 24 hours. The imaging probe $[Mn(PyC_3A)(H_2O)]^-$ is a leading contender for use in individuals with impaired renal function.

72. **Fu – Xian – Van et al., (2016)** used an acylation procedure to incorporate 2-hydrazino-6-methoxy-1,3-benzothiazole into diethylenetriamine pentaacetic (DTPA). By treating this ligand with $GdCl_3$. $6H_2O$, the corresponding non-ion Gd(III) complex that holds promise as a single molecule magnetic resonance imaging (MRI) contrast agent was produced. By measuring the longitudinal relaxivity (r_1), the effectiveness of the contrast agent was determined. The r1 of Gd(III)-DTPA-bisbenzothiazole hydrazide was up to 6.44 $mM^{-1}s\text{-}^{1}$, which was 1.8 times higher than that of the commercially available analogous MRI contrast agent Gd(III)-DTPA (r_1 = 3.64 $mM^{-1}s^{-1}$). Also, Gd(III)-DTPA-bisbenzothiazole hydrazide significantly improved signal contrast compared to Gd(III)-DTPA in in vitro MR images under a 0.5 T magnetic field. These findings show that this Gd(III) non-ion complex functions as a possible MRI contrast agent.

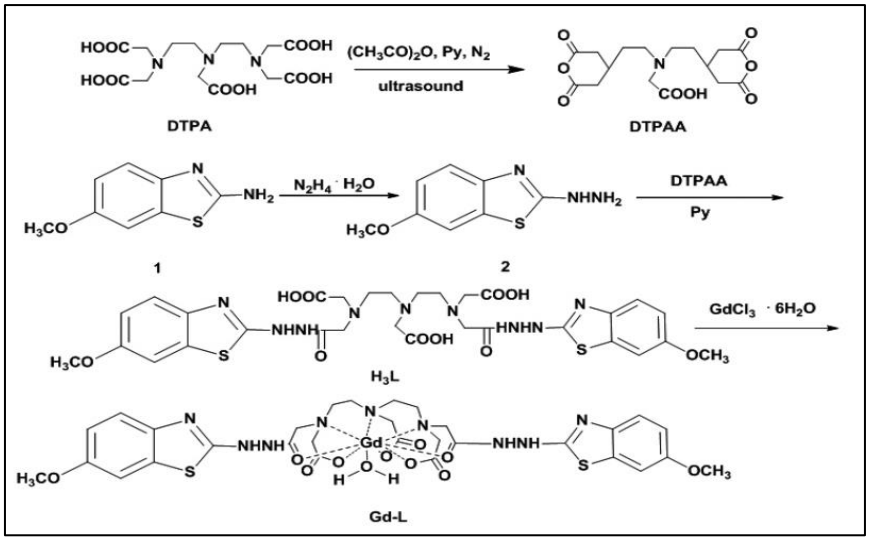

Fig 2.4: Synthesis of ligand(H_3L) and complex (Gd (III)-L)

73. By using the condensation reaction between DTPA bis(anhydride) and either 5-aminouracil or 5,6-diamino-uracil, **Alexandra S. Georgopoulou et al. (1999)** created two novel DTPA (diethylenetriaminepentaacetic acid) functionalised bis(amides) with pendant uracil moieties. These ligands are an example of the growing class of ligands that can join complementary organic bases in triple hydrogen bonds. These ligands, however, are distinct because they combine with various metal ions to generate water soluble complexes. The two

DTPA-uracil ligand syntheses, seven metal complexes, and the crystal structure of the bismuth complex of DTPA bis(4,5-diamino-6-hydroxy-2-mercaptopyrimidine) L1 are all reported in this article. The two arms on which the uracil moieties are located have a significant degree of rotational mobility in this solid state structure, which enables these groups to make numerous hydrogen bonds involving both uracil moieties on one side of the molecule.

74. **Dapeng Hao, MD, et al., (2012)** reviewed that the use of GBCAs in clinical MR scans is common. Because to the variances in their chemical structures, each GBCA differs in terms of in vitro and in vivo stability, colligative characteristics, osmolality, viscosity, protein binding capacity, and excretion patterns. Other than NSF, there is currently no discernible pattern of significant differences in the frequency or nature of adverse responses across the nine GBCAs. Patients who use Gd-DTPA-BMA, Gd-DTPA-BMEA, and Gd-DTPA are more likely to get NSF, a significant late adverse event. The most stable GBCAs, the macrocycles, are advised for use in individuals with kidney disease. Three NSF cases, while admittedly a very small number, have also been reported after the use of two of the macrocyclic contrast agents. Whether or not to give GBCAs to expectant moms, nursing mothers, and paediatric patients should be carefully considered. Physicians can safely produce high-quality contrast-enhanced MR images by being aware of the properties, stability, and safety of GBCAs.

75. **Bohuslav Drahos et al., (2012)** in their analysis consistently identifies patterns in how the donor-acceptor properties, rigidity of the ligand scaffold, and ligand structure affect the thermodynamic, kinetic, and redox stability of the Mn^{2+} complex. Relativly little can be predicted about the complexes' ability to relax, as measured by their relaxivity, water-exchange rate, and sometimes even their hydration number. Generally, for known Mn^{2+} complexes, the k_{ex} values range within three orders of magnitude. When assessing activation volumes, the mechanism of water exchange is typically associatively activated for complexes with six coordinates and dissociatively activated for chelates with seven coordinates. The hydration number largely determines the relaxivity of Mn^{2+} chelates: monohydrated EDTA-derivative complexes exhibit twice as low relaxivities as bishydrated ones, and even lower values were found for the non-hydrated complexes of DTPA and DOTA.

76. **MICHAEL MAGERSTA et al., (1986)** reviewed different methods have been devised for obtaining gadolinium(III)complexes of the ligands NOTA (1,4,7-triazacyclononane-N,N',N''-triaceticacid), DOTA (1,4,7,10-tetraazacyclododecane-\sN,N',N'',N'''-tetraaceticacid), TETA (1,4,8,11-tetraazacyclotetradecane-N,N',N'',N'''-

tetraacetic acid), and DTPA (diethylenetriaminepentaacetic acid) as solids for use as pharmaceuticals. Investigations have been done into how effective they are as relaxation agents for spectroscopy or as in vitro and in vivo contrast agents for NMR imaging. Studies on serum stability and the measurement of stability constants demonstrated that the Gd (DOTA) complex is a more stable compound than the Gd (DTPA). After injection of Gd (DOTA) and Gd, NMR images of tumours developed in athymic mice were obtained (DTPA).

77. **Daniel D. Schwert et al., (2002)** reviewed that for the past ten years, research has been conducted on contrast agents for magnetic resonance imaging based on metal ions other than gadolinium (III), such as manganese (II), manganese (III), iron (III), and copper (II). Despite the fact that these metal ions' inherent characteristics tend to make them less desirable than gadolinium (III)-based agents, the extensive body of literature on their biology has enabled the development of workable contrast agents. In animal models, both non-specific and specific medicines have been developed and evaluated. Specific agents have been developed and tested for organs such the liver, pancreas, adrenals, malignant tumours, and even the interiors of cells and neuronal tracts. (FerriSeltz®) are offered for human use in clinical settings. This article talks about the toxicity, relaxivity, image enhancement, and tissue specificity of several drugs.

78. A novel neutral gadolinium compound has been created and described by **Mark S. Konings et al., (1989)** that shows potential as a magnetic resonance imaging enhancing tool. Diethylenetriaminepentaacetic acid (DTPA) bicyclic anhydride's interaction with ethylamine provides a 71% yield of the DTPA-bis(ethy1amide) derivative DTPA-BEA (1). High yields of the Gd (III) complex and crystals of Gd (III) were produced from GdzOg and the acid form of 1. The coordination of the two amide carbonyl oxygen atoms to gadolinium is the most remarkable aspect of the structure. A nine-coordinate tricapped trigonal prism containing three amine nitrogens, three carboxylate oxygens, two amide oxygens, and a water molecule as its sites makes up the gadolinium coordination polyhedron.

79. For conventional magnetic resonance imaging (MRI) identification of amyloidal beta (Ab) plaques in Alzheimer's disease, there is currently no gadolinium-based contrast agent available (AD). The survival and quality of life of the patient would depend on its quick discovery. AD is characterised by Ab plaques, which are effectively bound by the common Indian spice curcumin (CUR). **Rameshwar Patil et al., (2015)** have developed a novel nanoimaging agent (NIA) based on naturally occurring poly(b-L-malic acid) (PMLA) that contains covalently bonded gadolinium-DOTA (Gd-DOTA) and naturally occurring CUR to

address this binding. MRI detects the all-in-one agent, which recognises and specifically binds to Ab plaques. By using ex vivo staining, it successfully identified Ab plaques in human and animal samples. In clinics, the technique may be helpful for the secure and non-invasive diagnosis of AD. The fluorescence of bound CUR, reporter Thioflavin-T, MRI employing ex vivo slices of sick human brain sections or of the brain of an AD animal model, and plaques generated by synthetic peptides were all used to monitor the binding process. Ab plaques were found in both species by the NIA (mouse and human).

80. Macrocyclic amino carboxylate (DOTA and DO3A) complexes of Gd- (III) and Fe(III) have been created, characterised, and tested as potential contrast agents for magnetic resonance imaging by **C. Allen Chang *et al.*, (1993)**. DOTA is 1,4,7,10-tetrakis(carboxymethy1)-1,4,7,10-tetraazacyclododecane, and D03A is 1,4,7-tris(carboxymethyl)-1,4,7 (MRI). Four nitrogens and three oxygens are coordinated to the iron in both Na[Fe(DOTA)] according to X-ray single-crystal investigations. Fe and SH_20 (D03A). $3H_20$. None of the fluids are coordinated to iron atoms; the carboxylate arm of the previous iron complex is not coordinated. Both of the Fe(II1) complexes are high spin (S=5/2) compounds, according to magnetic susceptibility and Mossbauer measurements. A brand-new hydrated complex of Gd(DO3A) called $[(Gd(DO3A)_3.Na_2CO_3]$ has been crystallised. Each enneacoordinate Gd atom is coordinated to two oxygens from the carbonate ion, two nitrogens from each carboxyl arm, and four nitrogens from the ligand in the structure $^{17}H_2O$. In the crystal structure, no water molecules are coordinated to the Gd atoms. Fe (III) chelates are less effective water proton relaxation agents than the Gd (DO3A) and Gd $(DOTA)^-$ species.

81. **Kumar, K et al., (1994)** studied the stability constants governing the formation of the Gd (III) and Y(III) complexes of three macrocyclic poly (amino carboxylates), DO3A, HP-DO3A, and DOTA, have been determined by potentiometric and spectrophotometric methods, respectively, at 25°C and at a constant ionic strength of 0.1 M ((TMA)Cl. In the presence of Na^+ ions, the ligands' initial protonation constant decreased, showing a preference for binding to Na^+. The Na^+ ion was found to be chelated deeply within the ligand cage, according to a crystal structure investigation of a complex of NaBr and the tetra-tert-butyl ester of DOTA.

82. The Gd(III) and Y(III) complexes' thermodynamic stability constants were in the following order: DOTA > HP- DO3A > DTPA > DO3A > EDTA. The [Na(t Bu-DOTA)] Br complex, the isostructural Gd(III) and Y(III) complexes of HP-D03A, as well as the H_2SO_4 salt of DO3A, have had their crystal structures identified. The ligand provided eight of the nine

coordinates for the Gd(III) and Y(III) ions, with a water molecule in the ninth (apical) position. With the exception of sodium being -0.3 A deeper in the ligand cavity, the geometry of the eight-coordinate binding of Na^+ in the DOTA tetraester was comparable to that in the (Gd/Y) HP-DO3A complexes. The protonated sec and transannular nitrogens of the metal-free DO3A ligand were preorganized for metal coordination.

83. Novel bifunctional poly(amino carboxylate) chelating compounds that enable chemoselective attachment to highly functionalized biomolecules are easily synthesised, as is detailed by **Sebastian Knor *et al*., (2007)** . We created novel bifunctional chelating agents with additional functional groups based on the well-known chelator 1,4,7,10-tetraazacyclodecane-1,4,7,10-tetraaceticacid (DOTA) by alkylating 1,4,7,10-tetraazacyclodecane (cyclen) with one equivalent of para-functionalized alkyl 2-bromophenyl-acetate and three equivalents of tert-butyl 2- bromoacetate. The resultant compounds, which have an extra carbonyl or alkyne activity, enable quick click reactions for site-specific labelling of functionally appropriate unprotected biomolecules. This was proven through the chemoselective oxime ligation and Cu I-catalyzed azide-alkyne cycloaddition that attached our novel DOTA compounds to the so-called somatostatin analogue Tyr3-octreotate. The radiometalized compound's initial biodistribution investigations in mice showed that the described DOTA conjugation can be used.

84. This study by **Mingqian Tan et al., (2010)** developed and manufactured a CLT1 peptide-targeted G3 nanoglobular Mn(II)-DOTA monoamide conjugate as a targeted MRI contrast agent for Oncofetal fibronectin or fibrin-fibronectin complexes can be seen using molecular methods in tumour stroma. On the surface of the G3 nanoglobule, the targeted contrast agent was made up of 42 Mn(II)-DOTA chelates and 2 peptides. At room temperature, the targeted agent had T1 and T2 relaxivities of 3.13 and 8.74 mM^{-1} s^{-1} per Mn(II) chelate, respectively, at 3 T (tesla). It could be easily eliminated by renal filtration and had a clearly defined nanosize (5.2 nm). At doses as low as 0.03 mmol- Mn/kg, the targeted nanoglobular contrast agent preferentially bonded to tumour tissue, producing considerable tumour contrast enhancement with negligible nonspecific enhancement in the liver of tumor-bearing animals. For MR cancer molecular imaging, the targeted G3 nanoglobular Mn(II)-DOTA conjugate holds promise as a non-gadolinium(III)-based MRI contrast agent.

85. **A. Dean Sherry et al., (1998)** has discovered that DTPA can be converted into propylamine or ester by converting one or even two of its terminal carboxyl groups. These

ligands can then form complexes with Gd^{3+} that, on average, contain fewer inner-sphere water molecules than $Gd(DTPA)^{2-}$ at room temperature and below. This implies that, while being weakly bound, the amide or ester moieties in these complexes interact sufficiently to prevent the entry of additional water molecules into the inner coordination sphere of $Gd^{3+.}$ As a model for a monoconjugated DOTA macromolecule, they now reported the synthesis, rate of production, thermodynamic stability, and field dependence of the longitudinal relaxation rate (l/Tl) of solvent water protons in solutions of Gd (DOTA-PA). The information suggests that when designing in vivo targeted MRI contrast agents, mono conjugated DOTA macromolecules may have certain advantages over the analogous DTPA-conjugated systems.

86. **Haroon Ur Rashid et al., (2016)** reviewed about macrocyclic tetraamine 1,4,7,10-tetraazacyclododecane, also known as cyclen. To create stable compounds with the Gd^{3+} ion, its derivatives serve as helpful ligands. As MRI contrast agents, these chelates are being researched. For application in vivo, the free Gd^{3+} ion is incredibly hazardous. A highly stable Gd^{3+} -chelate is created when a cyclen-based ligand is complexed with it because the cyclen is confined in the ligand's core cavity, which has already been generated. The potential toxicity of cyclen-based MRI contrast agents is reduced due to their improved thermodynamic and kinetic stability. As a result, these substances have proven to be the safest for use in clinical settings. The most crucial factor utilised to assess a contrast agent's efficacy is relaxivity. This parameter is influenced by a variety of variables. This article goes into great detail about how to make MRI contrast agents based on cyclen more relaxing. Two important ligands generated from cyclen are 1,4,7, 10-tetraazacyclododecane-1,4,7,10-tetraacetic acid (DOTA) and 1,4,7, 10-tetraazacyclododecane-1,4,7-triacetic acid (DO3A). Moreover, they serve as the foundation for the synthesis of new ligands. There are a few significant procedures for creating DOTA and DO3A derivatives that are detailed. Also highlighted is the coordination geometry of the chelates produced by these ligands and their derivatives. Via the suitable derivatization of DOTA and DO3A, new ligands can be created. Such ligands' Gd^{3+} -chelates function as effective MRI contrast agents with improved relaxivity, increased stability, improved clearance, lower toxicity, and higher water solubility.

87. In this study, new polymethylated macrocyclic ligands of potential interest for magnetic resonance imaging are synthesised and their structural characteristics are described by **Ramachandran S. Ranganathan et al., (2002)**. By cyclotetramerizing (2S)-1-benzyl-2-methylaziridine and then catalytic hydrogenation, M_4cyclen, or (2S,5S,8S,11S)-2,5,8,11-tetramethyl-1,4,7,10-tetraazacyclododecane, was produced. The ligands M^4DOTA and

M^4DOTMA, which stand for (R)-2-[(2S,5S,8S,11S)-4,7,10-tris-carboxymethyl-2,5,8,11-tetramethyl-1,4,7,10-tetraazacyclododecan-1-yl] propionic acid, respectively, were made by carboxyalkylating M_4cyclen in the presence of Na_2CO_3. If $NaHCO_3$ was the acid scavenger while adding the carboxylic arms, the triacetic ligand M_4DO3A, [(2S,5S,8S,11S)-4,7-bis-carboxymethyl-2,5,8,11-tetramethyl- 1,4,7,10-tetraazacyclododecan-1-yl]acetic acid, was produced in good yields without any traces of M_4DOTA. Under the same circumstances, cyclen produced M_4DOTA with an 82% yield. The elevated basicity of the substituted tetraamine, as shown by NMR titration, is attributed to the distinction in reactivity between cyclen and M_4cyclen. The methyl substituents are positioned in one of the two potential equatorial-like positions, either close to or distant from the carboxylic arms, in the one- and two-dimensional ^1H and ^{13}C NMR spectra of M_4DOTA and M_4DOTMA in the H_4L or H_6L^{2+} forms. The methyl groups are unable to occupy the axial-like locations because they are sterically too crowded. DOTMA, or (R)-2-[4,7,10-tris-((R)-carboxyethyl)- 1,4,7,10-tetraazacyclododecan-1-yl]propionic acid, adopts an elongated shape as well in the H_6L^{2+} form. The parent unsubstituted ligand DOTA cannot be subjected to a comprehensive NMR investigation due to the rigidification of the polymethylated ligands.

88. In order for DOTA (1,4,7,1O-tetraazacyclododecane-1,4,7,1O-tetracarboxylicacid) to complex the gadolinium (III) ion, an intermediate complex must first form, with a stability constant of P = 6.9 and an incompletely coordinated metal ion as demonstrated by NMR spectroscopy. The pH changes that occur during the complexation process were measured using dyes. Despite its low concentration, the $HDOTA^{3-}$ form is the most kinetically active species between pH 4 and 6 (k_f,HL= 1.0 X log 6 M^{-1} s^{-1}). By using an ion exchanger to scavenge the freed 15% $Gd3^+$, the dissociation of GdDOTA- was studied. Even in acidic solutions, the dissociation happens incredibly slowly. The acid-independent dissociation process can be disregarded because it is catalysed by the H* ions (k_d,H = 8.4 X 10" M^{-1} s^{-1}; k_d,= 5 X log s-'). log KML = 22.1 was used to get the stability constant of GdDOTA- from the formation and dissociation rates. This complex does not appear to be especially stable, in contrast to past studies. Yet, due to the exceptional kinetic inertness of GdDOTA-, it should be a highly safe MRI contrast agent.

89. Two polydisulfide Mn(II) complexes were created by **Zhen Ye et al., (2011)** as biodegradable macromolecular MRI contrast agents. The presence of endogenous free thiols caused the macromolecular Polydisulfide Mn(II) Complexes to breakdown easily. The r_1 relaxivity of both polydisulfide Mn(II) complexes was higher than that of $MnCl_2$ and

comparable to polydisulfide Gd(III) complexes. When exposed to Ca^{2+} ions, Mn-EDTA cystamine copolymers exhibited greater resistance to transmetallation than Mn-DTPA cystamine copolymers. Polydisulfide Mn (II) complexes led to a considerable augmentation of the contrast in the liver and heart, similar to other Mn (II) chelates that h ave been reported. Potentially useful contrast agents for MR imaging could be created from macro-molecular Mn(II) complexes.

90. The goal of the study by **Takahiro Mukai et al., (2002)** was to create a residualizing label based on indium-111 for calculating protein pharmacokinetics. The monoreactive DOTA derivative with a tetra uorophenyl group as the protein binding site (mDOTA) was created to prevent cross-linking of proteins. 1,4,7,10-Tetraazacyclododecane-N,N',N",N'" -tetraacetic acid (DOTA), which produced a highly stable and hydrophilic ^{111}In chelate, was chosen as the chelating site. A yield of 11% was obtained overall for the synthesis of mDOTA. Human serum albumin (HSA), galactosyl-neoglycoalbumin (NGA), and cytochrome c (cyt c) were used as model proteins in an investigation into the stability of ^{111}In-labelled proteins in murine plasma, radioactivity retention in protein catabolic sites, and radiochemical yields of ^{111}In-labelled proteins via mDOTA. After being incubated in murine plasma for 5 days, ^{111}In-labeled HSA via mDOTA remained remarkably stable. After injecting mice with ^{111}In- DOTA-NGA, it was shown that there was a prolonged retention of radioactivity in the catabolic sites because the radiometabolite was slowly removed from the lysosome. With a radiochemical yield of over 91%, ^{111}In-DOTA-cyt c was generated at a chelator concentration of 42.2 M. On the other hand, high radiochemical yields of ^{111}In-DOTA-lysine and ^{111}In-DOTA were produced at lower chelator concentrations. These results suggested that the ^{111}In-labelling agent mDOTA would be a suitable choice for calculating protein pharmacokinetics. These findings also indicated that creating ^{111}In-DOTA-labeled proteins with more specific activity would be preferable to adding a protein binding site distal from the unmodified DOTA structure.

91.Two distinct selective-protection techniques involving the creation of cyclen-bisaminal or phosphoryl cyclam derivatives were used by **Luís M. P. Lima et al., (2012)** to successfully synthesise a new 1,4,7,10-tetraazacyclododecane (cyclen) derivative bearing a picolinate pendant arm (HL1) and its 1,4,8,11-tetraazacyclotetradecane (cyclam) analogue HL2. Both compounds' coordination chemistry, particularly with Cu^{2+} and their acid-base characteristics in solid state and aqueous solution were studied. The single crystal X-ray diffraction structures of the compounds with the formulas $[Cu(HL)](ClO_4)\ 2H_2O$ (L = L1 or L2), $[CuL1](ClO_4)$, and $[CuL2]Cl_2.2H_2O$ were discovered after the synthesis of the copper(II)

complexes.These investigations established that the carboxylate group on the picolinate moiety is the site of complicated protonation. Both ligands combine with Cu^{2+} to create complexes that are extremely thermodynamically stable. Furthermore, both HL1 and HL2 show a significant preference for Cu^{2+} over Zn^{2+}. Spectrophotometry was used to assess the kinetic inertness of both Cu^{2+} complexes in acidic media, and the results showed that $[CuL2]^{+}$ is significantly more inert than $[CuL1]^{+}$. When compared to a list of copper(II) complexes of various macrocyclic ligands, the calculated half-life values further show the exceptionally high kinetic inertness of $[CuL2]^{+}$. The cyclam-based ligand HL2, which has a quick complexation process, a high level of kinetic inertness, and significant thermodynamic and electrochemical stability, is a particularly desirable receptor for copper(II).

92. By activating a single carboxyl group using N-hydroxysulfosuccinimide, **Michael R. Lewis et al., (1994)** have created a technique for attaching the macrocyclic chelating agent 1,4,7,10-tetraaza-cyclododecane N,N,N",N"'-tetraacetic acid (DOTA) to proteins (sulfo-NHS). DOTA conjugates of cytochrome c and the anti-carcinoembryonic antigen chimeric monoclonal antibody cT84.66 were made by adding the DOTA active ester reaction mixture to the proteins at pH 8.5–9.0. The sulfo-NHS active ester of DOTA was made in one step using 1-ethyl-3-[3-(dimethylamino)propyl]carbodiimide(EDC). The average number of chelators linked to the protein molecule increased from 2.64 to 8.79, according to mass spectrometry analysis of the cytochrome c conjugates, as the molar ratio of DOTA active ester to protein in the reaction mixture increased from 1:1 to 100:1. The radiolabeled proteins are physiologically inert according to stability analyses of the conjugates in human serum and the presence of a 5000–250 000-fold excess of diethylenetriaminepentaacetic acid (DTPA). In comparison to serum stability tests, kinetic examination of metal loss from a radiolabeled immunoconjugate in the presence of an enormous excess of DTPA may offer a more accurate indication of that immunoconjugate's in vivo stability.

93. Pharmaceuticals called magnetic resonance imaging (MRI) contrast agents are frequently utilised in MRI tests. **Dapeng Hao et al., (2012)** reviewed about the most widely employed MRI contrast agents (GBCAs) are those based on gadolinium. Nine GBCAs have been approved for use in clinical settings and are largely indicated for the total body, vascular, and central nervous system. To increase signal in T1-weighted MRI scans, where GBCAs are concentrated, GBCAs predominantly lower T1 in vivo. The effectiveness of GBCAs, which are water proton relaxation catalysts with a rate constant called relaxivity, makes them distinct from other medications. The relaxivity of each GBCA is influenced by a number of variables,

which are explored in terms of both current agents and potential molecular imaging agents currently being researched. Based on the chemistry of the chelating ligands, current GBCAs can be classified into four distinct structural kinds (macrocyclic, linear, ionic, and nonionic) whose main function is to shield the body against the dissociation of the highly poisonous Gd3 ion from the ligand. In this article, they explained how chemical structure affects formulation features such as inherent and in vivo stability towards dissociation. GBCAs still carry considerable risk even if they have a lower rate of serious adverse events than iodinated contrast agents.

94. It has become extremely popular to utilise lanthanides as probes for many biological experiments rather than radioisotopes. **Fazel Shabanpoo et al., (2010)** found that it is possible to add lanthanide chelates to peptides and proteins either in solution using a labelling kit that is readily accessible or by solid-phase peptide synthesis using the proper lanthanide chelate. Here, a thorough protocol for the latter is provided using a chimeric insulin-like peptide made of human insulin-like peptide 5 (INSL5) A-chain and relaxin-3 B-chain as a model peptide for the labelling of peptides or small proteins with diethylenetriamine-N, N, N″, N″-tetra-tert-butyl acetate-N′-acetic acid (DTPA) chelate or other similar one.

95. The macrocyclic chelator DOTA (1,4,7,10-tetraazacyclododecane-N,N,N,N-tetraacetic acid) has been used by **Margret Schottelius et al., (2003)** to derivatize Tyr 3-Lys 5 (Dde)-octreotide (TOC(Dde)) and Tyr 3-Lys 5 (Dde)-octreotate (TATE(Dde)) in the solution phase. By using SPPS and the Fmoc-strategy, the fully protected parent peptides were put together. H_2O_2 was used to create disulfide bonds after cleavage from the solid support in the coupling of TOC(Dde) and TATE(Dde) with DOTA in the presence of NHS, EDCI, and DIPEA in a water/DMF solvent solution was effective.

96. Within under 2 hours, the coupling reaction produced yields of >98% with no discernible side products. This procedure is consequently a quick and cost-effective replacement for the methods now in use for creating DOTATOC, DOTATATE, and other DOTA-peptide conjugates. Nevertheless, when bulky substituents are present in the haloacetamide, this approach fails to produce the tetra-substituted products, and in certain situations, this intermediate cannot be generated by traditional acylation procedures, limiting the amount of $DOTAMR_4$ compounds that are available for research. This work presents an improved approach for the synthesis of $DOTAMR_4$ by coupling DOTA to a suitable amine-containing reagent (i.e. protected amino-acids with the a-amino group free). Starting with

DOTA, a number of DOTAMR4 derivatives that are challenging or impossible to create using conventional approaches were quickly attained. Using this technology, a fresh protocol for the solution-phase synthesis of DOTA peptide derivatives was created by **Luis M. De Leon Rodrıguez et al., (2004)**. With the help of this technology, numerous additional DOTAMR4 peptide and non-peptide derivatives have been created in our labs, with a number of these fresh substances displaying intriguing molecular imaging capabilities.

97. The preparation of N-hydroxysulfosuccinimidyl DOTA and its conjugation to the human/murine chimeric anti-carcinoembryonic antigen antibody cT84.66 have been improved by **Michael R. Lewis et al., (2001)** using a straightforward, water-soluble method for conjugating monoclonal antibodies to 1,4,7,10-tetraazacy-clododecane-N,N′,N″,N‴-tetraacetic acid (DOTA). With this new technique, conjugation efficiency is increased by a factor of six, antibody cross-linking is reduced by a factor of three to seven, the population of conjugate species is more homogeneous, and the amount of chemicals required for conjugation is decreased by a factor of five. The cT84.66-DOTA conjugate was labelled with high specific activity for the inclusion of the majority of these radiometals, including ^{111}In, ^{90}Y, ^{88}Y, ^{64}Cu, and ^{67}Cu. Large-scale manufacturing and radiometal labelling of cT84.66-DOTA for clinical radioimmunotherapy trials are made possible by this improved conjugation method.

98. A promising radiopharmaceutical for tumour imaging has been created and tested **Deepa Sinha et al., (2009)** : 9m Tc-Diethylene triamine pentaacetic acid-bis (amide) conjugates. The compounds were created through the condensation of DTPA bis(anhydride) with various L-amino acids (methyl tryptophan and 5-hydroxy tryptophan), and they were then examined using IR, NMR, and mass spectroscopy to determine their composition. In physiological conditions, 99m Tc-labeled compounds were found to be stable for roughly 24 hours with a radiolabeling yield of more than 95%. All of these complexes' blood kinetic investigations revealed a bi-exponential pattern and fast washout from the blood circulation. Further in vivo research for targeted tumour imaging is encouraged by the preliminary findings with these amino acid-based ligands.

99. In an effort to develop new complexing agents with aminoacetic groups along the polymer chain whose complexing properties should be superior to their monomolecular homologues, EDTA (ethylenediaminetetraacetic acid), DTPA, etc., polycondensation of diethylenetriaminepentaacetic acid (DTPA) bisanhydride with diols and diamines was investigated. It has been investigated how to create linear, water-soluble polymers that will be

complexed with gadolinium. **Veronique Montembault et al. (1995)** produced polycondensates with different COOH function densities using a range of comonomers, allowing them to examine how effectively they were able to complex with various metallic cations.

100. The condensation reaction between DTPA bis(anhydride) and 5-aminouracil or 5,6-diamino-uracil has led to the production of two novel DTPA (diethylenetriaminepentaacetic acid) functionalised bis(amides) with pendant uracil moieties. These ligands are an example of the growing class of ligands that can join complementary organic bases in triple hydrogen bonds. These ligands, however, are distinct because they combine with various metal ions to generate water soluble complexes. The two DTPA-uracil ligand syntheses, seven metal complexes, and the crystal structure of the bismuth complex of DTPA bis(4,5-diamino-6-hydroxy-2-mercaptopyrimidine) L1 are all reported by **Alexandra S. Georgopoulou et al., (1999)** . The two arms on which the uracil moieties are located have a high degree of rotational freedom, which is the most significant characteristic of this solid state structure. This property enables these groups to make numerous hydrogen bonds involving both uracil moieties on one side of the molecule.

101. There has been the development of a novel family of paramagnetic macromolecular contrast agents for magnetic resonance imaging. By copolymerizing ethylenediaminetetraacetic acid dianhydride or diethylenetriarninepentaacetic acid dianhydride with diamine monomers, eight novel polyamide ligands were created. Moreover, their iron(IlI), manganese(II), and gadolinium(lIl) complexes were created by **Ming Ouyang et al., (1996).** Infrared spectra, chemical analysis, and ^{1}H nuclear magnetic resonance were used to describe all polyamide ligands and metal complexes. When compared to equivalent simple monomeric paramagnetic metal complexes, relaxivity experiments clearly shown that polyamide paramagnetic metal complexes had a better relaxing efficacy.

102. Diethylenetriaminepentaacetic acid (DTPA) dianhydride and octadecylester of tyrosine or phenylalanine were used by **Xia Zhao et al., (1997)** to create several novel amphiphilic ligands. They also created and described the metal complexes of Gd m, Yb H, and Mn H. The liposomes containing metal complexes were created by inserting amphipathic metal complexes into the liposomal vesicles' membrane. Liposomes that have been tagged with a paramagnetic metal exhibit high spin-lattice relaxivity These complexes were simple to incorporate into the liposomes' lamella due to their amphiphilic nature. High water proton spin-

lattice relaxation rates were seen in the metal complexes and tagged liposomes (1/7"1). Further research is being conducted, including imaging, biological, and toxicological tests.

103. **LIU, Ying-Chun et al., (2005)** described that multidentate ligands are frequently employed in the development of MRI contrast agents to limit the number of coordinated water molecules, which improves the stability of the complexes in vivo. As a result, the outer-sphere relaxivity becomes a significant factor in the total relaxivity. As no water molecule was coordinated to the metal ion in the title complex's ligands' nitrogen, amide, and carboxyl oxygen atoms, several water molecules were bound there by hydrogen bonds, making the outer-sphere relaxivity the only relaxivity component. Moreover, the complex's six five-membered chelate rings may further increase the stability of the compound. The complex is also water soluble. All of these details suggest that the title paramagnetic complex could be a potential option for an MRI contrast agent that targets the liver.

104. A novel ligand (H_2L), diethylenetriamine-N,N',N''-triacetylisoniazide N,N''-bisacetic acid, and its four non-ion transition metal complexes, ML nH_2O (M=Mn, n=4; M=Co, Ni, n=2; M=Cu, n=1), have been synthesized and characterised by **Ding-Wa Zhang et al., (2005)** on the basis of elemental analysis, molar conductivity, ^{1}H-NMR, FAB-MS, TG-DTA analysis and IR spectrum. Also, the complexes' relaxivities (R_1) were calculated. The values for MnL, CoL, NiL, CuL, as well as $Gd(DTPA)_2$, which was employed as a reference, are 6.94, 2.79, 2.52, 1.59, and 4.34 l $mmol^{-1}s^{-1}$, respectively. MnL has a higher relaxivity than $Gd(DTPA)_2$, for example. The findings suggest that the MnL complex could be used as an MRI contrast agent.

105. By combining EDTA (ethylenediaminetetraacetic acid) or DTPA (diethylenelriaminepentaacetic acid) dianhydride and ethyl ester of serine, threonine, and tyrosine, six novel aminocarboxylic compounds were created by **Zhuo Renx et al., (1996).** Moreover, their paramagnetic metal compounds were created. IR spectra, ^{1}H NMR, and elemental studies were used to characterise all ligands and paramagnetic metal complexes. The relaxation effectiveness research of the metal complexes revealed that they were more successful at relaxing than their matching unmodified metal complexes. Gadolinium complex of DTPA modified with tyrosine ethyl ester imaging investigation in mice revealed that this metal complex might ostensibly boost the signal strength of MR pictures.

106. A propionic acid substituted ethylenediamine N,N'-di-[(o-hydroxyphenyl) acetic acid] (P-EDDHA), which tightly complexes ^{67}Ga, was created by **Jochen Schuhmach et al.,**

as a chelating agent for labelling antibodies (Abs) with metallic radionuclides. Carbodiimide was used to couple the ^{67}Ga-P-EDDHA chelate to IgG in aqueous solution at a 1:1 molar ratio. 15% was the typical coupling yield. With commercially available ^{67}Ga, a specific activity of 4 mCi/mg IgG could be attained. Human serum was used to test the in vitro stability of the substance and revealed a half-life of approximately 120 hours for the release of ^{67}Ga from the labelled Ab during the initial stage of incubation. Its half-life in vitro is comparable to that determined for ^{111}In-DTPA labelled Abs. The in vivo formation of radioactive labelled transferrin via transchelation, as stated for ^{111}In-DTPA tagged Abs, should, however, be decreased by this labelling strategy due to the high stability of the ^{67}Ga-P-EDDHA chelate.

107. Every year, tens of millions of MRIs that have been contrast-enhanced are conducted worldwide. The contrast materials, which increase diagnostic precision, are nearly exclusively tiny, hydrophilic chelates based on gadolinium (III) described by **Jessica Wahsner et al., (2019)** . Concerns about these substances' long-term safety have surfaced in recent years, which has sparked research towards substitutes. The creation of novel molecularly focused contrast agents or agents with the ability to detect pathogenic alterations in the immediate environment has also received attention. This in-depth analysis details the current state of the art for contrast agents that have received clinical approval, their mode of action, and the variables affecting their safety. From there, they discussed various methods for producing MR image contrast, including relaxation, chemical exchange saturation transfer, and direct detection, as well as the kinds of molecules that work well in each case. Finally, they discussed initiatives to develop safer contrast agents, either by boosting relaxivity, fortifying them against metal ion release, or switching to gadolinium (III)-free substitutes.

108. **Erno Bruche et al., (2013)** reviewed the chemistry of gadolinium and its complexes formed with various organic ligands has become the primary research theme of several labs around the world since the realisation that paramagnetic MR contrast agents may play an important role in clinical imaging in the late 1970s and the everexpanding role of MRI in clinical radiology practises worldwide. Approximately 10 studies on the use of gadolinium as a T1 relaxation (contrast) agent for MRI first emerged in the literature in 1984. Over the course of these 25 years, publications increased annually, reaching approximately 1000 papers on this topic in 2010. Only a small portion of those deal with thermodynamic and kinetic measurements of novel gadolinium compounds, although the importance and interest in this subject remain strong. Since the first MRI contrast agent was introduced in 1987, we have learned a great deal about the thermodynamics and kinetics of lanthanide ion-ligand complexes.

As a result, scientists are now in a much better position to design lanthanide complexes that will be non-toxic in vivo even when they may not be quickly excreted from the body. As we advance towards the next generation of molecular imaging agents for medicine, this knowledge base is essential.

109. When employing pulsed electron-electron double resonance (PELDOR or DEER) at high fields or frequencies to measure nanometric distances, high-spin gadolinium (III) and manganese (II) complexes have replaced the traditional nitroxide radical spin labels. **Paul Demay-Drouhard et al., (2016)** reported that a model system made of two $[Mn(dota)]^2$ (MnDOTA; DOTA4 = 1,4,7,10-tetraazacyclododecane-1,4,7,10-tetraacetate) directly attached to the ends of a central rod-shaped oligo(phenylene-ethynylene) (OPE) spacer was successfully synthesised. Q-band PELDOR measurements on a bis-nitroxide analogue are used to confirm the OPE's stiffness. This paper presents an intriguing option for in-depth research on pulsed dipolar spectroscopic techniques on Mn (II) systems and demonstrates the possibility of MnDOTA-based spin labels for detecting reasonably low nanoscale distances.

110. 7-[2-(bis-carboxymethyl-amino)-ethyl] is a new decadentate ligand that can be made quickly and effectively. Acyclic and macrocyclic binding moieties for the compound 4,10-bis-carboxymethyl-1,4,7,10-tetraaza-cyclododec-1-yl-acetic acid (DEPA) are disclosed. A scalable and repeatable synthesis technique for 1,4,7-tris(tert-butoxycarbonylmethyl)tetraazacyclododecane, a precursor molecule of DEPA, was created by **Hyun-Soon Chong *et al*., (2015**) . DEPA was examined as a chelator of ^{177}Lu, ^{212} Bi, and ^{213}Bi for prospective application in radioimmunotherapy (RIT), an antibody-targeted cancer therapy, employing in vitro serum stability, in vivo biodistribution investigations, and spectroscopic complexation kinetics.

111. The imaging of plaques using magnetic resonance imaging (MRI) is a promising method. The objective of this study by **Amber L. Doiron *et al*., (2007)** was to produce polymeric particles of a small size with a high loading of gadolinium (III) diethylenetriaminepentaacetic acid (Gd-DTPA) and show their utility for MRI. To concentrate the MRI agent at an imaging site, a water-in-oil-in-oil double emulsion solvent evaporation process was utilised to encapsulate the agent in a poly(lactide-co-glycolide) (PLGA) or polylactide-poly(ethylene glycol) (PLA-PEG) particle. It was possible to produce PLGA particles with two different average sizes of 1.83 m and 920 nm as well as PLA-PEG particles with a mean diameter of 952 nm. Up to 30 weight percent of Gd-DTPA could be loaded, and

the in vitro release lasted for five hours. The particles' low cytotoxicity towards human umbilical vein endothelial cells (HUVEC) was demonstrated. The polymeric contrast agent formulation's capacity to produce contrast was comparable to that of Gd-DTPA by itself. These findings show the potential value of the polymeric particles loaded with contrast agents for MRI plaque detection.

MATERIALS & METHODS

3. MATERIALS AND METHODS

3.1 Preparation of DTPA based complexes:

Chemicals required like DTPA was purchased from TCI, 4-amino benzoic acid from SRL Chemicals and 6-amino naphthoic acid from Sigma Aldrich in 99% purity.

Solvents used:

- Acetic anhydride
- Pyridine
- Diethyl ether
- Dimethyl formamide (DMF)
- Anhydrous ether
- Triethylamine

STAGE I

Preparation of DTPA bis anhydride [DTPA Bis]:

In a double neck round bottom flask added DTPA mixture, acetic anhydride, pyridine and was heated in a magnetic stirrer at 80°C for 18 hours under nitrogen atmosphere. The mixture was cooled to room temperature, filtered, and the resulting solid was washed with acetic anhydride and diethyl ether. It was then placed in an oven to dry and the yield of dried product was noted. [112]

STAGE II

LIGAND 1

Preparation of DTPABis-4ABA (L1):

DTPA bis anhydride (0.8mmol) was dissolved in 7ml of DMF and 0.5ml of triethylamine (2.4mmol) were mixed under nitrogen atmosphere in a double neck round bottom flask. 4-amino benzoic acid (1.8mmol) was dissolved in 10ml of DMF and added to it. pH of the solution was maintained at 8. The reaction was heated at 40°C with stirring for 7 hours. Excess of solvent was evaporated using rotor evaporator and the product was precipitated using anhydrous ether. The white precipitate was filtered using vacuum pump and dried. The yield was noted.[113]

STAGE III

COMPLEX 1

Preparation of Mn-DTPABis-4ABA:

Manganese (II) chloride and DTPABis-4ABA (L1) were taken in a round bottom flask. The p^H was maintained at 8.4 using 1N $NaHCO_3$ solution and dissolved. To the solution added 2ml of 1N HCl to maintain the pH of the solution and kept in water bath at 70°C for 6 hours. Then the resulting solution was subjected to direct flame for 2 minutes in wavering manner and allowed to cool. The excess solvent was evaporated and complex was formed. The yield was noted.[114]

STAGE II

LIGAND 2

Preparation of DTPABis- 6ANA (L3):

DTPA bis anhydride (0.4 mmol) was dissolved in 4ml of DMF and 0.5ml of triethylamine (2.4mmol) were mixed under nitrogen atmosphere in a double neck round bottom flask. 6-amino naphthoic acid (0.9mmol) was dissolved in 5ml of DMF and added to it. p^H of the solution was maintained at 8. The reaction was heated at 40°C with stirring for 7 hours. The solution was reduced to half in order to remove excess of solvent and kept for drying to obtain a red wine colour product. The yield of the product was noted.

STAGE III

COMPLEX 2

Preparation of MnDTPABis- 6ANA:

Manganese (II) chloride and DTPABis- 6ANA (L2) were taken in a round bottom flask. The p^H was maintained at 8.4 using 1N $NaHCO_3$ solution and dissolved. To the solution added 2ml of 1N HCl to maintain the pH of the resulting solution and kept in water bath at 70°C for 6 hours. Then the resulting solution was subjected to direct flame for 2 minutes in wavering manner and allowed to cool. The excess solvent was evaporated and complex was formed. The yield was noted.

3.2 Preparation of EDTA based complexes:

Chemicals required like EDTA was purchased from TCI, 4-amino benzoic acid from SRL Chemicals and 6-amino naphthoic acid from Sigma Aldrich were purchased in 99% purity.

Solvents used:

- Acetic anhydride
- Pyridine
- Diethyl ether
- Dimethyl formamide (DMF)
- Triethylamine

STAGE I

Preparation of EDTA bisanhydride [EDTABis]:

In a double neck round bottom flask added EDTA mixture, acetic anhydride, pyridine and was heated in a magnetic stirrer at 80°C for 18 hours under nitrogen atmosphere. The mixture was cooled to room temperature, filtered, and the resulting solid was washed with acetic anhydride and diethyl ether. It was then placed in an oven to dry and the yield of dried product was noted.

STAGE II

LIGAND 3

Preparation of EDTABis -4ABA (L3):

EDTA bis anhydride (0.8mmol) was dissolved in 7ml of DMF and 0.5ml of triethylamine (2.4mmol) were mixed under nitrogen atmosphere in a double neck round bottom flask. 4-amino benzoic acid (1.8mmol) was dissolved in 10ml of DMF and added to it. pH of the solution was maintained at 8. The reaction was heated at 40°C with stirring for 7 hours. The solution was reduced to half in order to remove excess of solvent and kept for drying to obtain a off white colour product. The yield of the product was noted.

STAGE III

COMPLEX 3

Preparation of [Mn-EDTABis-4ABA]:

Manganese (II) chloride and EDTABis -4ABA (L3) were taken in a round bottom flask. The p^H was maintained at 8.4 using 1N $NaHCO_3$ solution and dissolved. To the solution added 2ml of 1N HCl to maintain the pH of the resulting solution and kept in water bath at 70°C for 6 hours. Then the resulting solution was subjected to direct flame for 2 minutes in wavering manner and allowed to cool. The excess solvent was evaporated and complex was formed. The yield was noted.

STAGE II

LIGAND 4

Preparation of DTPABis -6ANA (L4):

DTPA bis anhydride (0.4 mmol) was dissolved in 4ml of DMF and 0.5ml of triethylamine (2.4mmol) were mixed under nitrogen atmosphere in a double neck round bottom flask. 6-amino naphthoic acid (0.9mmol) was dissolved in 5ml of DMF and added to it. p^H of the solution was maintained at 8. The reaction was heated at 40°C with stirring for 7 hours. The solution was reduced to half in order to remove excess of solvent and kept for drying to obtain a red wine colour product. The yield of the product was noted.

STAGE III

COMPLEX 4

Preparation of Mn-DTPABis-6ANA:

Manganese (II) chloride and DTPABis -6ANA (L4) were taken in a round bottom flask. The p^H was maintained at 8.4 using 1N $NaHCO_3$ solution and dissolved. To the solution added 2ml of 1N HCl to maintain the pH of the resulting mixture and kept in water bath at 70°C for 6 hours. Then the resulting solution was subjected to direct flame for 2 minutes in wavering manner and allowed to cool. The excess solvent was evaporated and complex was formed. The yield was noted.

3.3 All the synthesised compounds were subjected to various spectroscopic techniques like

- Ultra violet visible spectroscopy
- Infrared spectroscopy
- Nuclear magnetic resonance spectroscopy
- Electron spin resonance spectroscopy
- Thermogravimetric analysis
- Fluorescence spectroscopy
- Anti-bacterial studies

3.3.1 ULTRA VIOLET VISIBLE SPECTROSCOPY:

The UV-visible spectra of the ligands and complexes with suitable concentrations in DMSO and H2O were obtained by Ultraviolet Visible Double Beam Spectrometer using quartz cell and the solvent effect was eliminated by placing the solvents DMSO and H2O in reference cell.

3.3.2 FOURIER TRANSFORM INFRARED SPECTROSCOPY(FTIR):

Infrared spectrum of compounds was obtained using Shimadzu IR spectrometer. The compounds were directly placed in zinc selenide sample cavity; the spectra of compounds were obtained using interferogram technique.

3.3.3 NUCLEAR MAGNETIC SPECTROSCOPY(NMR):

All the ligands exhibit different signals with correct intensity ratio. The spectrums were recorded in a BRUKER modern 400 MHz instrument with Tetramethyl silane (TMS) as an internal standard. Deuterated DMSO and D2O were used as solvents to record the spectrum. Chemical shifts were quoted in parts per million.

3.3.4 ELECTRON SPIN RESONANCE SPECTROSCOPY (ESR):

Spectrum of complexes were recorded using JOEL Model JES FA200.

3.3.5 THERMO GRAVIMETRIC ANALYSIS (TGA):

Thermo gravimetric analysis were done for samples. This gives the information about thermal stability and thermal decomposition of complexes. Their stability was determined using TG/DTA-EXSTAR/6300 (Thermo Gravimetric Analyser). The thermograms were obtained from continuous nitrogen flow with the sample which is placed in an alumina pan. The plots were made for weight loss against temperature.

3.3.6 FLUORESCENCE SPECTROSCOPY:

The fluorescence spectra of the ligands and complexes with suitable concentrations in DMSO and H2O were obtained by Agilent Cary Eclipse fluorescence Spectrometer.

3.3.7 ANTI-BACTERIAL TEST

(Kirby-Bauer method)

Procedure

Inoculum Preparation

Growth Method

The growth method is performed as follows

1. At least three to five well-isolated colonies of the same morphological type are selected from an agar plate culture. The top of each colony is touched with a loop, and the growth is transferred into a tube containing 4 to 5 ml of a suitable broth medium, such as Nutrient broth.

2. The broth culture is incubated at 35°C until it achieves or exceeds the turbidity (usually 2 to 6 hours)

3. The turbidity of the actively growing broth culture is adjusted with sterile saline or broth to obtain a turbidity. This results in a suspension containing approximately 1 to 2 x 10^8 CFU/ml for *E.coli and Staphylococccus aureus.*

Inoculation of Test Plates

1. Optimally, within 15 minutes after adjusting the turbidity of the inoculum suspension, a sterile cotton swab is dipped into the adjusted suspension. The swab should be rotated several times and pressed firmly on the inside wall of the tube above the fluid level. This will remove excess inoculum from the swab.

2. The dried surface of a Nutrient agar plate is inoculated by streaking the swab over the entire sterile agar surface. This procedure is repeated by streaking two more times, rotating the plate approximately 60° each time to ensure an even distribution of inoculum. As a final step, the rim of the agar is swabbed.

3. The lid may be left ajar for 3 to 5 minutes, but no more than 15 minutes, to allow for any excess surface moisture to be absorbed before applying the drug impregnated disks.

4. The media was punctured by making a well of 6 mm in diameter and filled with 20 µl of a sample. Further the petriplates were placed inversely for complete diffusion and inhibition zones were examined by measuring the diameter (mm) formed around the well after 24 hrs incubation at 37°C. The zones were measured by using standard (Hi-Media) scale.

RESULTS & DISCUSSION

4. RESULTS AND DISCUSSION

All the synthesized compounds were characterised by various spectroscopic techniques.

4.1 ULTRA-VIOLET VISIBLE SPECTROSCOPY:

The electronic spectra of DTPA compounds showed an absorption band in the range 240-270 nm which may be attributed to π→π* transition of the aromatic moiety of ligands**.** This absorption band remained unaltered in their complexes. A shoulder around 320-400 nm may be due to the ligand to metal charge transfer (LMCT) transition. The weak absorption at 550 nm may be assigned to the spin allowed d-d transition.**[115]** The λ_{max} of EDTA based ligands show good absorption at 290nm – 310 nm. Complex of 6 amino naphthoic acid showed a weak n→π* transition showing good absorption near 310 nm. The complexes Mn-EDTABis-4ABA and Mn-EDTABis-6ANA showed a hypsochromic shift compared to the ligands.

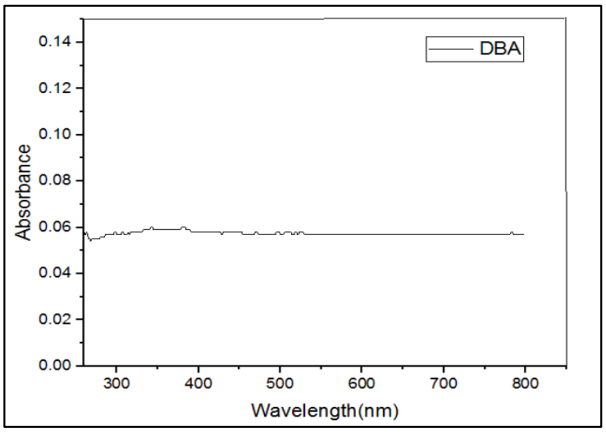

DTPABis-4ABA

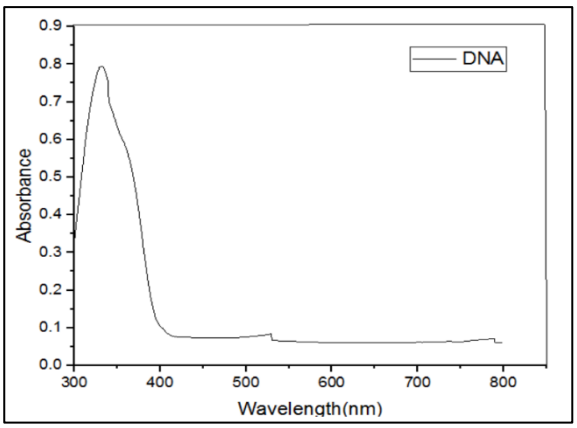

DTPABis-6ANA

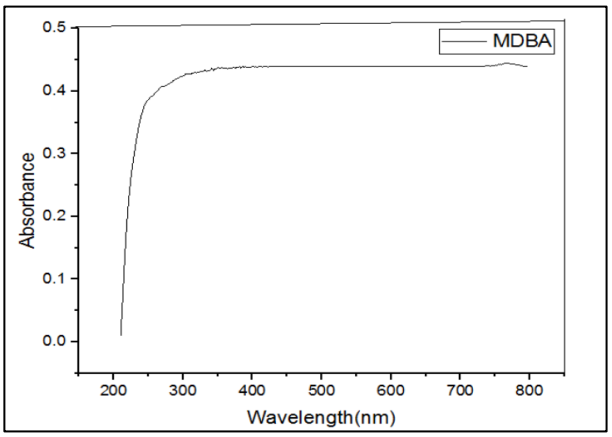

MnDTPABis-4ABA

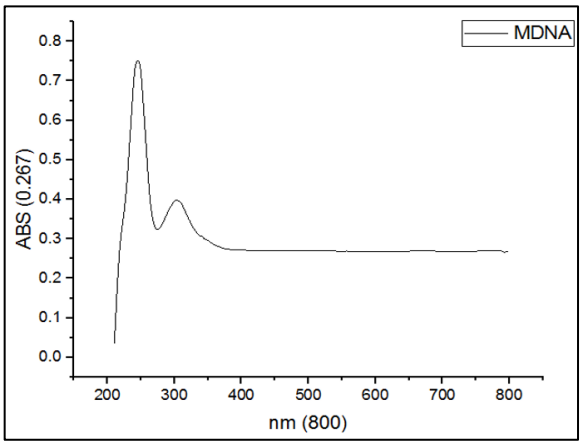

Mn DTPABis-6ANA

Fig 4.1: UV-visible spectra of DTPA based ligands and complexes

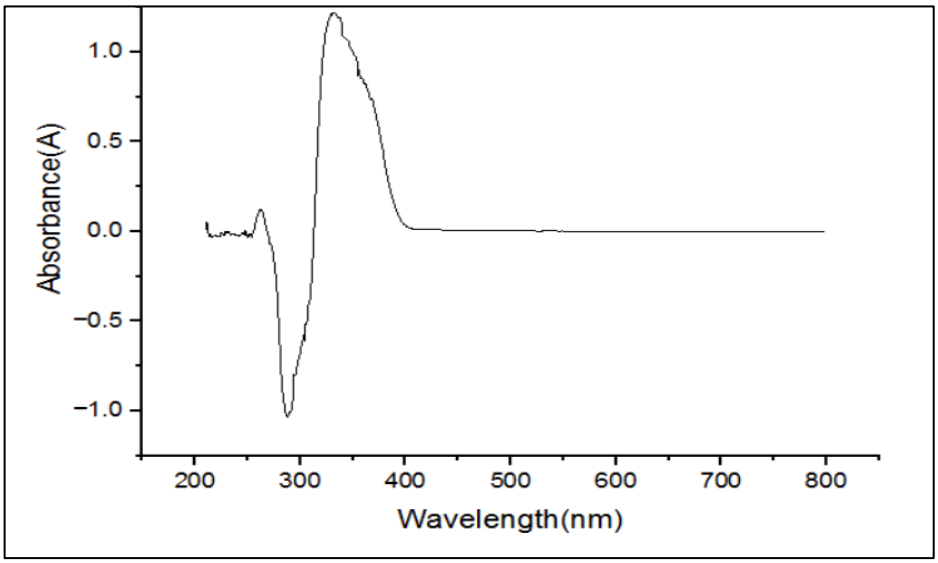

EDTABis-6ANA

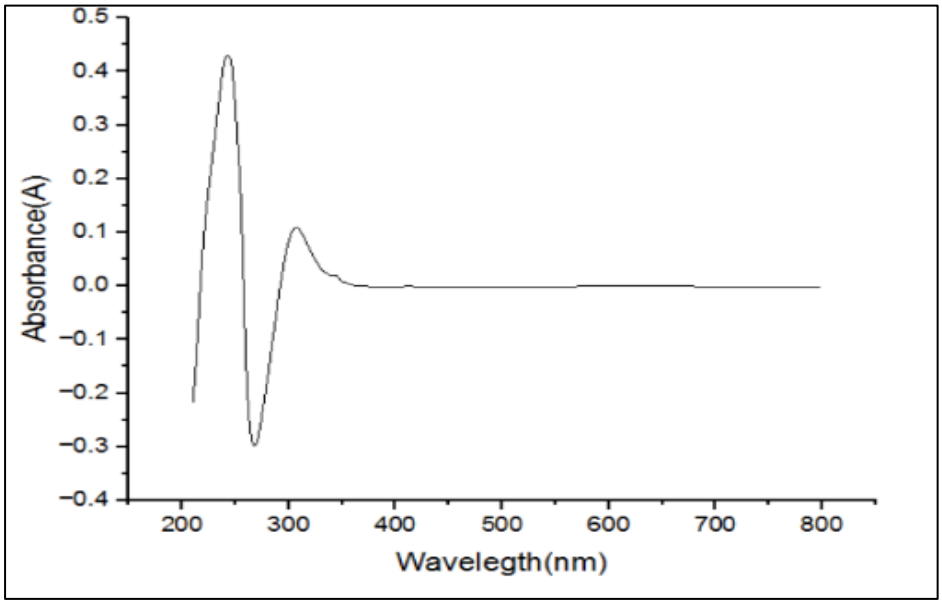

MnEDTABis-6ANA

Fig 4.2: UV-visible spectrums of EDTA based ligands and complexes

4.2 FOURIER TRANSFORM INFRARED SPECTRA:

In the IR spectrum of EDTA-Bis a peak at 1749 cm^{-1} corresponded to symmetric C=O stretch of anhydride and a peak at 1255 cm^{-1} corresponded to C-O stretch. A peak around 1062 cm^{-1} and 930 cm^{-1} corresponded to C-N stretch and OH bend respectively. **[116]**

In the IR spectrum of DTPA-Bis a peak at 1771 cm^{-1} corresponded to symmetric C=O stretch of anhydride, 1689 cm-1 corresponded to C=O stretch of carboxylic acid and a peak at 1342 cm^{-1} corresponded to C-O stretch. A peak around 1110 cm^{-1} and 949 cm^{-1} corresponded to C-N stretch and OH bend respectively.

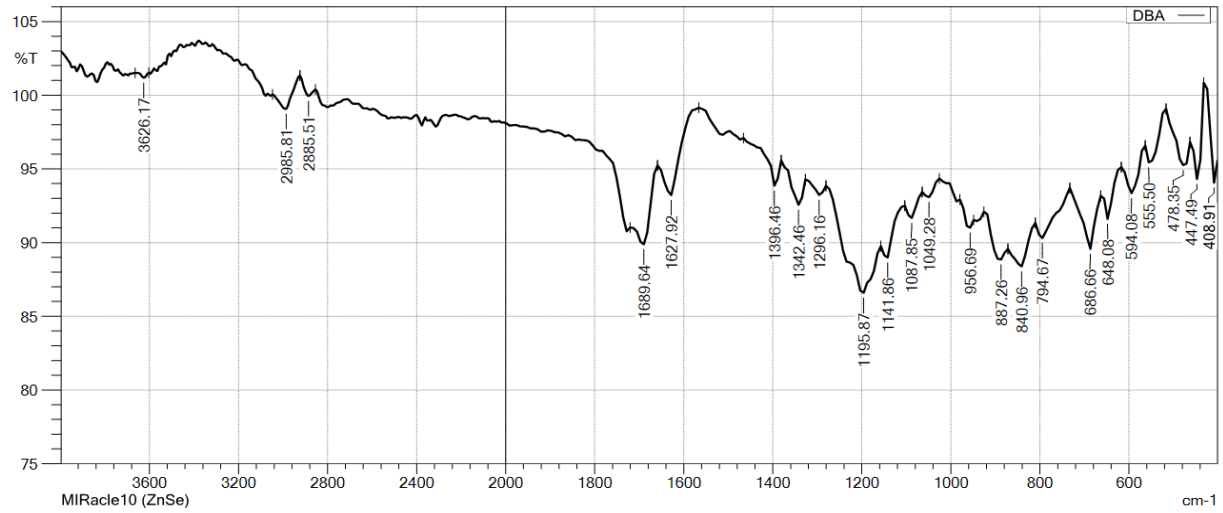

Fig 4.3: IR spectrum of DTPA-Bis

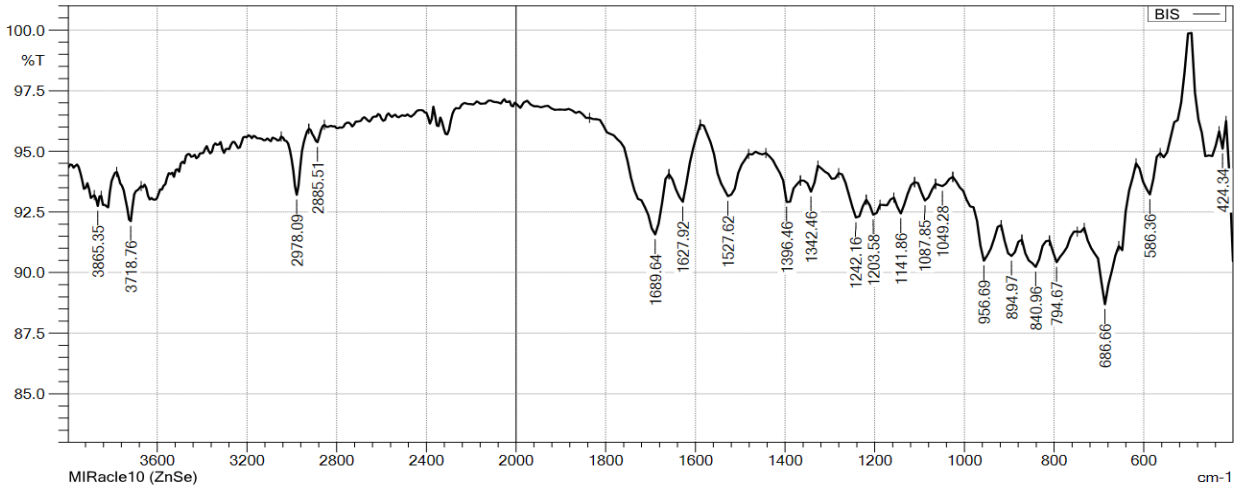

Fig 4.4: IR spectrum of EDTA-Bis

In the IR spectrum of DTPABis-4ABA, the strong band at 1689 cm^{-1} can be attributed to the absorption of carboxyl groups υ(C=O). The three bands at 1627, 1527 and 1396 cm^{-1} could be assigned to absorptions of amide respectively. In the band of wavelength 1620 cm^{-1} assigned to amide absorptions in DTPABis-6ANA, two weak bands at 2916 cm^{-1} revealed the OH stretching of carboxylic acid, 1087 cm^{-1} exhibited the NH stretching. **[117-121]**

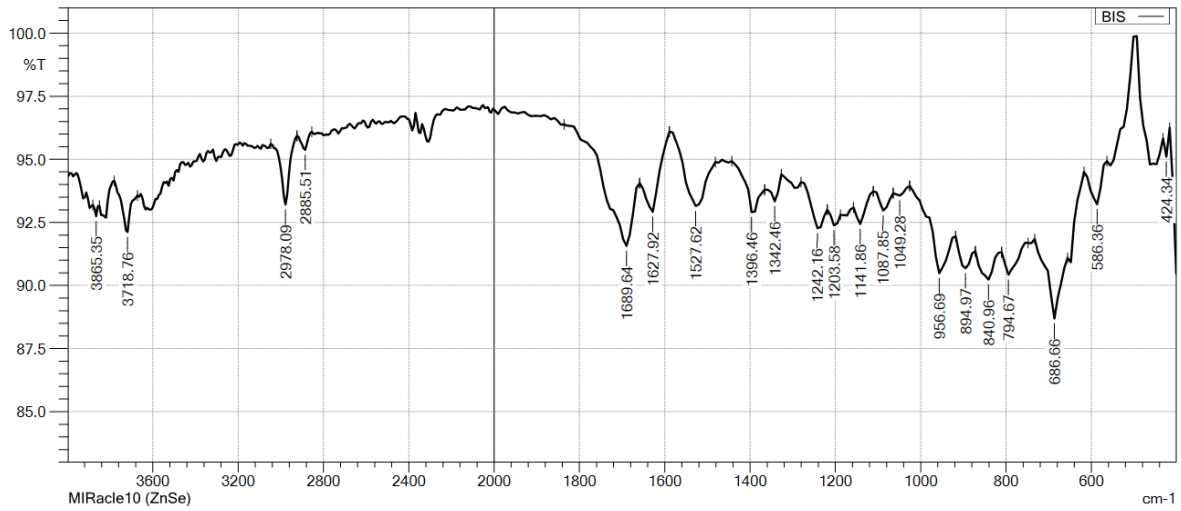

Fig4.5: IR spectrum of DTPABis-4ABA

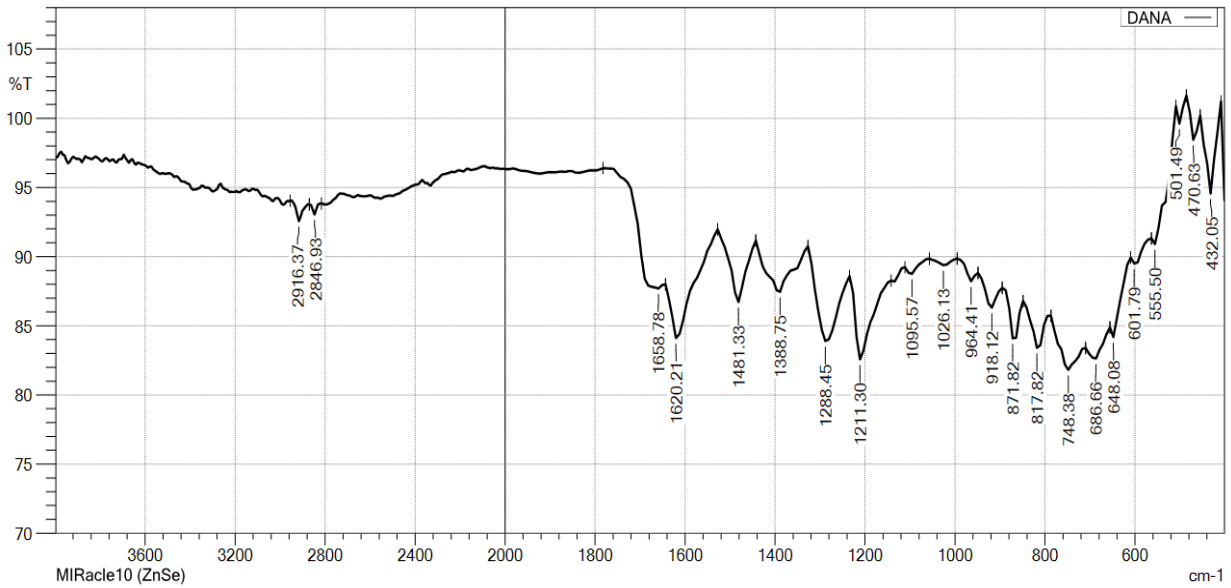

Fig 4.6: IR spectrum of DTPABis-6ANA

In the IR spectrum of EDTABis-4ABA, the strong band at 1658 cm^{-1} can be attributed to the absorption of carboxyl groups υ(C=O). The three bands at 1597, 1473 and 1396 cm^{-1} could be assigned to absorptions of amide respectively. In the band of wavelength 1620 cm^{-1} assigned to amide absorptions in EDTABis-6ANA, two weak bands at 2924 cm^{-1} revealed the OH stretching of carboxylic acid, 1103 cm^{-1} exhibited the NH stretching.

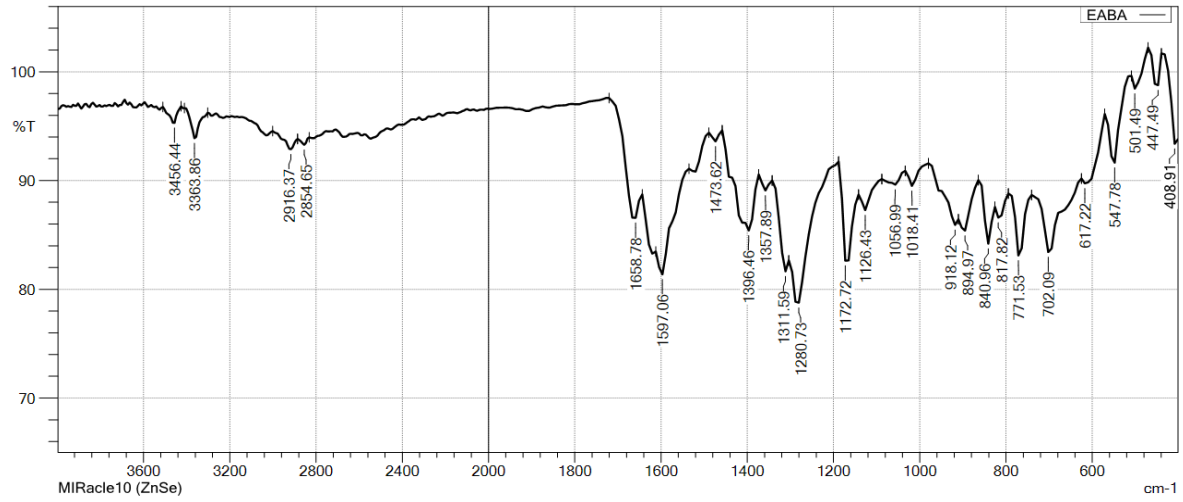

Fig 4.7: IR spectrum of EDTABis-4ABA

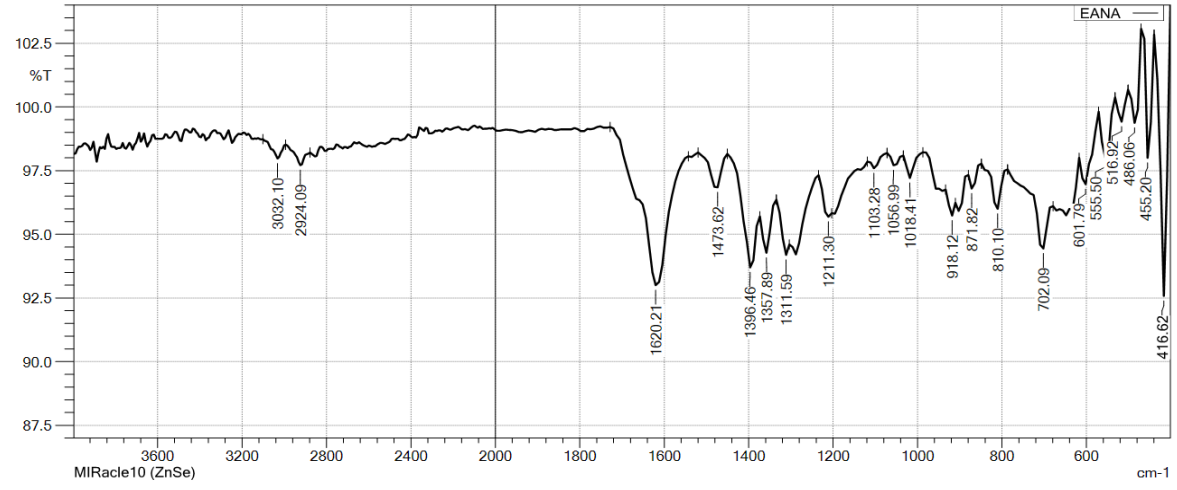

Fig 4.8: IR spectrum of EDTABis-6ANA

In the IR spectrum of the metal complex Mn-DTPABis-4ABA the peaks at 1627, 1527 and 1396 cm^{-1} disappeared and strong absorption peaks at 1550cm^{-1} and 1404 cm^{-1} were present. This indicated the formation of the complex. The metal – oxygen bond at 509 cm^{-1} was present in the IR spectra of MnDTPABis-4ABA. In the band of wavelength 1620 cm^{-1} assigned to amide absorptions in DTPABis-6ANA, two weak bands at 2916 cm^{-1} revealed the OH stretching of carboxylic acid, 1087 cm^{-1} exhibited the NH stretching.

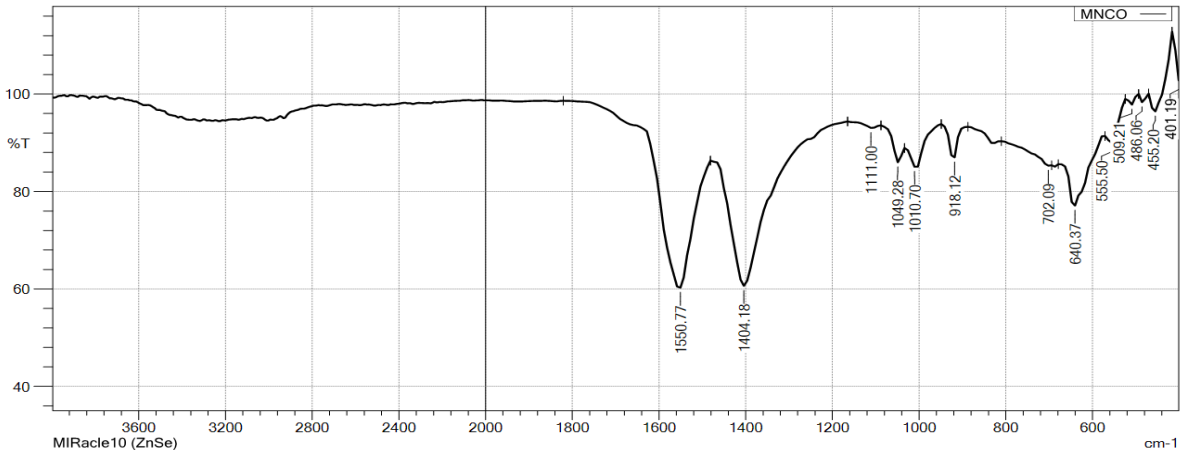

Fig 4.9: IR spectrum of Mn-DTPABis-4ABA

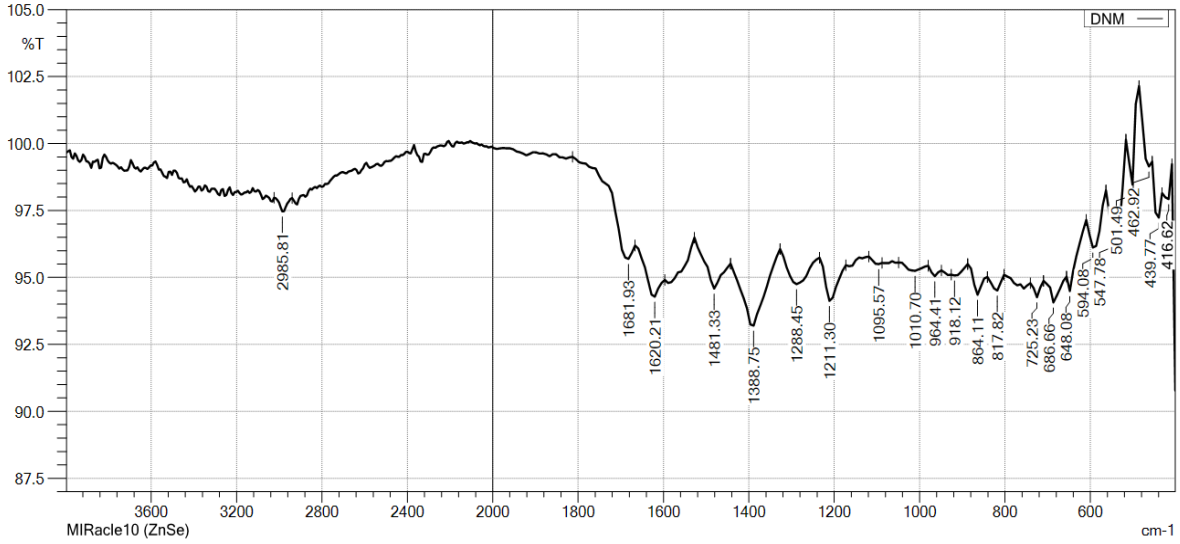

Fig 4.10: IR spectrum of Mn-DTPABis-6ANA

In the IR spectrum of the metal complex Mn-EDTABis-4ABA the peaks at 1627, 1527 and 1396 cm^{-1} disappeared and strong absorption peaks at 1550cm^{-1} and 1404 cm^{-1} were present. This indicated the formation of the complex. The metal – oxygen bond at 510 cm^{-1} was present in the IR spectra of MnEDTABis-4ABA. In the band of wavelength 1620 cm^{-1} assigned to amide absorptions in EDTABis-6ANA, two weak bands at 2931 cm^{-1} revealed the OH stretching of carboxylic acid, 1149 cm^{-1} exhibited the NH stretching.

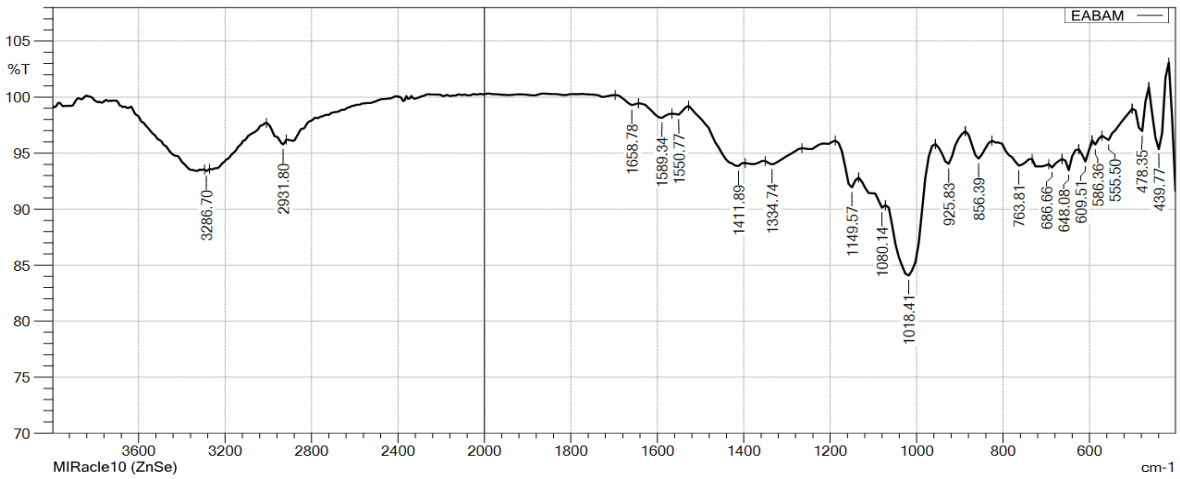

Fig 4.11: IR spectrum of Mn-EDTABis-4ABA

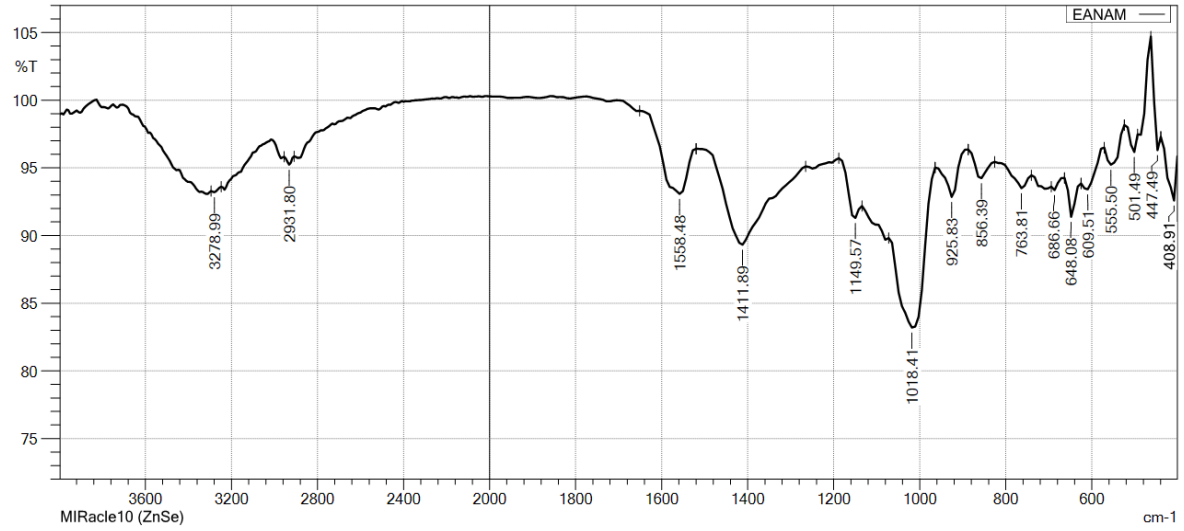

Fig 4.12: IR spectrum of Mn-EDTABis-6ANA

Table 2: Vibrational frequencies of ligands and complexes

	υ (C=O) anhydride	υ(C-N)	υ(C=O) carboxyl	υ(N-H)	υ(Mn-O)
DTPABis	1771	1110	1689	1087	-
EDTABis	1749	1062	1658	1056	-
DTPABis-4ABA	-	1110	1689	1087	-
EDTABis-4ABA	-	1062	1658	1056	-
DTPABis-6ANA	-	1110	1692	1087	-
EDTABis-6ANA	-	1062	1658	1056	-
Mn-DTPABis-4ABA	-	1110	1689	1087	509
Mn-EDTABis-4ABA	-	1062	1658	1056	510
Mn- DTPABis-6ANA	-	1110	1692	1087	501
Mn-EDTABis-6ANA	-	1062	1658	1056	501

4.3 NUCLEAR MAGNETIC SPECTRA OF LIGANDS:

A peak at δ=2.5 ppm and a peak at δ=2.6 ppm corresponds to DMSO d6 solvent of DTPABis-4ABA and DTPABis-6ANA respectively. A peak at δ=7.6(d) ppm corresponds to the four aromatic protons of 4-amino benzoic acid and the peak at δ=7.8(d) ppm corresponds to the six aromatic protons of 6-amino naphthoic acid. A triplet appearing at the range of δ=2.9-3-3(t) ppm corresponds to the four methylene protons of N-CH_2-CH_2-N- group in DTPABis.^{1}H NMR showed a sharp singlet at around δ = 3.4- 3.7ppm(s) corresponding to the four methylene protons of N-CH_2-C=O, which showed the chemical equivalence of methylene groups in

DTPABis-4ABA and DTPABis-6ANA respectively. A peak at 5.8 corresponds to amine protons and a singlet at 10.5 corresponds to carboxylic acid.

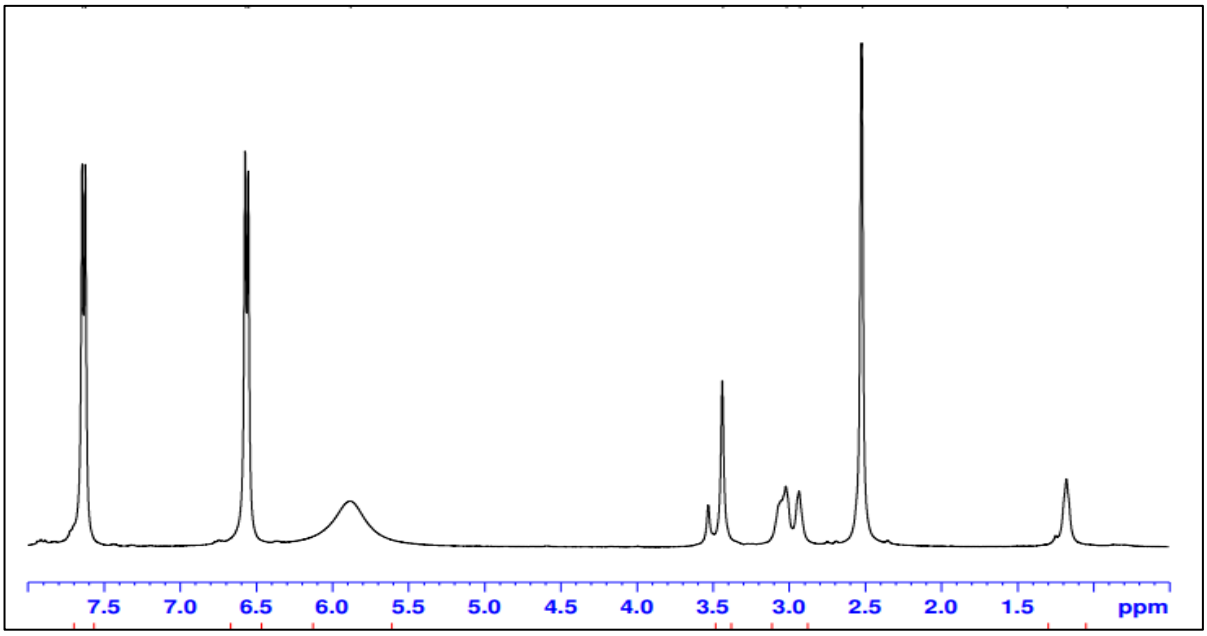

Fig 4.13: ^{1}H NMR of DTPABis-4ABA

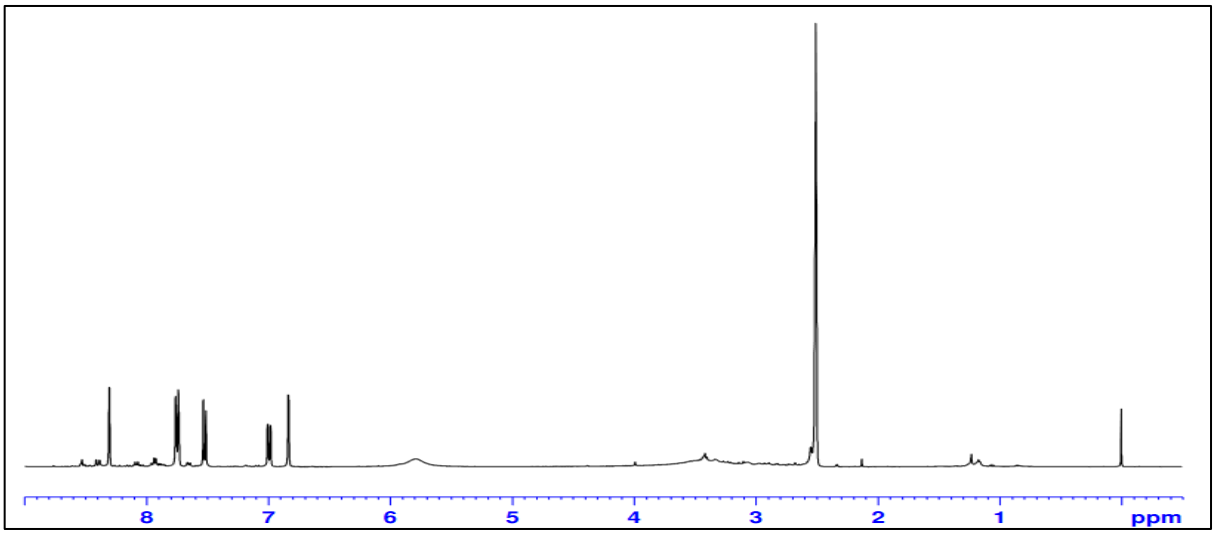

Fig 4.14: ^{1}H NMR of DTPABis-6ANA

A peak at δ=2.7 ppm and a peak at δ=2.6 ppm corresponds to DMSO d6 solvent of EDTABis-4ABA and EDTABis-6ANA respectively. A peak at δ=7.8(d) ppm corresponds to the four aromatic protons of 4-amino benzoic acid and the peak at δ=7.7(d) ppm corresponds to the six aromatic protons of 6-amino naphthoic acid. A triplet appearing at the range of δ=2.83(t) ppm corresponds to the four methylene protons of N-CH_2-CH_2-N- group in EDTABis.^{1}H NMR showed a sharp singlet at around δ = 3.5ppm(s) corresponding to the four methylene protons of N-CH_2-C=O, which showed the chemical equivalence of methylene groups in EDTABis-4ABA and EDTABis-6ANA respectively. A peak at 5.8 and 5.9 corresponds to amine protons. [122]

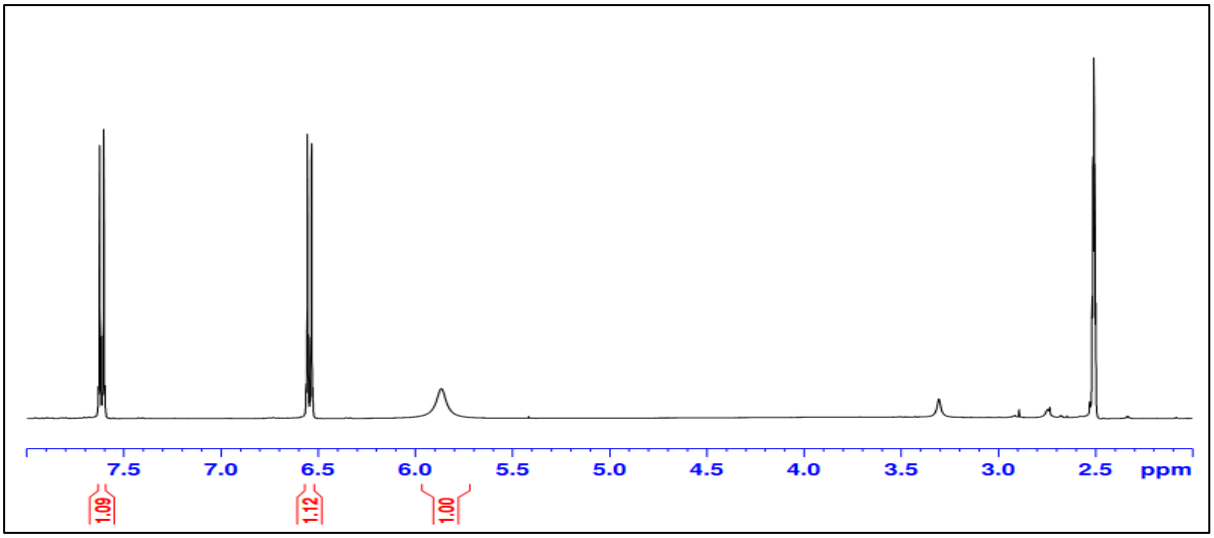

Fig 4.15: ^{1}H NMR of EDTABis-4ABA

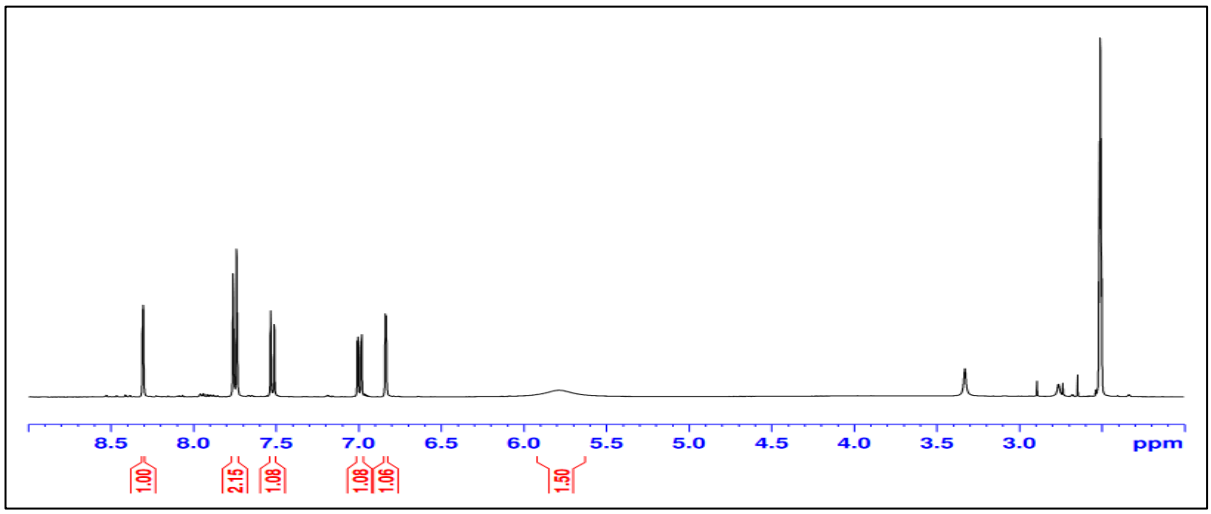

Fig 4.16: ^{1}H NMR of EDTABis-6ANA

Table 3: NMR peaks of ligands

	-N**H**	-COO**H**	Ar-**H**	N-**CH₂**-C=O	N-**CH₂**-C**H₂**-N
EDTABis-4ABA	5.9	-	7.8	3.5	2.8
EDTABis-6ANA	5.8	10.6	7.7	3.4	2.9
DTPABis-4ABA	5.8	10.5	7.6	3.4	2.9
DTPABis-6ANA	5.8	10.6	7.8	3.7	3.3

4.4 ELECTRON SPIN RESONANCE SPECTRUM of DTPABis-6ANA:

The effective g value of 2.04 indicated that dipolar interactions between manganese ions are present. This is because Mn (II) ions have a $3d^5$ electronic configuration for the ^{55}Mn nucleus, with a nuclear spin of I=5/2. As a result, the EPR spectrum of the Mn (II) complex at room temperature displays a characteristic six-line hyperfine splitting.

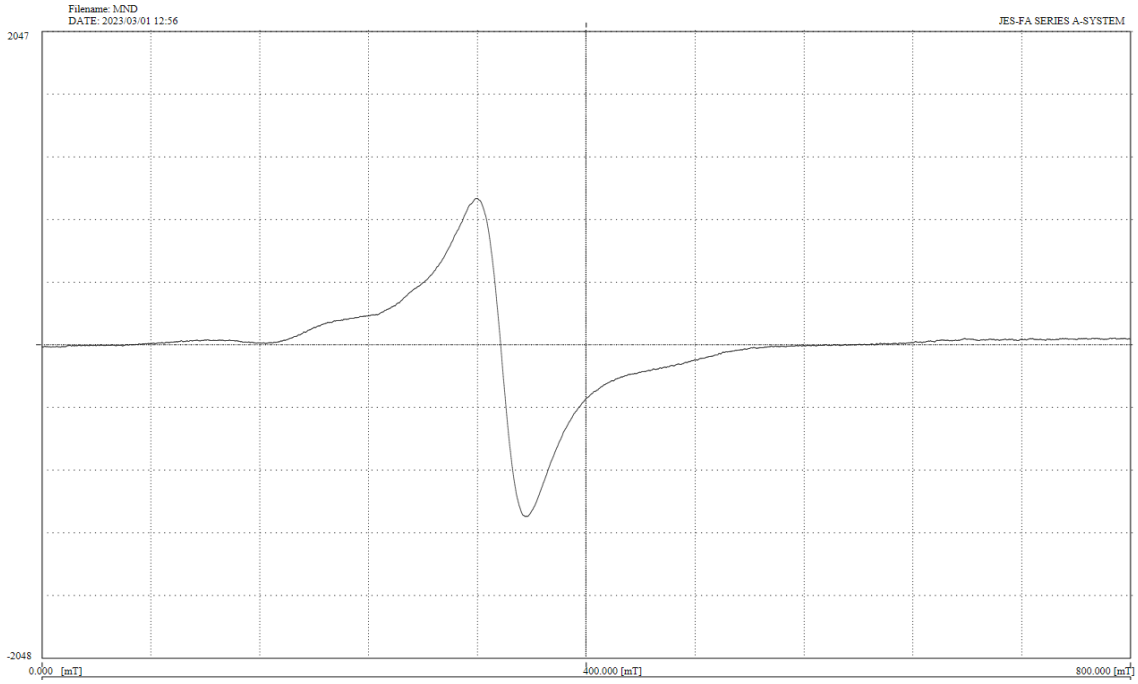

Fig 4.17: ESR spectrum of MnDTPABis-6ANA

However, if the symmetry around the Mn (II) ion is distorted due to complexation, the resonances become anisotropic, and a randomly oriented sample may exhibit a broad line. The broad signal observed in the present work suggests that the symmetry around the Mn (II) ion in the complex is distorted.

4.5 THERMO GRAVIMETRIC STUDIES:

Thermo Gravimetric Analysis (TGA) provides detailed information about the decomposition temperature of the analyte at various temperatures.

TGA was taken for MnDTPABis-6ANA and MnEDTABis-4ABA.

For MnDTPABis-6ANA, at temperature 90°C there is a slight weight loss due to loss of water molecules. The weight loss at 110°C corresponds to sodium bicarbonate. At 320°C the weight loss is due to degradation of 6-amino naphthoic acid. The weight loss at 470°C is due to loss of DTPA molecule. After 650°C the metal decomposes as metal oxide.

For MnEDTABis-4ABA, at temperature 90°C there is a slight weight loss due to loss of water molecules. The weight loss at 110°C corresponds to sodium bicarbonate. The weight loss at 360°C corresponds to loss of 4-amino benzoic acid. At 450°C the weight loss is due to decomposition of EDTA. After 650°C the metal decomposes as metal oxide.

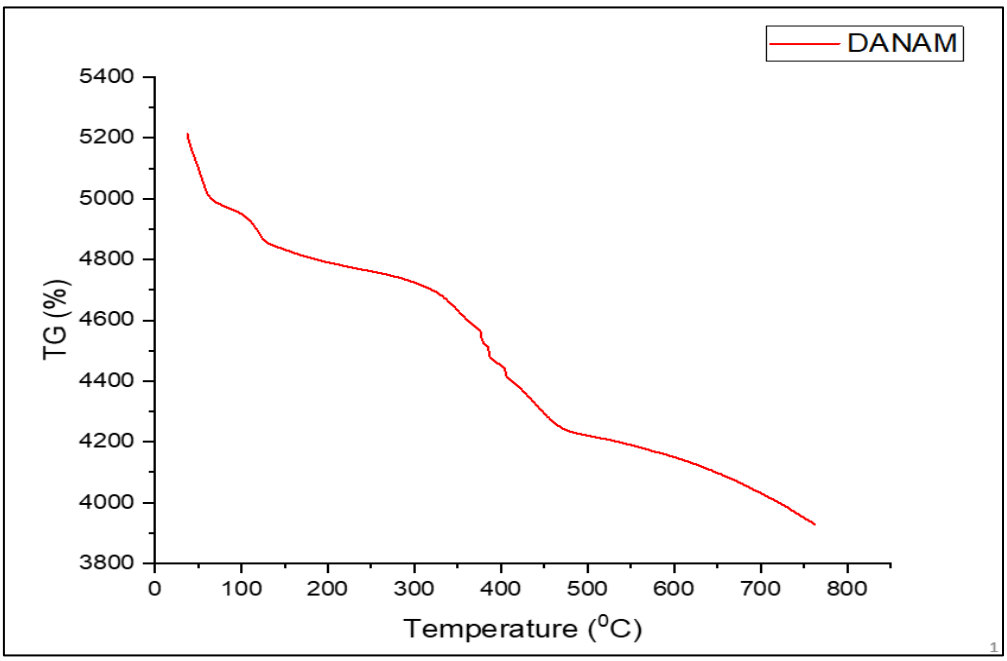

Fig 4.18: Thermogram of MnDTPABis-6ANA

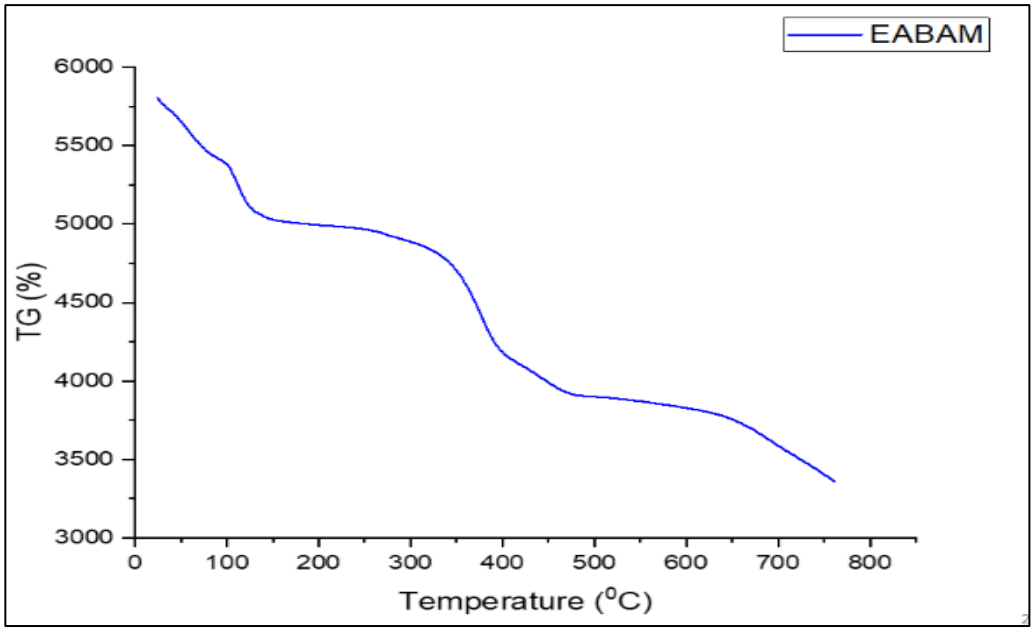

Fig 4.19: Thermogram of MnEDTABis-4ABA

4.6 FLUORESCENCE SPECTROSCOPY:

Photoluminescence measurements allow us to evaluate the impact caused on the emission properties of the ligands due to coordination of the transition metal cations. Excitation of the ligand 4-aminobenzoicacid at 278 and 378 nm resulted in an emission maximum at 350 and 450nm. Excitation of the ligand 6-amino naphthoic acid at 278 and 345 nm resulted in an emission maximum at 420 and 420nm **[123].** Similarly, the complex with 4-aminobenzoic acid also exhibited emission shift from 248 and 305 to 410nm. The complex with 6- amino naphthoic acid also exhibited emission shift from 243 and 302 to 420 and 410nm. In EDTA complexes, ligands EDTABis-4ABA and EDTABis-6ANA showed good fluorescence intensity at 353nm and 421nm respectively. The complex MnEDTABis-6ANA showed the maximum intensity at 411nm. Comparing the fluorescence activity of Gd-DTPA complexes, Mn – DTPA bis anhydride complexes showed good fluorescence emission. Emission wavelength of commercial contrast agent Gd-DTPA was at 305 nm **[124]** due to f–f transition of central Gd^{3+}, whereas the emission wavelength of the prepared Mn – DTPA bis anhydride complexes exhibit at 410 nm. This red shift might be due to the increased π-conjugation because of the formation of C - N bond based on aromatic group of DTPA bis-anhydride with 4-aminobenzoic acid and 6-amino naphthoic acid. Compared to Mn – DTPA bis anhydride complexes, the range of fluorescent intensity of Gd-DTPA was low and nearly negligible. And MnEDTABis-6ANA showed the maximum intensity out of all the complexes. These results suggest that Manganese complexes of DTPA and EDTA with 4-amino benzoic acid and 6-amino naphthoic acid could be used in fluorescence imaging techniques. Further studies of this compounds may also lead to imaging properties which can be used as contrast agents.

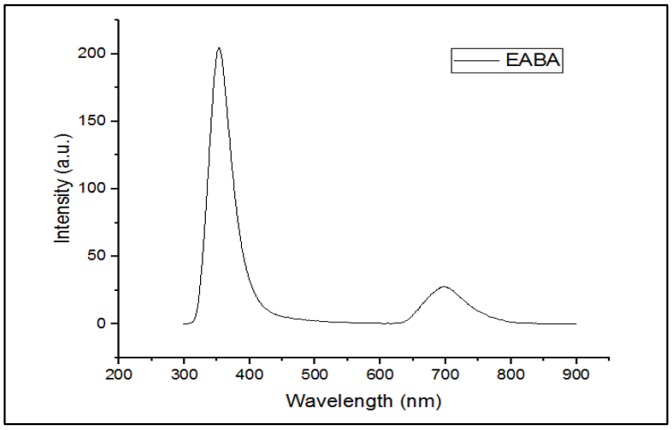

EDTABis-4ABA

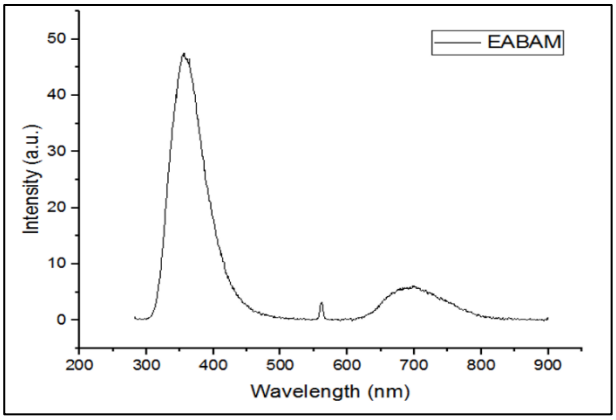

MnEDTABis-4ABA

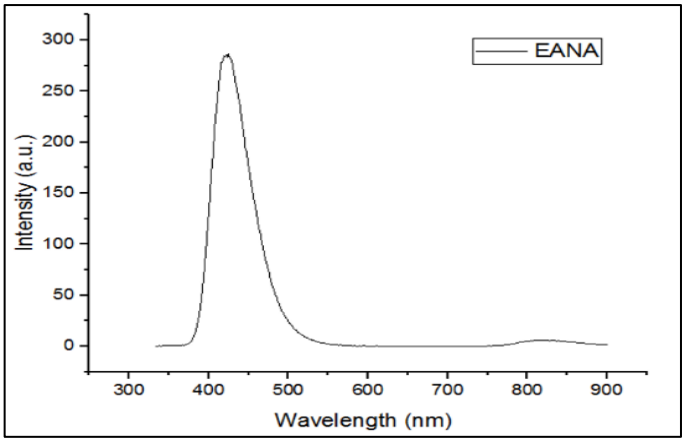

EDTABis-6ANA

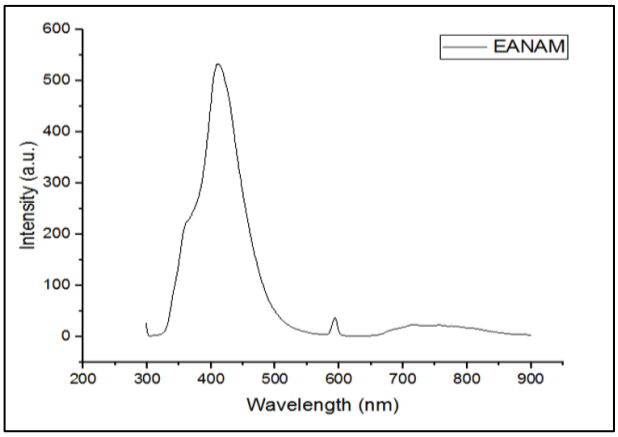

MnEDTABis-6ANA

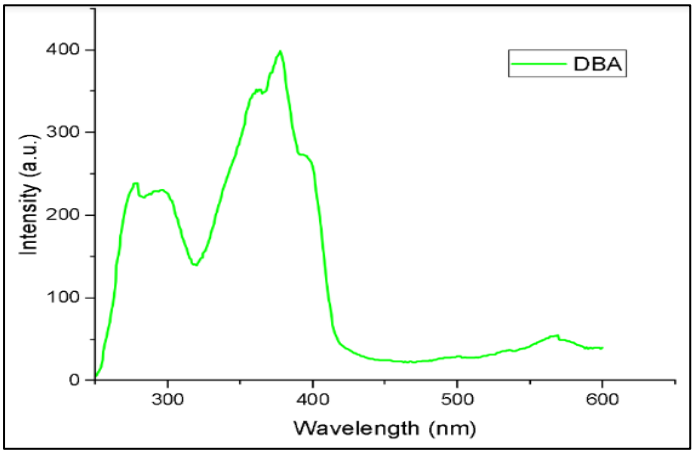

DTPABis-4ABA

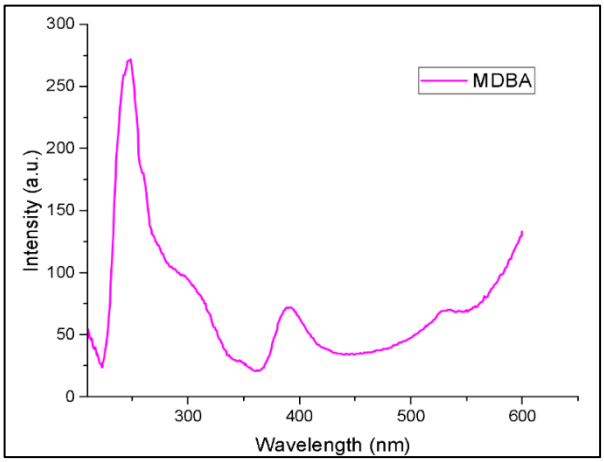

MnDTPABis-4ABA

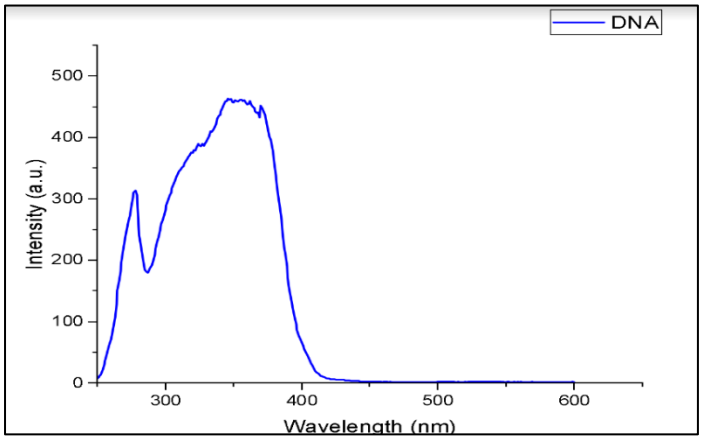

DTPABis-6ANA

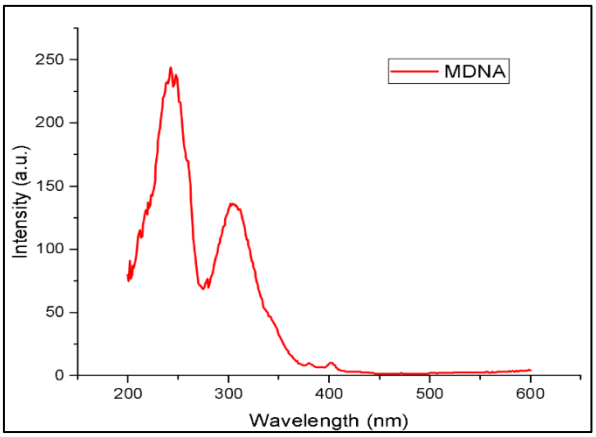

MnDTPABis-6ANA

Fig4.20: Emission Spectrum of ligands and complexes of EDTA &DTPA compounds

4.7 ANTI-BACTERIAL ACTIVITIES:

The Mn complexes showed good antimicrobial activity against various pathogens depending upon nature of the ligand in the complexes and concentration of the complexes. The zone of inhibition of the complexes and ligands is given in table. Generally, the activity of the complexes can be explained on the basis of chelation. This increased activity upon chelation is attributed to Tweedy's chelation theory, according to which, the chelation reduces the polarity of the metal atom mainly because of the positive charge of the metal partially shared with donor atoms present on the ligand and there is electron delocalization over the whole chelate ring . This, in turn, increases the lipophilic character of the metal chelate and favours its permeation through the lipid layers of the bacterial membranes. Generally, it is suggested that the chelated complexes deactivate various cellular enzymes, which play a vital role in various metabolic pathways. of these microorganisms. Other factors such as solubility, conductivity and dipole moment, affected by the presence of metal ions, may also increase the biological activity of the metal complexes compared to the ligand [125]. These complexes may also disturb the respiration process of the cell and thus block the synthesis of proteins, which restricts further growth of the organism. All the ligands and complexes showed moderate activities towards the tested microbe *Staphylococcus aureus.*

The ligands and complexes of EDTA and DTPA with 4 – amino benzoic acid and 6-amino naphthoic acid were tested against a gram-positive bacteria *Staphylococcus aureus* and a gram-negative bacteria *E. coli* with the standards Ampicillin and Rifampicin at 20µl concentration. Considering the ligands of DTPA, 6-amino naphthoic acid with DTPA bisanhydride showed good activity against the bacteria. In EDTA ligands, 6-aminonaphthoic acid showed good resistance against *Staphylococcus aureus* and 4-aminobenzoic acid showed good resistance against E.*coli.* The complexes also showed considerable activity against the bacteria. In DTPA complexes, complex of 4-amino benzoic acid showed good resistance to *E. coli.* In EDTA complexes, 6-amino naphthoic acid showed good activity against E.coli. Also, to conclude further, it can be said that complexes of EDTA showed good bacterial resistant activity than DTPA complexes.

Table 4: Zone of inhibition of DTPA based ligands and complexes

Sample	Zone of Inhibition (mm)	
	Staphylococcus aureus	*E.coli*
Standard (Rifampicin)	35mm	19mm
DTPABis	16mm	15mm
DTPABis-4ABA	16mm	16mm
DTPABis-6ANA	15mm	17mm
MnDTPABis-4ABA	16mm	15mm
MnDTPABis-6ANA	18mm	14mm

Fig 4.21: Zone of inhibition of DTPA compounds

Table5: Zone of inhibition of EDTA based ligands and complexes

Sample	Zone of Inhibition (mm)	
	Staphylococcus aureus	*E.coli*
Standard (Ampicillin)	13mm	14mm
EDTABis	18mm	15mm
EDTABis-4ABA	13mm	18mm
MnEDTABis-4ABA	9mm	10mm
EDTABis-6ANA	15mm	13mm
MnEDTABis-6ANA	9mm	13mm

Fig 4.22: Zone of inhibition of EDTA compounds

SUMMARY &CONCLUSION

5.SUMMARY AND CONCLUSION

Metal complexes of poly amino carboxylic acids were synthesised and subjected to various spectroscopic techniques to confirm their structure and nature. The IR and NMR spectral techniques revealed the structural information. The excitation and emission spectrum gave the data related to absorption and emission nature of ligand and complexes. The IR bands of C-N and of metal with oxygen revealed the formation of ligands and complexes respectively. The biological effect of compounds was studied by anti-bacterial test. The ligands and complexes of EDTA and DTPA compounds showed good resistant activity against gram positive bacteria *Staphylococcus aureus* and gram negative bacteria *E.coli.* From the fluorescence spectrums of ligands and compounds, all the ligands and complexes showed good fluorescence activities with moderate and excellent emissions. These compounds maybe further studied to utilise them for imaging techniques. Since the compounds also showed good biological activities, which were compatible with the human body, these compounds may also be studied further in usage as contrast agents in MRI imaging technique. Further the polyamino carboxylic acids like EDTA, EGTA, TTHA, DTPA etc.., maybe also attached with different amino acids and their complexes will be studied for imaging purposes.

BIBILIOGRAPHY

1. Werner, E. J., Datta, A., Jocher, C. J., & Raymond, K. N. (2008). High-relaxivity MRI contrast agents: where coordination chemistry meets medical imaging. *Angewandte Chemie International Edition*, *47*(45), 8568-8580.
2. Caravan, P. (2009). Protein-targeted gadolinium-based magnetic resonance imaging (MRI) contrast agents: design and mechanism of action. *Accounts of chemical research*, *42*(7), 851-862.
3. Salzer, R. (Ed.). (2012). *Biomedical imaging: principles and applications*. John Wiley & Sons.
4. http://www.maggiephilbin.com/wp-content/uploads/2010/11/mri-scanner.jpg
5. Mitchell, H. H., Hamilton, T. S., Steggerda, F. R., & Bean, H. W. (1945). The chemical composition of the adult human body and its bearing on the biochemistry of growth. *Journal of Biological Chemistry*, *158*(3), 625-637.
6. McMahon, K. L., Cowin, G., & Galloway, G. (2011). Magnetic resonance imaging: the underlying principles. *journal of orthopaedic & sports physical therapy*, *41*(11), 806-819.
7. The Chemistry of Contrast Agents in Medical Magnetic Resonance Imaging, ed. A. E. Merbach, and E´. Tóth, John Wiley & Sons, Chichester (England), 2001
8. Damadian, R., Zaner, K., Hor, D., & DiMaio, T. (1974). Human tumors detected by nuclear magnetic resonance. *Proceedings of the National Academy of Sciences*, *71*(4), 1471-1473.
9. http://casemed.case.edu/clerkships/neurology/NeurLrngObjectives/MRI.htm
10. Boros, E., Gale, E. M., & Caravan, P. (2015). MR imaging probes: design and applications. *Dalton transactions*, *44*(11), 4804-4818.
11. Bluthirnschranke nach Infarkt nativ und KM.png
12. Aime, S., Botta, M., Fasano, M., & Terreno, E. (1998). Lanthanide (III) chelates for NMR biomedical applications. *Chemical Society Reviews*, *27*(1), 19-29.
13. Qiao, R., Yang, C., & Gao, M. (2009). Superparamagnetic iron oxide nanoparticles: from preparations to in vivo MRI applications. *Journal of Materials Chemistry*, *19*(35), 6274-6293.
14. Maiocchi, A. (2003). The use of molecular descriptors in the design of gadolinium (III) chelates as MRI contrast agents. *Mini Reviews in Medicinal Chemistry*, *3*(8), 845-859.
15. Schmitt-Willich, H. (2007). Stability of linear and macrocyclic gadolinium based contrast agents. *The British journal of radiology*, *80*(955), 581-582.

16. Port, M., Idée, J. M., Medina, C., Robic, C., Sabatou, M., & Corot, C. (2008). Efficiency, thermodynamic and kinetic stability of marketed gadolinium chelates and their possible clinical consequences: a critical review. *Biometals*, *21*(4), 469-490.
17. Major, J. L., & Meade, T. J. (2009). Bioresponsive, cell-penetrating, and multimeric MR contrast agents. *Accounts of chemical research*, *42*(7), 893-903.
18. Runge, V. M., Dickey, K. M., Williams, N. M., & Peng, X. (2002). Local tissue toxicity in response to extravascular extravasation of magnetic resonance contrast media. *Investigative radiology*, *37*(7), 393-398.
19. Runge, V. M., Price, A. C., Wehr, C. J., Atkinson, J. B., & Tweedle, M. F. (1985). Contrast enhanced MRI. Evaluation of a canine model of osmotic blood-brain barrier disruption. *Investigative radiology*, *20*(8), 830-844.
20. Dietz, B. (2014). *Positron emission tomography quantification of stem cells in cardiovascular disease* (Master's thesis).
21. Lutz, A. M., Seemayer, C., Corot, C., Gay, R. E., Goepfert, K., Michel, B. A., ... & Weishaupt, D. (2004). Detection of synovial macrophages in an experimental rabbit model of antigen-induced arthritis: ultrasmall superparamagnetic iron oxide–enhanced MR imaging. *Radiology*, *233*(1), 149-157.
22. Lauffer, R. B. (1987). Paramagnetic metal complexes as water proton relaxation agents for NMR imaging: theory and design. *Chemical reviews*, *87*(5), 901-927.
23. Raymond, K. N., & Pierre, V. C. (2005). Next generation, high relaxivity gadolinium MRI agents. *Bioconjugate chemistry*, *16*(1), 3-8.
24. M. Bottrill, L. Kwok and N. J. Long, Chem. Soc. Rev., 2006, 35, 557
25. Geraldes, C. F., & Laurent, S. (2009). Classification and basic properties of contrast agents for magnetic resonance imaging. *Contrast media & molecular imaging*, *4*(1), 1-23.
26. Lee, S. Y., Kang, M. S., Jeong, W. Y., Han, D. W., & Kim, K. S. (2020). Hyaluronic acid-based theranostic nanomedicines for targeted cancer therapy. *Cancers*, *12*(4), 940.
27. Chandra, T., Pukenas, B., Mohan, S., & Melhem, E. (2012). Contrast-enhanced magnetic resonance angiography. *Magnetic Resonance Imaging Clinics*, *20*(4), 687-698.
28. (a) K. Wai-Y. Chan, S. Barra, M. Botta and Wing-T. Wong, J. Inorg. Biochem., 2004, 98, 677; (b) S. Gu, Hee-K. Kim, G. H. Lee, Bong-S. Kang, Y. Chang and Tae-J. Kim, J. Med. Chem., 2011, 54, 143; (c) A. Takács, R. Napolitano, M. Purgel, A. C. Bényei, L. Zékány, E. Brücher, I. Tóth, Z. Baranyai and S. Aime, Inorg. Chem., 2014, 53, 1858; (d)B. Jebasningh and V. Alexander, Inorg. Chem., 2005, 44, 9434

29. Hart, J. R. (2000). Ethylenediaminetetraacetic acid and related chelating agents. *Ullmann's encyclopedia of industrial chemistry*.
30. DeBusk, R. (2002). Ethylenediaminetetraacetic acid (EDTA), University of Maryland Medical Center Website
31. Auld, D. S. (1995). Methods in Enzymology: Proteolytic Enzymes: Aspartic and Metallo Peptidases..
32. Paolieri, M. (2017). Ferdinand Münz: EDTA and 40 years of inventions. *Bull. Hist. Chem*, *42*(2), 133-140.
33. Holleman, A. F.; Wiberg, E. (2001). *Inorganic Chemistry*. San Diego: Academic Press. ISBN 978-0-12-352651-9
34. Deblonde, G. J. P., Kelley, M. P., Su, J., Batista, E. R., Yang, P., Booth, C. H., & Abergel, R. J. (2018). Spectroscopic and computational characterization of diethylenetriaminepentaacetic acid/transplutonium chelates: evidencing heterogeneity in the heavy actinide (III) series. *Angewandte Chemie International Edition*, *57*(17), 4521-4526.
35. Fomenko, V. V., Polynova, T. N., Porai-Koshits, M. A., Varlamova, G. L., & Pechurova, N. I. (1973). Crystal structure of copper (II) diethylenetriaminepentaacetate monohydrate. *Journal of Structural Chemistry*, *14*(3), 529-529.
36. Fisher, Anna E.O.; Maxwell, Suzette C.; Naughton, Declan P. (2004). "Superoxide and hydrogen peroxide suppression by metal ions and their EDTA complexes". *Biochemical and Biophysical Research Communications*. **316** (1): 48–51
37. Zech, C. J., Herrmann, K. A., Reiser, M. F., & Schoenberg, S. O. (2007). MR imaging in patients with suspected liver metastases: value of liver-specific contrast agent Gd-EOB-DTPA. *Magnetic resonance in medical sciences*, *6*(1), 43-52.
38. Niendorf, H. P., Haustein, J., Cornelius, I., Alhassan, A., & Clauss, W. (1991). Safety of gadolinium-DTPA: extended clinical experience. *Magnetic resonance in medicine*, *22*(2), 222-228.
39. Ao, M., Wang, Z., Ran, H., Guo, D., Yu, J., Li, A., ... & Zheng, Y. (2010). Gd-DTPA-loaded PLGA microbubbles as both ultrasound contrast agent and MRI contrast agent—A feasibility research. *Journal of Biomedical Materials Research Part B: Applied Biomaterials*, *93*(2), 551-556.

40. Schuhmann-Giampieri, G., Schmitt-Willich, H., Press, W. R., Negishi, C., Weinmann, H. J., & Speck, U. (1992). Preclinical evaluation of Gd-EOB-DTPA as a contrast agent in MR imaging of the hepatobiliary system. *Radiology*, *183*(1), 59-64.

41. Wen, X., Jackson, E. F., Price, R. E., Kim, E. E., Wu, Q., Wallace, S., ... & Li, C. (2004). Synthesis and characterization of poly (L-glutamic acid) gadolinium chelate: a new biodegradable MRI contrast agent. *Bioconjugate chemistry*, *15*(6), 1408-1415.

42. Lattuada, L., & Lux, G. (2003). Synthesis of Gd-DTPA-cholesterol: a new lipophilic gadolinium complex as a potential MRI contrast agent. *Tetrahedron letters*, *44*(20), 3893-3895.

43. Shahbazi-Gahrouei, D., Williams, M., Rizvi, S., & Allen, B. J. (2001). In vivo studies of Gd-DTPA-monoclonal antibody and gd-porphyrins: Potential magnetic resonance imaging contrast agents for melanoma. *Journal of Magnetic Resonance Imaging: An Official Journal of the International Society for Magnetic Resonance in Medicine*, *14*(2), 169-174.

44. Langereis, S., de Lussanet, Q. G., van Genderen, M. H., Meijer, E. W., Beets-Tan, R. G., Griffioen, A. W., ... & Backes, W. H. (2006). Evaluation of Gd (III) DTPA-terminated poly (propylene imine) dendrimers as contrast agents for MR imaging. *NMR in Biomedicine: An International Journal Devoted to the Development and Application of Magnetic Resonance In vivo*, *19*(1), 133-141

45. Lee, H. Y., Jee, H. W., Seo, S. M., Kwak, B. K., Khang, G., & Cho, S. H. (2006). Diethylenetriaminepentaacetic Acid− Gadolinium (DTPA-Gd)-Conjugated Polysuccinimide Derivatives as Magnetic Resonance Imaging Contrast Agents. *Bioconjugate chemistry*, *17*(3), 700-706.

46. Lee, H. Y., Jee, H. W., Seo, S. M., Kwak, B. K., Khang, G., & Cho, S. H. (2006). Diethylenetriaminepentaacetic Acid− Gadolinium (DTPA-Gd)-Conjugated Polysuccinimide Derivatives as Magnetic Resonance Imaging Contrast Agents. *Bioconjugate chemistry*, *17*(3), 700-706.

47. Sun, G., Feng, J., Jing, F., Pei, F., & Liu, M. (2003). Synthesis and evaluation of novel polysaccharide-Gd-DTPA compounds as contrast agent for MRI. *Journal of magnetism and magnetic materials*, *265*(2), 123-129.

48. Nakamura, T., Ohana, T., Yabuno, H., Kasai, R., Suzuki, T., & Hasebe, T. (2012). Simple fabrication of Gd (III)-DTPA-nanodiamond particles by chemical modification for use as magnetic resonance imaging (MRI) contrast agent. *Applied physics express*, *6*(1), 015001.

49. Doiron, A. L., Chu, K., Ali, A., & Brannon-Peppas, L. (2008). Preparation and initial characterization of biodegradable particles containing gadolinium-DTPA contrast agent for enhanced MRI. *Proceedings of the National Academy of Sciences*, *105*(45), 17232-17237.

50. Gupta, A., Stait-Gardner, T., De Campo, L., Waddington, L. J., Kirby, N., Price, W. S., & Moghaddam, M. J. (2014). Nanoassemblies of Gd–DTPA–monooleyl and glycerol monooleate amphiphiles as potential MRI contrast agents. *Journal of Materials Chemistry B*, *2*(9), 1225-1233.

51. Gupta, A., de Campo, L., Rehmanjan, B., Willis, S. A., Waddington, L. J., Stait-Gardner, T., ... & Moghaddam, M. J. (2015). Evaluation of Gd-DTPA-monophytanyl and phytantriol nanoassemblies as potential MRI contrast agents. *Langmuir*, *31*(4), 1556-1563.

52. Molnar, E., Camus, N., Patinec, V., Rolla, G. A., Botta, M., Tircso, G., ... & Platas-Iglesias, C. (2014). Picolinate-containing macrocyclic Mn2+ complexes as potential MRI contrast agents. *Inorganic Chemistry*, *53*(10), 5136-5149.

53. Drahoš, B., Kubíček, V., Bonnet, C. S., Hermann, P., Lukeš, I., & Tóth, É. (2011). Dissociation kinetics of Mn 2+ complexes of NOTA and DOTA. *Dalton Transactions*, *40*(9), 1945-1951.

54. Uzal-Varela, R., Perez-Fernandez, F., Valencia, L., Rodríguez-Rodríguez, A., Platas-Iglesias, C., Caravan, P., & Esteban-Gomez, D. (2022). Thermodynamic Stability of Mn

(II) Complexes with Aminocarboxylate Ligands Analyzed Using Structural Descriptors. *Inorganic Chemistry*, *61*(35), 14173-14186.

55. Belyanin, M. L., Stepanova, E. V., Valiev, R. R., Filimonov, V. D., Usov, V. Y., Borodin, O. Y., & Ågren, H. (2016). Design, synthesis and evaluation of a new Mn–Contrast agent for MR imaging of myocardium based on the DTPA-phenylpentadecanoic acid complex. *Chemical Physics Letters*, *665*, 111-116.

56. Wang, X., Xu, L., Ren, Z., Fan, M., Zhang, J., Qi, H., & Xu, M. (2019). A novel manganese chelated macromolecular MRI contrast agent based on O-carboxymethyl chitosan derivatives. *Colloids and Surfaces B: Biointerfaces*, *183*, 110452.

57. Ye, C. H., Sun, H. L., Wang, X. Y., Li, J. R., Nie, D. B., Fu, W. F., & Gao, S. (2004). Preparation of three terbium complexes with p-aminobenzoic acid and investigation of crystal structure influence on luminescence property. *Journal of Solid State Chemistry*, *177*(10), 3735-3742.

58. Chen, K., Li, P., Zhu, C., Xia, Z., Xia, Q., Zhong, L., ... & Zhu, J. (2021). Mn (II) complex of lipophilic group-modified ethylenediaminetetraacetic acid (EDTA) as a new hepatobiliary MRI contrast agent. *Journal of Medicinal Chemistry*, *64*(13), 9182-9192

59. Moghaddam, M. J., De Campo, L., Waddington, L. J., & Drummond, C. J. (2010). Chelating phytanyl-EDTA amphiphiles: self-assembly and promise as contrast agents for medical imaging. *Soft Matter*, *6*(23), 5915-5929.

60. Islam, M. K., Kim, S., Kim, H. K., Park, S., Lee, G. H., Kang, H. J., ... & Chang, Y. (2017). Manganese complex of ethylenediaminetetraacetic acid (EDTA)–benzothiazole aniline (BTA) conjugate as a potential liver-targeting MRI contrast agent. *Journal of medicinal chemistry*, *60*(7), 2993-3001.

61. Carvalho, J. F., Kim, S. H., & Chang, C. A. (1992). Synthesis and metal complex selectivity of macrocyclic DTPA and EDTA bis (amide) ligands. *Inorganic Chemistry*, *31*(20), 4065-4068.

62. Frey, S. T., Chang, C. A., Carvalho, J. F., Varadarajan, A., Schultze, L. M., Pounds, K. L., & Horrocks Jr, W. D. (1994). Characterization of lanthanide complexes with a series of amide-based macrocycles, potential MRI contrast agents, using Eu3+ luminescence spectroscopy and molecular mechanics. *Inorganic Chemistry*, *33*(13), 2882-2889.

63. Troughton, J. S., Greenfield, M. T., Greenwood, J. M., Dumas, S., Wiethoff, A. J., Wang, J., ... & Caravan, P. (2004). Synthesis and evaluation of a high relaxivity manganese (II)-based MRI contrast agent. *Inorganic chemistry*, *43*(20), 6313-6323.

64. Mishra, A., Fousková, P., Angelovski, G., Balogh, E., Mishra, A. K., Logothetis, N. K., & Tóth, É. (2008). Facile synthesis and relaxation properties of novel bispolyazamacrocyclic Gd3+ complexes: an attempt towards calcium-sensitive MRI contrast agents. *Inorganic Chemistry*, *47*(4), 1370-1381.

65. Liu, D. S., Sui, Y., Li, C. H., Cheng, W. T., Wang, T. W., & You, X. Z. (2011). Synthesis, structure and magnetic properties of a two-dimensional manganese (II) complex with a maximum denticity of ethylenediaminetetraacetic ligand. *Inorganica Chimica Acta*, *376*(1), 112-117.

66. Liu, D. S., Qiu, Z. J., Xiao, Y. L., Shen, Y. J., Zhou, Q., Chen, W. T., & Sui, Y. (2019). A novel tetranuclear Pb2+ compound based on ethylenediaminetetraacetate and azide mixed-ligands: Synthesis, structure and properties. *Journal of Solid State Chemistry*, *279*, 120952.

67. Baroni, S., Colombo Serra, S., Fringuello Mingo, A., Lux, G., Giovenzana, G. B., & Lattuada, L. (2016). Synthesis and relaxometric characterization of a new Mn (II)-EDTA-deoxycholic acid conjugate complex as a potential MRI blood pool agent. *ChemistrySelect*, *1*(8), 1607-1612.

68. Wang, X. F., Gao, J., Wang, J., Zhang, Z. H., Wang, Y. F., Chen, L. J., ... & Zhang, X. D. (2008). Crystal structures of seven-coordinate (NH 4) 2 [Mn II (edta)(H 2 O)]· 3H 2 O,(NH 4) 2 [Mn II (cydta)(H 2 O)]· 4H 2 O and K 2 [MN II (hdtpa)]· 3.5 H 2 O complexes. *Journal of Structural Chemistry*, *49*, 724-731

69. Cheng, W., Ganesh, T., Martinez, F., Lam, J., Yoon, H., Macgregor, R. B., ... & Zhang, X. A. (2014). Binding of a dimeric manganese porphyrin to serum albumin: towards a gadolinium-free blood-pool T 1 MRI contrast agent. *JBIC Journal of Biological Inorganic Chemistry*, *19*, 229-235.

70. Raymond, K. N., & Pierre, V. C. (2005). Next generation, high relaxivity gadolinium MRI agents. *Bioconjugate chemistry*, *16*(1), 3-8.
71. Gale, E. M., Atanasova, I. P., Blasi, F., Ay, I., & Caravan, P. (2015). A manganese alternative to gadolinium for MRI contrast. *Journal of the American Chemical Society*, *137*(49), 15548-15557.
72. Wan, F. X., Zhang, T. K., Li, Y., Li, C. C., & Jiang, L. (2016). Synthesis and study on magnetic resonance imaging performance of gd (iii)-dtpa-bisbenzothiazol hydrazide. *Journal of the Chilean Chemical Society*, *61*(2), 2861-2863.
73. Georgopoulou, A., & Williams, D. (1999). Synthesis of water soluble DTPA complexes with pendant uracil moieties capable of forming complementary hydrogen bonds. *Journal of the Chemical Society, Dalton Transactions*, (4), 547-552.
74. Hao, D., Ai, T., Goerner, F., Hu, X., Runge, V. M., & Tweedle, M. (2012). MRI contrast agents: basic chemistry and safety. *Journal of Magnetic Resonance Imaging*, *36*(5), 1060-1071.
75. Drahoš, B., Lukeš, I., & Tóth, É. (2012). Manganese (II) complexes as potential contrast agents for MRI. *European Journal of Inorganic Chemistry*, *2012*(12), 1975-1986.
76. Magerstädt, M., Gansow, O. A., Brechbiel, M. W., Colcher, D., Baltzer, L., Knop, R. H., ... & Naegele, M. (1986). Gd (DOTA): an alternative to Gd (DTPA) as a T1, 2 relaxation agent for NMR imaging or spectroscopy. *Magnetic Resonance in Medicine*, *3*(5), 808-812.
77. Non-Gadolinium-Based MRI Contrast Agents Daniel D. Schwert 1, Julian A. Davies 1, Nicholas Richardson.
78. Konings, M. S., Dow, W. C., Love, D. B., Raymond, K. N., Quay, S. C., & Rocklage, S. M. (1990). Gadolinium complexation by a new diethylenetriaminepentaacetic acid-amide ligand. Amide oxygen coordination. *Inorganic Chemistry*, *29*(8), 1488-1491.
79. Patil, R., Gangalum, P. R., Wagner, S., Portilla-Arias, J., Ding, H., Rekechenetskiy, A., ... & Holler, E. (2015). Curcumin targeted, polymalic acid-based MRI contrast agent for the detection of Aβ plaques in Alzheimer's disease. *Macromolecular bioscience*, *15*(9), 1212-1217.

80. Chang, C. A., Francesconi, L. C., Malley, M. F., Kumar, K., Gougoutas, J. Z., Tweedle, M. F., ... & Wilson, L. J. (1993). Synthesis, characterization, and crystal structures of M (DO3A)(M= iron, gadolinium) and Na [M (DOTA)](M= Fe, yttrium, Gd). *Inorganic Chemistry*, *32*(16), 3501-3508.
81. Kumar, K., Chang, C. A., Francesconi, L. C., Dischino, D. D., Malley, M. F., Gougoutas, J. Z., & Tweedle, M. F. (1994). Synthesis, stability, and structure of gadolinium (III) and yttrium (III) macrocyclic poly (amino carboxylates). *Inorganic Chemistry*, *33*(16), 3567-3575.
82. Knör, S., Modlinger, A., Poethko, T., Schottelius, M., Wester, H. J., & Kessler, H. (2007). Synthesis of Novel 1, 4, 7, 10-Tetraazacyclodecane-1, 4, 7, 10-Tetraacetic Acid (DOTA) Derivatives for Chemoselective Attachment to Unprotected Polyfunctionalized Compounds. *Chemistry–A European Journal*, *13*(21), 6082-6090.
83. Tan, M., Wu, X., Jeong, E. K., Chen, Q., Parker, D. L., & Lu, Z. R. (2010). An effective targeted nanoglobular manganese (II) chelate conjugate for magnetic resonance molecular imaging of tumor extracellular matrix. *Molecular pharmaceutics*, *7*(4), 936-943.
84. Sherry, A. D., Brown, R. D., Geraldes, C. F., Koenig, S. H., Kuan, K. T., & Spiller, M. (1989). Synthesis and characterization of the gadolinium (3+) complex of DOTA-propylamide: a model DOTA-protein conjugate. *Inorganic Chemistry*, *28*(3), 620-622.
85. Rashid, H. U., Martines, M. A. U., Jorge, J., de Moraes, P. M., Umar, M. N., Khan, K., & Rehman, H. U. (2016). Cyclen-based Gd3+ complexes as MRI contrast agents: Relaxivity enhancement and ligand design. *Bioorganic & medicinal chemistry*, *24*(22), 5663-5684.
86. Ranganathan, R. S., Pillai, R. K., Raju, N., Fan, H., Nguyen, H., Tweedle, M. F., ... & Jacques, V. (2002). Polymethylated DOTA ligands. 1. synthesis of rigidified ligands and studies on the effects of alkyl substitution on acid− base properties and conformational mobility. *Inorganic chemistry*, *41*(25), 6846-6855.
87. Wang, X., Jin, T., Comblin, V., Lopez-Mut, A., Merciny, E., & Desreux, J. F. (1992). A kinetic investigation of the lanthanide DOTA chelates. Stability and rates of formation and of dissociation of a macrocyclic gadolinium (III) polyaza polycarboxylic MRI contrast agent. *Inorganic Chemistry*, *31*(6), 1095-1099
88. Ye, Z., Jeong, E. K., Wu, X., Tan, M., Yin, S., & Lu, Z. R. (2012). Polydisulfide manganese (II) complexes as non-gadolinium biodegradable macromolecular MRI contrast agents. *Journal of Magnetic Resonance Imaging*, *35*(3), 737-744.

89. Mukai, T., Namba, S., Arano, Y., Ono, M., Fujioka, Y., Uehara, T., ... & Saji, H. (2002). Synthesis and evaluation of a monoreactive DOTA derivative for indium-111-based residualizing label to estimate protein pharmacokinetics. *Journal of pharmacy and pharmacology*, *54*(8), 1073-1081.
90. Lima, L. M., Esteban-Gómez, D., Delgado, R., Platas-Iglesias, C., & Tripier, R. (2012). Monopicolinate cyclen and cyclam derivatives for stable copper (II) complexation. *Inorganic Chemistry*, *51*(12), 6916-6927.
91. Lewis, M. R., Raubitschek, A., & Shively, J. E. (1994). A facile, water-soluble method for modification of proteins with DOTA. Use of elevated temperature and optimized pH to achieve high specific activity and high chelate stability in radiolabeled immunoconjugates. *Bioconjugate chemistry*, *5*(6), 565-576.
92. Hao, D., Ai, T., Goerner, F., Hu, X., Runge, V. M., & Tweedle, M. (2012). MRI contrast agents: basic chemistry and safety. *Journal of Magnetic Resonance Imaging*, *36*(5), 1060-1071.
93. Shabanpoor, F., Separovic, F., & Wade, J. D. (2011). General method for selective labelling of double-chain cysteine-rich peptides with a lanthanide chelate via solid-phase synthesis. *Journal of Peptide Science*, *17*(3), 169-173.
94. Schottelius, M., Schwaiger, M., & Wester, H. J. (2003). Rapid and high-yield solution-phase synthesis of DOTA-Tyr3-octreotide and DOTA-Tyr3-octreotate using unprotected DOTA. *Tetrahedron letters*, *44*(11), 2393-2396.
95. De León-Rodríguez, L. M., Viswanathan, S., & Sherry, A. D. (2010). Improved synthesis of DOTA tetraamide ligands for lanthanide (III) ions: A tool for increasing the repertoire of potential PARACEST contrast agents for MRI and/or fluorescent sensors. *Contrast media & molecular imaging*, *5*(3), 121-125.
96. Lewis, M. R., Kao, J. Y., Anderson, A. L. J., Shively, J. E., & Raubitschek, A. (2001). An improved method for conjugating monoclonal antibodies with N-hydroxysulfosuccinimidyl DOTA. *Bioconjugate chemistry*, *12*(2), 320-324.
97. Sinha, D., Shukla, G., Tiwari, A. K., Chaturvedi, S., Chuttani, K., Chandra, H., & Mishra, A. K. (2009). 99mTc-DTPA-amino acids conjugate as specific SPECT pharmaceuticals for tumor imaging. *Chemical biology & drug design*, *74*(2), 159-164.
98. Montembault, V., Soutif, J. C., & Brosse, J. C. (1996). Synthesis of chelating molecules as agents for magnetic resonance imaging, 31. Polycondensation of diethylenetriaminepentaacetic acid bisanhydride with diols and diamines. *Reactive and Functional Polymers*, *29*(1), 29-39.

99. Georgopoulou, A., & Williams, D. (1999). Synthesis of water soluble DTPA complexes with pendant uracil moieties capable of forming complementary hydrogen bonds. *Journal of the Chemical Society, Dalton Transactions*, (4), 547-552.

100. Ouyang, M., Zhuo, R., & Fu, G. (1996). Synthesis and relaxivity of polyamide paramagnetic metal complexes for magnetic resonance imaging. *Polymers for Advanced Technologies*, *7*(8), 671-674.

101. Zhao, X., Zhuo, R., Lu, Z., & Liu, W. (1997). Synthesis, characterization and relaxivity of amphiphilic chelates of DTPA derivatives with GdIII, YbIII and MnII. *Polyhedron*, *16*(16), 2755-2759.

102. Ying-Chun, L., Jing, Z., Quan, L., Shu-Lan, M., Miao-Qiong, X., & Wen-Xiang, Z. (2005). Structural Characterization and Relaxivity Study of a New Paramagnetic Mn (II) Complex of DTPA-BpABA. *Chinese Journal of Chemistry*, *23*(8), 1012-1016.

103. Zhang, D. W., Yang, Z. Y., Zhang, S. P., & Yang, R. D. (2006). Synthesis, characterization and relaxation properties of four non-ion transition metal manganese (II), cobalt (II), nickel (II) and copper (II) complexes with derivatives from diethylene triamine pentaacetic acid and isoniazid. *Transition metal chemistry*, *31*, 333-336.

104. Renxi, Z., Gongcheng, F., Ming, O., Xia, Z., & Zhengrong, L. (1996). Modified DTPA, EDTA ligands and their paramagnetic metal complexes as contrast agents for MRI. *Wuhan University Journal of Natural Sciences*, *1*, 225-229.

105. Alhamami, M., Cheng, W., Lyu, Y., Allen, C., Zhang, X. A., & Cheng, H. L. M. (2018). Manganese-porphyrin-enhanced MRI for the detection of cancer cells: A quantitative in vitro investigation with multiple clinical subtypes of breast cancer. *PLoS One*, *13*(5), e0196998.

106. Matzku, S., Schuhmacher, J., Kirchgeßner, H., & Brüggen, J. (1986). Labeling of monoclonal antibodies with a 67Ga-phenolic aminocarboxylic acid chelate: Part II. Comparison of immunoreactivity and biodistribution of monoclonal antibodies labeled with the 67Ga-chelate or with 131I. *European journal of nuclear medicine*, *12*(8), 405-412.

107. Wahsner, J., Gale, E. M., Rodríguez-Rodríguez, A., & Caravan, P. (2018). Chemistry of MRI contrast agents: current challenges and new frontiers. *Chemical reviews*, *119*(2), 957-1057.

108. Brücher, E. O., Tircsó, G., Baranyai, Z., Kovács, Z., & Sherry, A. D. (2013). Stability and toxicity of contrast agents. *The chemistry of contrast agents in medical magnetic resonance imaging*, 157-208.

109. Demay-Drouhard, P., Ching, H. V., Akhmetzyanov, D., Guillot, R., Tabares, L. C., Bertrand, H. C., & Policar, C. (2016). A Bis-Manganese (II)–DOTA Complex for Pulsed Dipolar Spectroscopy. *ChemPhysChem*, *17*(13), 2066-2078.

110. Chong, H. S., Lim, S., Baidoo, K. E., Milenic, D. E., Ma, X., Jia, F., ... & Lewis, M. R. (2008). Synthesis and biological evaluation of a novel decadentate ligand DEPA. *Bioorganic & medicinal chemistry letters*, *18*(21), 5792-5795

111. Doiron, A. L., Chu, K., Ali, A., & Brannon-Peppas, L. (2008). Preparation and initial characterization of biodegradable particles containing gadolinium-DTPA contrast agent for enhanced MRI. *Proceedings of the National Academy of Sciences*, *105*(45), 17232-17237.

112. Kakkar, D., Tiwari, A. K., Chuttani, K., Kaul, A., Singh, H., & Mishra, A. K. (2010). Comparative evaluation of glutamate-sensitive radiopharmaceuticals: Technetium-99m–glutamic acid and technetium-99m–diethylenetriaminepentaacetic acid–bis (Glutamate) conjugate for tumor imaging. *Cancer biotherapy & radiopharmaceuticals*, *25*(6), 645-655.

113. Renxi, Z., Gongcheng, F., Ming, O., Xia, Z., & Zhengrong, L. (1996). Modified DTPA, EDTA ligands and their paramagnetic metal complexes as contrast agents for MRI. *Wuhan University Journal of Natural Sciences*, *1*, 225-229.

114. Belyanin, M. L., Stepanova, E. V., Valiev, R. R., Filimonov, V. D., Usov, V. Y., Borodin, O. Y., & Ågren, H. (2016). Design, synthesis and evaluation of a new Mn–Contrast agent for MR imaging of myocardium based on the DTPA-phenylpentadecanoic acid complex. *Chemical Physics Letters*, *665*, 111-116.

115. (a) K. Wai-Y. Chan, S. Barra, M. Botta and Wing-T. Wong, J. Inorg. Biochem., 2004,98, 677; (b) S. Gu, Hee-K. Kim, G. H. Lee, Bong-S. Kang, Y. Chang and Tae-J. Kim,J.Med. Chem., 2011, 54, 143; (c) A. Takács, R. Napolitano, M. Purgel, A. C. Bényei,L.Zékány, E. Brücher, I. Tóth, Z. Baranyai and S. Aime, Inorg. Chem., 2014, 53, 1858; (d) B. Jebasningh and V. Alexander, Inorg. Chem., 2005, 44, 9434.

116. http://casemed.case.edu/clerkships/neurology/NeurLrngObjectives/MRI.htm

117. Maiocchi, A. (2003). The use of molecular descriptors in the design of gadolinium (III) chelates as MRI contrast agents. *Mini Reviews in Medicinal Chemistry*, *3*(8), 845-859.

118. Schmitt-Willich, H. (2007). Stability of linear and macrocyclic gadolinium based contrast agents. *The British journal of radiology*, *80*(955), 581-582.

119. Major, J. L., & Meade, T. J. (2009). Bioresponsive, cell-penetrating, and multimeric MR contrast agents. *Accounts of chemical research*, *42*(7), 893-903.

120. Runge, V. M., Dickey, K. M., Williams, N. M., & Peng, X. (2002). Local tissue toxicity in response to extravascular extravasation of magnetic resonance contrast media. *Investigative radiology*, *37*(7), 393-398.

121. Runge, V. M., Price, A. C., Wehr, C. J., Atkinson, J. B., & Tweedle, M. F. (1985). Contrast enhanced MRI. Evaluation of a canine model of osmotic blood-brain barrier disruption. *Investigative radiology*, *20*(8), 830-844.

122. Leydier, A., Lin, Y., Arrachart, G., Turgis, R., Lecerclé, D., Favre-Reguillon, A., ... & Pellet-Rostaing, S. (2012). EDTA and DTPA modified ligands as sequestering agents for uranyl decorporation. *Tetrahedron*, *68*(4), 1163-1170.

123. Huang, Y., Boamah, P. O., Gong, J., Zhang, Q., Hua, M., & Ye, Y. (2016). Gd (III) complex conjugate of low-molecular-weight chitosan as a contrast agent for magnetic resonance/fluorescence dual-modal imaging. *Carbohydrate polymers*, *143*, 288-295.

124. Huang, Y., Cao, J., Zhang, Q., Lu, Z. R., Hua, M. Q., Zhang, X. Y., & Gao, H. (2016). Chitosan oligosaccharide based Gd-DTPA complex as a potential bimodal magnetic resonance imaging contrast agent. *Magnetic Resonance Imaging*, *34*(1), 1-7

125. Al-Amiery, A., Yasmein K. Al- Majeidy Abdulreazak, H. and Abood, H., *Bioinorg Chem Appl*. 2011, 2011, 483101